Journal of Research of the National Bureau of Standards

Volume 90 **Number 1** **January-February**

ISSN 0160-1741 **Library of Congress Catalog Card No.. 63-37059**

The Journal of Research of the National Bureau of Standards features advances in measurement methodology and analyses consistent with the NBS responsibility as the nation's measurement science laboratory. It includes reports on instrumentation for making accurate and precise measurements in fields of physical science and engineering, as well as the mathematical models of phenomena which enable the predictive determination of information in regions where measurements may be absent. Papers on critical data, calibration techniques, quality assurance programs, and well characterized reference materials reflect NBS programs in these areas. Special issues of the Journal are devoted to invited papers in a particular field of measurement science. Occasional survey articles and conference reports appear on topics related to the Bureau's technical and scientific programs. As a special service to subscribers each issue contains complete citations to all recent NBS publications in NBS and non-NBS media.

Issued six times a year. Annual subscriptions: domestic $17.00; foreign $21.25. Single copy, $3.00 domestic; $3.75 foreign.

United States Government Printing Office, Washington: 1985
Order all publications from the Superintendent of Documents
U.S. Government Printing Office, Washington, DC 20402

The Secretary of Commerce has determined that the publication of the periodical is necessary in the transaction of the public business required by law of this Department. Use of funds for printing this periodical has been approved by the Director of the Office of Management and Budget through April 1, 1985.

A New Feature—Conference Reports

The many conferences, symposia and workshops held at NBS each year play a valuable role in our efforts to identify the most important problems in measurement science. These meetings, which range from small groups of individuals whose focus is a specific area of technical expertise to large international conferences which cover broad aspects of work of current interest, define the "state of the art" in various disciplines and outline the direction of future work in that area. Summaries of such conferences, e.g., the "Report on the Sixth International Symposium on Temperature" by B. W. Mangum and G. T. Furukawa, J. Res. NBS **87**, 387 (1982) have appeared in previous issues of the Journal.

As a service to our readers, the *Journal of Research* is providing a new section entitled "Conference Reports" which will provide summaries of meetings held recently at NBS. The first two such reports summarizing recently held conferences on Optical Fiber Measurements and Large-Scale Computational Problems appear in the present issue. Similar reports will appear in future issues.

John W. Cooper
for the Board of Editors

Journal of Research of the National Bureau of Standards
Volume 90, Number 1, January–February 1985

Development of a One-Micrometer-Diameter Particle Size Standard Reference Material

G. W. Mulholland, A. W. Hartman, G. G. Hembree, Egon Marx, and T. R. Lettieri
National Bureau of Standards, Gaithersburg, MD 20899

Accepted: October 11, 1984

The average diameter of the first micrometer particle size standard (Standard Reference Material 1690), an aqueous suspension of monosized polystyrene spheres with a nominal 1 μm diameter, was accurately determined by three independent techniques. In one technique the intensity of light scattered by a diluted suspension of polystyrene spheres was measured as a function of scattering angle, using a He-Ne laser polarized in the vertical direction. The second technique consisted of measuring as a function of angle the intensity of light scattered from individual polystyrene spheres suspended in air, using a He-Cd laser with light polarized parallel and perpendicular to the scattering plane. The measurement of row length by optical microscopy for polystyrene spheres arranged in close-packed, two-dimensional hexagonal arrays was the basis of the third technique. The measurement errors for each technique were quantitatively assessed. For the light scattering experiments, this required simulation with numerical experiments. The average diameter determined by each technique agreed within 0.5% with the most accurate value being 0.895±0.007 μm based on light scattering by an aqueous suspension. Transmission electron microscopy, flow through electrical sensing zone counter measurements, and optical microscopy were also used to obtain more detailed information on the size distribution including the standard deviation (0.0095 μm), fraction of off-size particles, and the fraction of agglomerated doublets (1.5%).

Key words: array sizing; index of refraction; light scattering; Mie scattering; particle counting; particle size standards; polystyrene spheres; size distribution; transmission electron microscopy.

1. Introduction

This paper describes the measurements performed to accurately characterize the average particle size of the nominal one-micrometer polystyrene spheres particle size standard (Standard Reference Material 1690). The spheres were purchased from Dow Chemical Company.[1] They have a nearly monosize distribution and are dispersed in water at a weight concentration of 0.5%.

About the Authors: G. W. Mulholland is a research chemist in NBS' Center for Fire Research. A. W. Hartman, G. G. Hembree, Egon Marx, and T. R. Lettieri are physicists in the Bureau's Center for Manufacturing Engineering.

The three techniques used for measuring average particle size were: light scattering from individual spheres suspended in air, light scattering from an aqueous suspension of the spheres, and optical row-length measurements of spheres arranged in two dimensional arrays. The selection of these techniques resulted in part from a detailed review of all the generic measurement techniques appropriate for the dimensional calibration of microscopic-particle size standards by Swyt [1][2]. These same three techniques were used previously by others in characterizing a batch of monosize polystyrene spheres produced by Dow Chemical Co. (batch number LS-1028-E). Phillips et al. [2] obtained a diameter of 1.20 μm by single particle scattering measurements, Rowell et al. [3] obtained 1.21 μm by measurement of light scattering from a suspension of particles, and Bierhuizen and Ferron [4] obtained 1.20 μm based on array sizing. The good agreement among these independent

[1]Certain materials are identified in this paper in order to adequately specify the experimental procedure. Such identification does not imply recommendation or endorsement by the National Bureau of Standards, nor does it imply that the materials or equipment identified are necessarily the best available for the purpose.

[2]Figures in brackets refer to literature references at the end of this paper.

measurements gave us confidence that an accurate particle size standard was achievable.

Our study represents an extension of the earlier work in regard to the accuracy achievable by the three techniques. The major effort of our study was directed at performing the measurements in such a way as to maximize the accuracy in the determination of the mean particle size. This required the use of accurate calibration standards for magnification and angular alignment in addition to a quantitative error analysis.

Perhaps the most widely accepted technique for measuring the particle size of polystyrene spheres has been transmission electron microscopy (TEM). This is the basis of the particle size information that is provided with the monosize polystyrene spheres marketed by the manufacturer. We also had intended to use the TEM as one of our primary techniques, but we were unable to find an accurate method for calibrating the magnification of the microscope. The relatively wide range of values for particle diameter (from 1.10 to 1.26 μm) reported by five independent TEM measurements [3] for Dow Latex LS-1028-E also suggests that the method is unsatisfactory for highly accurate particle size measurements. While we did not use the TEM for determining average size, we did use it for determining the standard deviation, σ_P, of the size distribution.

Methods that have been used by others for measuring the particle size of polystyrene spheres include flow ultramicroscopy, ultracentrifugation, quasi-elastic scattering, and small-angle x-ray scattering. Some general design limitations of these instruments are given below. Our choice of light scattering and optical array sizing techniques was based on their being at least competitive with other methods in regard to sizing accuracy, and on our familiarity with the measurement methods and the theoretical basis.

Both the quasi-elastic scattering technique and small-angle x-ray scattering work best for particles smaller than about 1 μm. The former technique [5] measures, in effect, the particle diffusion coefficient, which increases with decreasing particle size. The resolution is limited for 1 μm particles but improves with decreasing size. This is just the opposite of angular–intensity light scattering and array sizing where the resolution drops off markedly for particle sizes less than about 0.5 μm diameter. Small-angle x-ray scattering [6] is also best for small particle sizes because of the small wavelengths of the x-rays.

Davidson et al. [7] obtained an uncertainty of about $\pm 4\%$ at the 95% confidence level for flow ultramicroscopy based on counting 300 particles. The major source of uncertainty was attributed to the statistical uncertainty in the average counting rate. The uncertainty in the number of particles counted is simply equal to the square root of that number. Van den Hul and Vanderhoff [8] obtained a mean diameter for Dow Latex LS-1028-E about 18% less than the mean of the other techniques listed by Rowell et al. [3] using ultracentrifugation. A major drawback in the technique for this application is the small density difference, 1.00 versus 1.05, between water and the polymer. Nevertheless, Van den Hul et al. point out that all the deviation from other measurements cannot be accounted for by the uncertainty in the density difference. Apparently no detailed error analysis has been made for the ultracentrifuge applied to particle measurements.

While the major focus of our study was the accurate determination of the number average particle diameter D_n, we also obtained information regarding the size distribution including the standard deviation, σ_P, of the particle size distribution, the fraction of off-size particles, and the fraction of agglomerated doublets. In addition, we obtained an estimate of the deviation from sphericity based on TEM measurements. A brief description of the emulsion polymerization technique for producing polystyrene spheres and the factors affecting the stability of the suspension is given in the Appendix.

2. Light Scattering From Individual Spheres

We determined the diameter of the polystyrene spheres by measuring the angular distribution of the intensity of the light scattered by a single sphere and comparing measured intensities with those computed for different values of the diameter, D, and the refractive index, n.

The particles were levitated electrostatically in a Differential II light-scattering photometer developed by Wyatt and Phillips [9]. This type of instrument has been used to determine D and n for spheres with diameters 1.099 μm (Phillips et al. [2]), 0.796 μm (Cook and Kerker [10]), 1.011, 0.794, and 0.600 μm (McRae [11]), and 1.01, 5.7, and 11.9 μm (Davis and Ravindran [12]). The sizes given above are nominal sizes provided by Dow Chemical Company, the manufacturer of the particles. Bottiger et al. [13] have developed the capability of measuring all 16 components of the Mueller matrix, the light-scattering phase matrix, for a single polystyrene sphere. They also collected the particles on the tip of a needle for subsequent observation in an electron microscope.

A detailed error analysis enabled us to make a quantitative statement regarding the accuracy of this technique. This and other aspects of the experiment and data analysis have been previously reported by Marx and Mulholland [14].

2.1 Experimental Method

An aerosol made up of polystyrene spheres is generated by nebulizing a suspension of the spheres in distilled, filtered water; the water evaporates rapidly leaving charged spheres. One of these spheres is then levitated electrostatically in an optical cell with electrodes as shown in figure 1. The particle is kept in the light beam of a He-Cd laser ($\lambda=441.6$ nm) by means of a servocontrol.

The scattered light reaches a photomultiplier (having an S-21 response) via a traveling periscope, which has an acceptance angle of about 2° and which moves in a horizontal arc of almost 180°. We found that the output of the angle encoder deviates by as much as 3° from the true angle, and we performed an angle calibration using an accurately indexed protractor.

We use a half-wave retardation plate to change the polarization of the incident light.

A typical sequence of measurements begins with a scan of the background, then a particle is captured and one or more scans is performed to measure the light scattered by that particle. A rotation of the half-wave plate by 45° then changes the polarization of the incident beam by 90°, and one or more scans is performed to measure the scattered light, followed by a background measurement for the new polarization. The light intensity-angle data pair closest to each integer angle over the range 20° to 160° is stored on magnetic tape.

2.2 Data Analysis

The data are matched to the results of the calculations of the angular distribution of the intensity of the light scattered by a uniform sphere, as found by Mie and others [15–17].

The values of D and n are determined by minimizing the quality of fit

$$Q(D,n)=\frac{1}{N}\sum_{i=1}^{N}(E_i-\alpha T_i(D,n))^2, \tag{1}$$

where N is the number of data points, E_i is the measured intensity at the angle θ_i, T_i is the computed value for the same angle, and α is an overall scaling factor required because we do not measure absolute intensities. The expression for the α that minimizes Q is given by

$$\alpha=\left(\sum_{i=1}^{N}E_iT_i\right)/\sum_{i=1}^{N}T_i^2. \tag{2}$$

The least-squares fit is then determined by a grid search in the Dn-plane for progressively finer grids. This procedure can be speeded up using an iterative search such as the Marquardt-Levenberg algorithm after an initial coarse grid search.

Other measures of the quality of fit are possible, and we consider mainly those that involve a change of variables. Specifically, we use the transformed intensity

$$I_1(\theta)=I(\theta)\sin^2(\theta/2), \tag{3}$$

because it tends to equalize the height of all the peaks for a particle of a size around 1 μm in diameter. In the original variable $I(\theta)$, the large peak at small angles is overemphasized. On the other hand, the use of $I_1(\theta)$ overemphasizes the values at angles close to 180°, which are small with large relative errors.

2.3 Results

The theoretical best fit curves are plotted in figure 2 for a single polystyrene sphere with and without the weighting function. There are four independent determinations of the best fit diameter; two based on vertical polarization and two based on horizontal polarization data. The best fit values range from 0.898 to 0.905 μm, which is a range of about 0.8%. A small portion of the table of values of $Q(n,D)$ near the minimum is given in

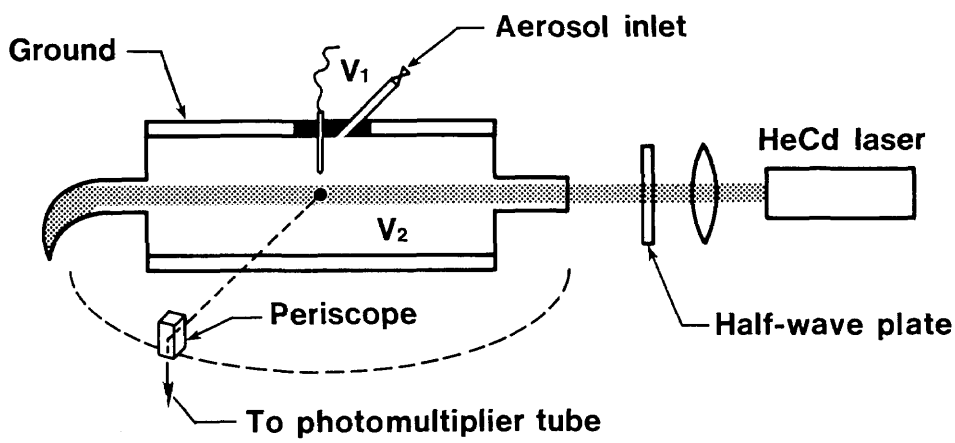

Figure 1–Single particle scattering instrument (Differential II). The pillbox shaped scattering cell has a pin electrode (V_1) separated by an insulator from the ground plate electrode and opposite to the base plate electrode (V_2).

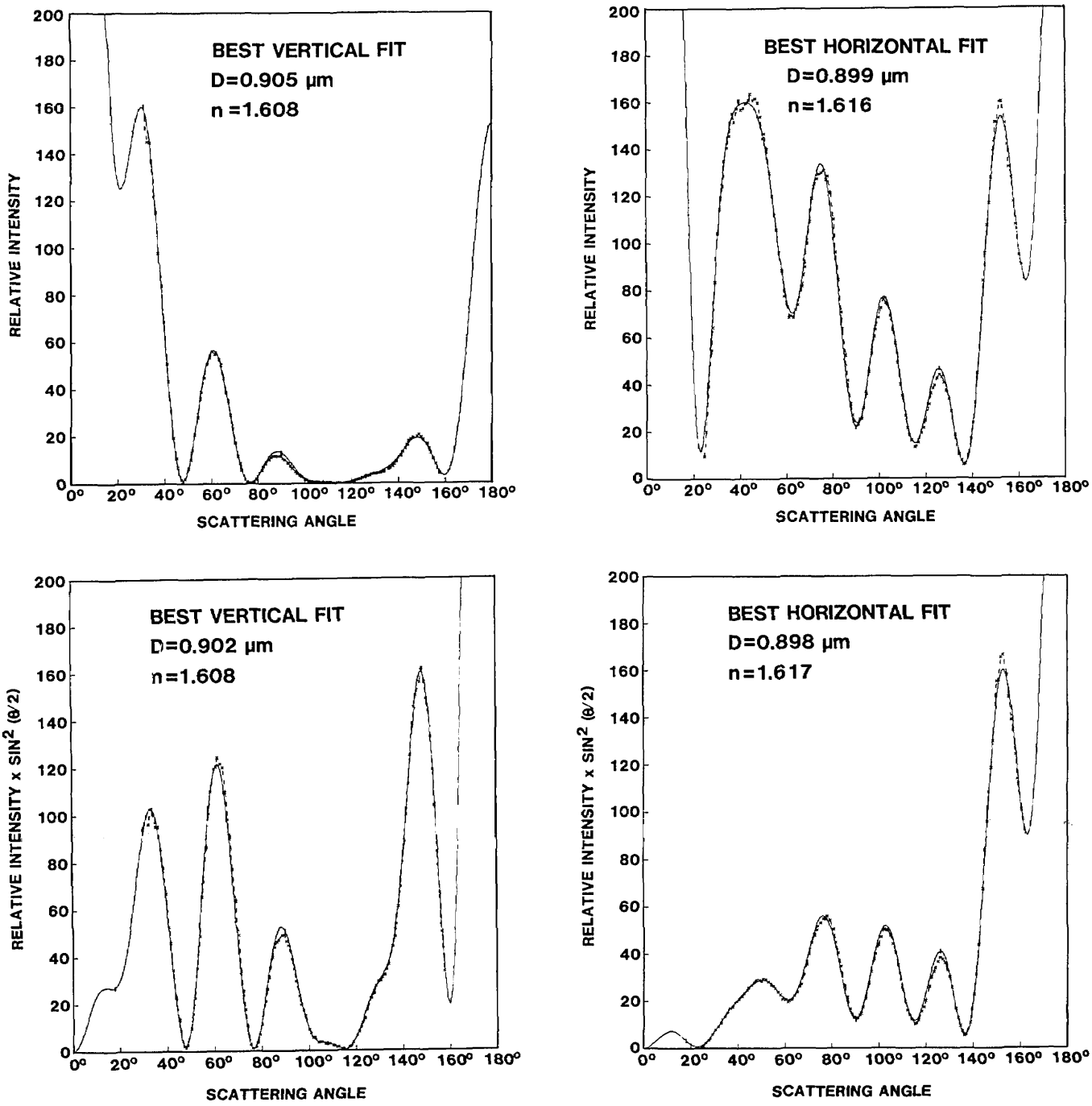

Figure 2–Best fits to the intensity of scattered light versus angle data for a single polystyrene sphere as determined by the least squares method with (bottom) and without (top) the $\sin^2\theta/2$ weighting factor. Data (– – –x– – –x); theory (_____).

table 1. The quantity Q varies rapidly with respect to D for fixed n (column) and rapidly with respect to n for fixed D (row) but is rather insensitive in the diagonal direction along which the product nD is almost constant. In a three-dimensional plot of $1/Q$ as a function of n and D, there is a very sharp peak when the surface is viewed in one direction but almost a ridgelike appearance in the other as shown in figure 3. The relative insensitivity of Q to correlated changes in n and D necessitates that careful angle calibrations and detailed data analysis be performed in order to obtain accurate values for n and D.

The results for the eight SRM 1690 particles analyzed are contained in table 2 including the averages for the

Table 1. Normalized values of Q near the minimum for a SRM 1690 particle.

	Vertical Polarization						Horizontal Polarization				
n	1.600	1.604	1.608	1.612	1.616	n	1.608	1.612	1.616	1.620	1.624
D,μm						D,μm					
0.899	4.75	3.18	2.18	1.70	1.69	0.893	14.22	9.78	6.36	4.07	3.03
0.901	2.34	2.15	1.48	1.29	1.50	0.895	9.58	5.93	3.37	2.01	1.92
0.903	2.31	1.47	1.09	1.15	1.58	0.897	5.90	3.11	1.51	1.16	2.13
0.905	1.65	1.10	1	1.29	1.92	0.899	3.35	1.55	1	1.81	4.06
0.907	1.32	1.06	1.20	1.70	2.52	0.901	2.15	1.46	2.16	4.35	8.13
0.909	1.32[a]	1.33	1.70	2.40	3.39	0.903	2.59	3.24	5.40	9.25	14.92

[a]The minimum value of Q in each column is underlined to illustrate the slow variation of Q on a diagonal.

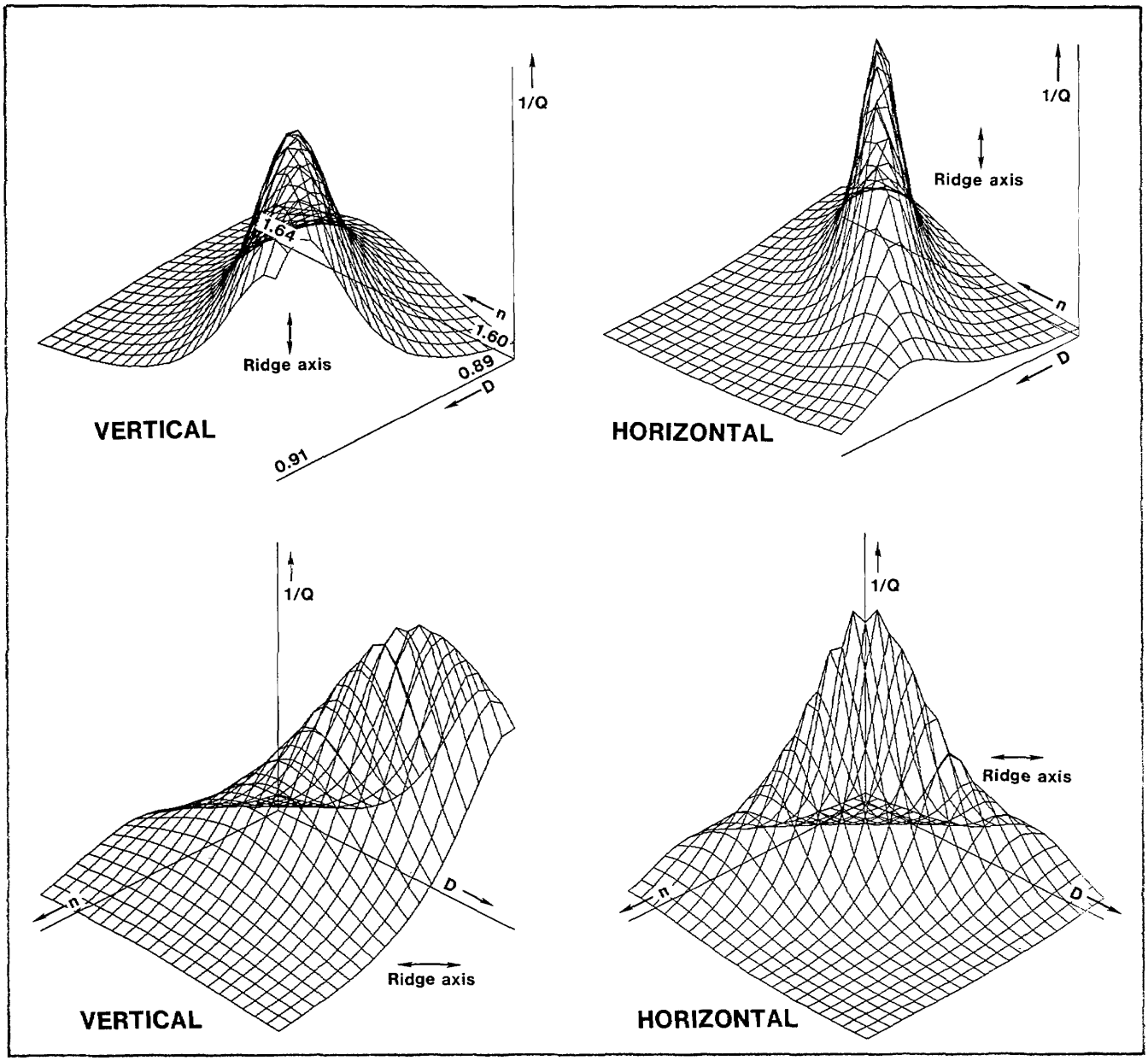

Figure 3–Two views of the three-dimensional surface of the inverse of the quality of fit, $1/Q$, as a function of the index of refraction, n, and the diameter, D, over a range of a few percent from the best value. The ridges cause difficulties for an accurate determination of the correct values of n and D.

Table 2. Radius and index of refraction for eight particles from SRM 1690.

	Harmonic Mean[a]		Vertical Polarization		Horizontal Polarization	
	Radius μm	Refractive Index	Radius μm	Refractive Index	Radius μm	Refractive Index
	0.4545	1.614	0.4550	1.614	0.4535	1.610
	0.4570	1.613	0.4570	1.613	0.4530	1.623
	0.4490	1.618	0.4530	1.605	0.4490	1.618
	0.4465	1.612	0.4510	1.600	0.4460	1.614
	0.4480	1.613	0.4515	1.610	0.4480	1.613
	0.4505	1.613	0.4535	1.610	0.4505	1.613
	0.4535	1.608	0.4535	1.608	0.4535	1.610
	0.4394	1.606	0.4402	1.603	0.4394	1.610
Average	0.4498	1.612	0.4518	1.608	0.4491	1.614
σ	0.0051	0.004	0.0048	0.005	0.0045	0.004

[a]Harmonic mean refers to the determination of the best fit radius and refractive index by taking the harmonic mean, Q_h, of the Q's for the cases of vertically and horizontally polarized light, Q_V and Q_H respectively (i.e., $2/Q_h = 1/Q_V + 1/Q_H$).

diameter and index of refraction, 0.900 μm and 1.612, respectively. The average particle size in this report refers to the number average defined as follows:

$$D_n = \frac{\sum_{i=1}^{N} D_i}{N}, \quad (4)$$

where N refers to the number of particles measured. The particle size is not perfectly uniform ($\sigma_P = 0.010$) and we expect to see a spread in the measured diameters. On the other hand, the refractive index should be the same for all particles, and we attribute the variation to experimental error.

For one particle we took nine scans with vertically polarized light and three more with horizontal polarization. The results of the analysis are shown in table 3. The standard deviation for the diameter, 0.0022 μm, is smaller than the one previously calculated for groups of particles, but that for the index of refraction, 0.005, is about the same, suggesting that this parameter does not change, at least for particles of the same size.

2.4 Error Analysis

To study the effects of experimental errors on the best fit parameters, we modified the program that produces the theoretical values of the scattered intensities to add

Table 3. Results for repeated scans for one particle.

Run	Unweighted Fit		Weighted Fit			
	Radius μm	Refractive Index	Radius μm	Refractive Index	n=1.608[a] Radius μm	n=1.615 Radius μm
1−V	0.4402	1.601	0.4380	1.612	0.4384	0.4366
2−V	0.4364	1.620	0.4376	1.614	0.4398	0.4378
3−V	0.4392	1.606	0.4366	1.618	0.4386	0.4372
4−V	0.4402	1.603	0.4398	1.605	0.4388	0.4372
5−V	0.4394	1.606	0.4410	1.601	0.4390	0.4372
6−V	0.4380	1.610	0.4398	1.604	0.4386	0.4368
7−V	0.4398	1.604	0.4386	1.610	0.4388	0.4370
8−V	0.4394	1.606	0.4388	1.609	0.4390	0.4372
9−V	0.4394	1.607	0.4400	1.604	0.4392	0.4374
1−H	0.4394	1.610	0.4402	1.601	0.4398	0.4384
2−H	0.4380	1.612	0.4402	1.612	0.4386	0.4374
3−H	0.4384	1.614	0.4364	1.620	0.4394	0.4382
Average	0.4390	1.608	0.4389	1.609	0.4390	0.4374
σ	0.00110	0.0053	0.00150	0.0063	0.00047	0.00053

[a]The last two columns correspond to values of the radii obtained for a fixed value of the refractive index (unweighted fit). The first value is obtained for the best fit to all particles of this size, and the second one is the published bulk value.

simulated errors and generate a file of "data" to be processed by the same procedure as described above. Noise obtained using a random number generator with a maximum amplitude of 1–3% of the intensity at each angle was added to all curves.

The major component of the random error is attributed to the noise in the intensity of the scattered light. This noise can be monitored by fixing the angle and recording a trace of the intensity versus time. The general characteristics of such a trace show that there are two components of this noise. The smaller component, about 2% of the intensity, affects each angle reading independently; the larger component, which we think comes from the motion of the particle within the laser beam when the servocontrol is activated, is about 5% and has a lower frequency so that it affects intensity readings in groups of about 10 degrees for the data collection speed that we used. The uncertainty in particle size for a 0.900 μm particle diameter was found to be at most 0.3% or 0.0027 μm. As described above, the observed variability in particle diameter for 12 repeat scans of the same particle resulted in a σ of 0.0022 μm, which is consistent with most of the error being attributed to noise in the intensity of the scattered light.

The quantity of primary interest is the random error associated with the determination of the average particle diameter. The standard deviation of the size distribution, σ_P, is much larger than the σ associated with repeat measurements and will ultimately limit the accuracy in the mean size determination. Our measured σ_P of the particle diameters based on eight particles is 0.010 μm; an estimate based on our electron microscopy for about 160 particles, as discussed below, is slightly smaller, 0.0095 μm. The component of the overall uncertainty in particle diameter resulting from the width of the size distribution is given by

$$R = t_m(0.025)\frac{\sigma_P}{\sqrt{n}}, \tag{5}$$

where n is the number of particles (eight in this case) and $t_m(0.025)$ is the Student t-value for m degrees of freedom and for 95% confidence level. The number of degrees of freedom relates to the determination of σ_P and is one less than the number of particles sized by electron microscopy, 159. We obtain a value of R equal to 0.0066 μm.

The sources of systematic errors include angle drift, δ_θ, polarization misalignment, δ_P, wavelength uncertainty, δ_λ, and non-volatile impurities, δ_I. There is an error on the order of 2% if the angle encoder output is not calibrated. To this is added the problem of a slight drift in the calibration that was apparently electronic in origin. Over the two days during which the light scattering measurements were performed on the eight polystyrene spheres, the angle drift was about 0.08°. Including this drift in a numerical simulation, we find the uncertainty in particle size due to the drift, δ_θ, to be 0.0028 μm.

The mixture of polarization states comes primarily from imperfections in the optical components and the misalignment of the periscope. The imperfections in the half-wave plate and other optical components allow the leakage of a small fraction of light (1 part in 200) at the orthogonal polarization direction. The error from the inclination of the periscope with respect to the scattering plane is comparable to the error due to the optical imperfections. A combined estimate of these effects comes to $\delta_P = 0.0018$ μm.

The least important error is the uncertainty in the wavelength of the He-Cd laser, $\delta_\lambda = 0.00007$ μm.

In addition to instrumental errors, there are uncertainties associated with the nature of the particle. While the polystyrene spheres are often considered to be homogeneous, we expect the existence of a surface coating from the non-volatile emulsifier added during the preparation of the particles. If we assume that all the emulsifier resides on the particle surface, we find that the diameter is increased by 0.0008 μm, so that $\delta_I = -0.0008$. There is also a contribution to the surface coating from the 2 ppm impurities in the distilled water in which the particles are suspended, but it is negligible in comparison with the emulsifier contribution.

An estimate of the total uncertainty, U_T, is obtained by adding the random error, R, to the sum of the absolute values of the systematic errors.

$$U_T = R + |\delta_\theta| + |\delta_P| + |\delta_I| \tag{6}$$

Using the values given above, we obtain $U_T = 0.012$ μm with a number average size of 0.900 μm.

The above analysis includes effects for which we have quantitative estimates. Two other possible systematic error sources are slight asphericity of the particle and possible inhomogeneity of the particle resulting from strain as the water evaporates from the particle. Transmission electron microscope measurements of the particle described in section 5 indicate an asphericity of 0.6% at a precision of about 0.3%. Over the course of our measurements the particle would have undergone extensive rotation as a result of Brownian motion. We have no quantitative estimate of this effect, though we intuitively expect our value to be close to the volume equivalent sphere diameter.

3. Light Scattering From a Suspension of Spheres

Light scattering measurements on a suspension of particles is complementary to single-particle scattering measurements. The signal-to-noise performance for sin-

gle-particle measurements is limited by the small scattering intensity and by particle movement in the beam. For scattering from a particle suspension the signal-to-noise ratio is much improved because of the large number of particles in the scattering volume and because of the use of photon counting. An accurately indexed rotary table was used for our light-scattering measurements with a suspension, whereas a rapidly-traversing periscope with some drift in the angle calibration was used for the single-particle measurements. One disadvantage of measurements with a suspension is that there is one more unknown in the measurement, namely the size distribution, compared to the single-particle measurements where particle size and the index of refraction are the only unknowns.

There have been a number of studies of light scattering by nearly monosized suspensions. Kerker's book [17] includes several studies of the determination of the mean size and standard deviation based on the angular dependence of the polarization ratio. Our instrument design is similar to the one described by Wims and Myers [18]. The recent determination of particle size of polystyrene spheres by Rowell et al. [3] by light scattering measurements is similar to our study in terms of measurement technique and data analysis.

3.1 Design of the Photometer

A schematic diagram of the light scattering photometer for particle suspension is shown in figure 4. A 5-mW intensity-stabilized He-Ne laser beam is directed to the center of a 10-cm diameter scattering cell with optical flat windows on opposite sides. Incident light is vertically polarized and only the vertically polarized component of the scattered light is detected (VV scattering). A beam stop is positioned in the cell to minimize the amount of reflected light reaching the detector. The collection optics (figs. 4 and 5) consist of two apertures, a $1\times$ microscope objective, a vertical polarizer, and a glass diffusing screen. The scattered light is detected by a low-noise photomultiplier tube with a small (2.5 mm diameter) photo cathode. The output pulses from the anode are amplified, discriminated, and then counted over a 10-second time interval. The typical number of counts per 10-second interval at the first peak is about 200,000, with repeat measurements agreeing within about 1%. The lowest count was on the order of 10,000.

For some measurements, part of the laser beam is split off and sent into a reference photomultiplier. Output counts from the reference amplifier-discriminator are used as clock pulses to the photon counter. In this manner, a ratio is taken between the signal photon counts and reference photon counts, thus cancelling out the laser intensity fluctuations. This is not a significant effect for the intensity stabilized He-Ne laser, but it is significant for the He-Cd laser to be discussed later.

A rotary table with an accuracy and reproducibility of ± 1 arc second (0.0003°) is used for the angle measurements. The rotary table is indexed at two-degree increments. The PMT is mounted rigidly to an arm attached to the rotary table. Using a micrometer adjustment and a dial indicator, the center of the scattering cell is made coincident with the center of rotation of the

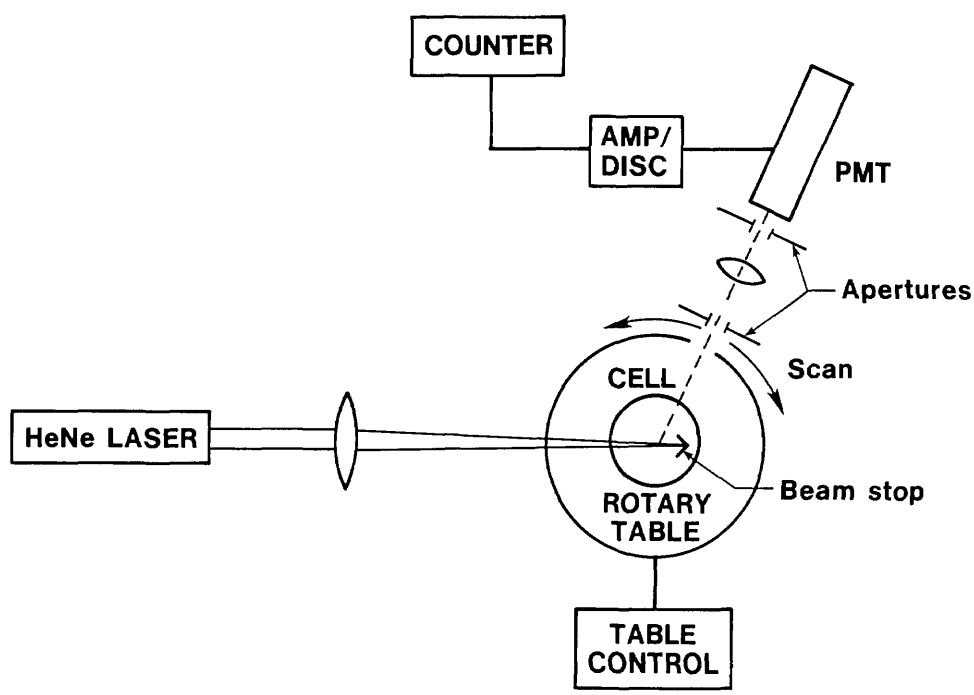

Figure 4–Light scattering photometer for particle suspension. Optical windows not shown.

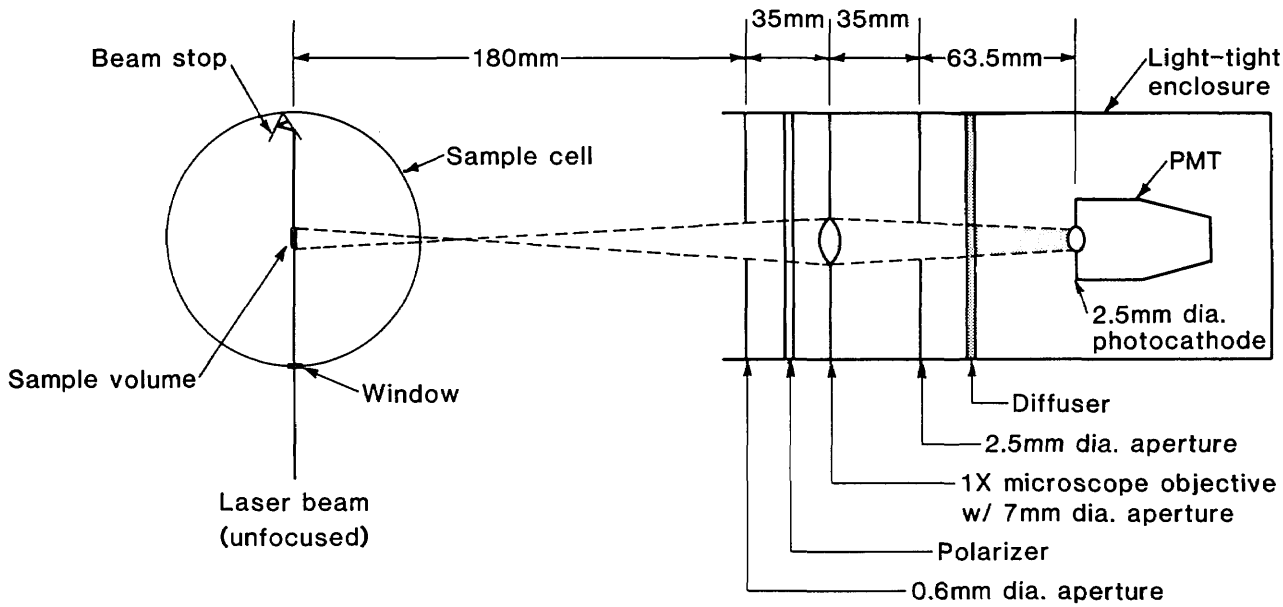

Figure 5–Design of detector optics for minimizing acceptance angle.

rotary table. Next the laser is mounted so that the beam goes through the center of the two optical flats and reflects back on itself. The pinholes in the detector system are then positioned in the center of the laser beam. The estimated deviation of the zero angle alignment, including a slight error in positioning the cell (about 0.05 mm) and in the pinhole positioning (about 0.2 mm), leads to an uncertainty in the zero angle of about 0.07°. The effect of this uncertainty on the particle size determination will be discussed in subsection 3.4.

It is important to have a small acceptance angle for the detector in order to obtain good size resolution. This is accomplished in our design by using two pinholes before the detector as indicated in figure 5. In addition, a collection lens is used to limit the depth of field. With these optics in the collection arm, the measured acceptance angle is about $\pm 1°$ as measured at the 70% transmission points. This compares favorably with the calculated acceptance angle of $\pm 1.3°$ at the zero transmission points. The two-degree acceptance angle gives a calculated sample volume on the order of $1.3 \times 10^{-2} cm^3$ (13 mm^3).

3.2 Sample Preparation and Experimental Procedure

Clean glassware and "particle free" water are used to minimize extraneous particles in the suspension. After each experiment, the cell is washed with detergent, rinsed, and then cleaned in hot nitric acid for a couple of hours. After rinsing the cell and cover glass 8 to 10 times with deionized, filtered water, the cell is dried without water marks by directing a particle-free flow of air over the external surface of the cell. Deionized water with a resistivity of about 18 megohm-centimeter is used for rinsing glassware and for sample dilution. A pleated membrane filter with a 0.2-μm pore size is also used on the water outlet to remove particulates.

In order to minimize multiple scattering, the particle suspension is diluted to a concentration on the order of 10^6 particles/cm^3. Dilution of approximately four orders of magnitude is required to dilute the standard samples, which are 0.5% by weight.

After positioning the optical cell, a beam stop is inserted in the cell to minimize reflected light. Measurements are performed every two degrees from 20° to about 140°, requiring about 30 minutes per experiment. At each angle, two intensity measurements are made to check for consistency and to avoid spurious data resulting from contamination particles which occasionally enter the scattering volume.

3.3 Data Analysis

For the case of light scattering from a suspension, there are three unknown parameters: the number-average size, D_n, the standard deviation of the size distribution, σ_P, and the index of refraction of the polystyrene sphere. We assume the size distribution to be normal. For the narrow size distribution of interest here, there is little difference between a log-normal distribution, which others have assumed for the polystyrene spheres, and a normal distribution. Determinations of size distributions of polystyrene spheres by electron microscopy support this assumption. In carrying out our data analysis, we assume the index of refraction to be known, and treat D_n and σ_P as unknown parameters. In

values of Q as a function of D_n and σ_P are given in table 4 for this case (experiment A3). We consider this second definition of quality of fit to be superior to the first because all the data are significant. For our data, both techniques produce very nearly the same result; for example, D_n for the first method is 0.894 compared to 0.896 for the second method.

3.4 Results

One drop from one of the SRM 1690 vials, selected at random from 1000 vials, was used in preparing each of the 10 samples. Light-intensity-versus-angle data were taken for each sample and the best-fit parameters were calculated. The results of the measurements are presented in table 5. The average value of D_n, $\bar{D}_n$, for experiments A2 through J1 was found to be 0.895 μm with a standard deviation associated with the average size, σ_{D_n}, of 0.0007. The average value of the standard deviation of the size distribution, σ_P, was found to be 0.029 μm. Also indicated in table 5 are four repeat measurements for one sample with the scans performed sequentially over a period of about three hours. The standard deviation for the average size for the repeat measurements is less than 0.0003 μm. We think that the larger standard deviation obtained for the 10 samples is a result of the sample preparation and cell positioning and not of differences in the vials; in any event, both standard deviations are small and represent a minor component of the overall error as discussed in subsection 3.5.

Table 4. The quality of fit, Q, for experiment A3 with weighting factor

	σ_P,μm	0.021	0.023	0.025	0.027
D,μm					
0.8945		0.158	0.147	0.149	0.165
0.8950		0.147	0.140	0.146	0.167
0.8955		0.140	0.137	0.148	0.172
0.8960		0.139	0.140	0.154	0.181
0.8965		0.143	0.147	0.164	0.192

Table 5. Best-fit values for D_n for 10 samples of SRM 1690 based on light scattering from a particle suspension.

Sample[a]	D_n,μm	σ	photon counts/10s[d]	Q
A2	0.8945	0.029	197,000	0.276
B	0.8965	0.025	165,000	0.287
C	0.8945	0.031	177,000	0.321
D	0.8940	0.031	179,500	0.272
E	0.8955	0.029	172,900	0.288
F	0.8950	0.029	150,500	0.224
G	0.8945	0.027	166,000	0.246
H	0.8950	0.027	97,500	0.166
I	0.8945	0.031	142,700	0.231
J1[b]	0.8955	0.029	137,200	0.280
J2	0.8950	0.029	137,000	0.221
J3	0.8955	0.027	137,500	0.234
J4	0.8955	0.029	136,000	0.217
A3[c]	0.8955	0.023	167,500	0.137

[a]The sample concentration is approximately 7.0×10^5 particles/cm^3.
[b]The numerals refer to repeat measurements of the same sample.
[c]Sample A3 was prepared and the measurements made six months after the other measurements.
[d]Measured at 30 °C.

Scattering measurements were also performed with a He-Cd laser with $\lambda=441.6$ nm, as a test for consistency. The appropriate values for the indices of refraction of water and polystyrene for this wavelength at 23 °C are 1.3395 and 1.615, respectively. Because of the lower intensity stability of the He-Cd laser, the ratio of signal photon counts to reference counts was taken as described in subsection 3.1. In this case D_n was found to be 0.896 with $\sigma_P=0.031$.

3.5 Error Analysis

The major elements of the random error component of the overall uncertainty are the photon counting noise and the fluctuation in the number of particles in the scattering volume. The percentage noise arising from the statistical nature of photon counting goes as $1/\sqrt{N}$ so that even for a low count of 10,000 the noise is only 1%. Another $1/\sqrt{N}$ term is caused by the fluctuation in the number of particles in the scattering volume. For a number concentration of 7×10^5 particles/cm^3 and a typical scattering volume of 1.3×10^{-2} cm^3, the number of particles is 9.1×10^3 leading to a noise of 1.0%. Assuming the two fluctuations to be independent, we obtain a combined noise of 1.5%. The effect of this noise was simulated by the same technique as described in subsection 2.4 and found to change the particle size by 0.0006 μm. This is comparable to the observed σ, 0.0007, for the measurements with the 10 samples. The random component of the uncertainty is calculated as in subsection 2.4,

$$R = t_{n-1}(0.025)\frac{\sigma}{\sqrt{n}}, \tag{11}$$

where n refers to the number of samples. In this case the number of degrees of freedom is $n-1$. We obtain for R a value of 0.0005 μm, which is a factor of 13 less than for the single-particle measurements.

The primary component of the systematic error is uncertainty in the refractive index of the particle with lesser contributions from multiple scattering, finite acceptance angle of detector, misalignment of detector, and reflected light. The uncertainty in the angle mea-

subsection 3.5 we consider the sensitivity of the results to the assumed value of the index of refraction.

For a distribution of particle sizes, the theoretically predicted scattering intensity, $I(\theta_i,D_n,n)$, is the single-particle scattering intensity, $T(\theta_i,D_j,n)$, averaged over the size distribution and the acceptance angle of the detector.

$$I(\theta_i,D_n,\sigma_P)=\frac{1}{\sqrt{(2\pi)}\sigma_P}\sum_{j=1}^{m}\exp\left[-\frac{(D_j-D_n)^2}{2\sigma_P{}^2}\right]\{T(\theta_i,D_j,n)$$

$$+0.7T(\theta_i-1,D_j,n)+0.7T(\theta_i+1,D_j,n)\} \quad (7)$$

where m represents the number of size increments and the terms with θ_i+1 and θ_i-1 take into account the effects due to the finite acceptance angle of the detector. The quality of fit, Q, for the particle suspension experiment is defined by the same type of expression as eq (1),

$$Q=\frac{1}{N}\sum_{i=1}^{N}[E_i-\alpha I(\theta_i,D_n,\sigma_P)]^2, \quad (8)$$

where the index i refers to angle, and E_i is the measured scattered intensity at θ_i. The expression for α is the same as given by eq (2) but with $I(\theta_i)$ replacing T_i.

For the refractive index of the polystyrene spheres, we use the value 1.588 for bulk polystyrene at $\lambda=632.8$ nm given by Boundy and Boyer [19]. The refractive index of water at 23 °C was taken to be 1.3315 based on measurements by Tilton and Taylor [20]. The appropriate wavelength and index of refraction for a particle suspended in water are the ratios of the respective values in vacuum to the refractive index of water giving

$$\frac{\lambda_{vac}}{n_{water}}=0.4752\ \mu m$$

$$\frac{n_{PSL}\ (vac)}{n_{water}}=1.1925.$$

The number of intervals in the size distribution, m, is typically taken to be 10 or 20. The size increment, Δ, from D_j to D_{j+1} is chosen to be

$$\Delta=\frac{4\sigma_P}{m-1} \quad (9)$$

so that the average in eq (7) covers the full size distribution regardless of the value of σ_P. For a specified value of D_n and σ_P, the quantity I is calculated at two degree intervals from 20° to 140°. The value of Q is determined from eqs (8) and (2). The best-fit values for D_n and σ_P are determined by finding the minimum Q for a range of values for D_n and σ_P. The range for D_n is typically 0.893–0.898 μm in increments of 0.0005 μm, and, for σ_P, from 0.021 to 0.039 μm in increments of 0.002 μm. Typical experimental data and best-fit results are shown in figure 6.

We also consider a second definition of quality of fit based on weighting the intensities by a function of the angle. Specifically, we consider

$$I_1(\theta_i)=I(\theta_i)\sin^4\left(\frac{\theta_i}{2}\right), \quad (10)$$

which reduces the contributions to the quality of fit from the large peaks at small scattering angles. As seen in figure 7, which is based on the same data as figure 6, the weighted peaks and valleys are approximately uniform in amplitude throughout the angular range. The

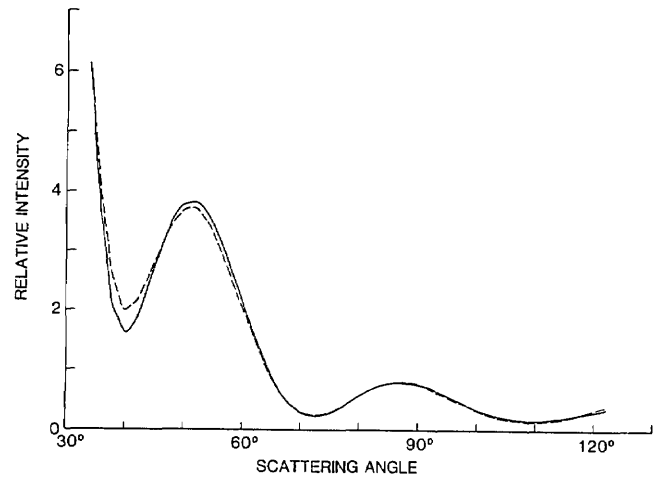

Figure 6–Best fit curve for the intensity of scattered light as a function of angle with $D_n=0.893$ μm and $\sigma_P=0.027$ μm. Data (– – –); theory (_____).

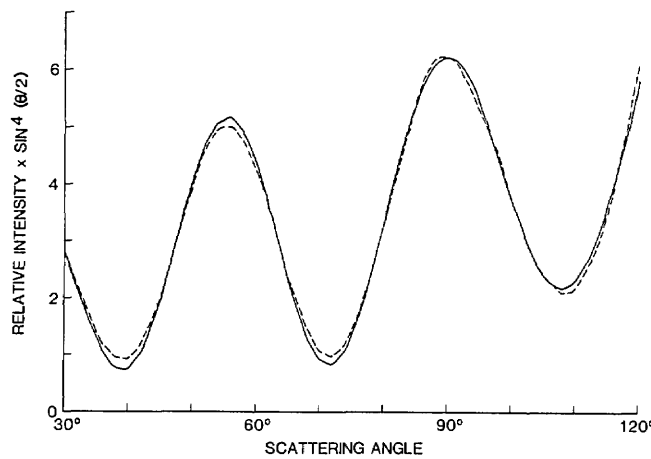

Figure 7–Best fit curve for the intensity of scattered light weighted by $\sin^4(\theta/2)$ as a function of angle with $D_n=0.896$ μm and $\sigma_P=0.023$ μm. The experimental data is the same as for figure 6. Data (– – –); theory (_____).

surement and in the wavelength of light is negligible in comparison to these others.

The values of the refractive index of polystyrene spheres obtained by various investigators were extrapolated to the He-Ne laser wavelength using the following dispersion equation:

$$n = A + \frac{B}{\lambda^2}. \tag{12}$$

The constants A and B are obtained from the measured value of n at one wavelength together with Starkie's [21] value of 31.0 for the dispersion ratio defined as

$$\frac{n_{5893} - 1}{n_{4861} - n_{6563}} = 31. \tag{13}$$

The resulting values given in table 6 are close to the bulk value of 1.588 but, based on these data, we cannot rule out the possibility of the refractive index of the particle being slightly different from that of the bulk. The range of values obtained for liquid suspensions of the particles extends from 1.577 to 1.594 and is based, respectively, on transmitted light intensity measurements by Smart and Willis [22] and interferometric measurements by Heller and Pugh [23]. In both cases the data analysis is the most straightforward for small particle sizes, and only the small particle size results are given in table 6.

Table 6. Refractive index of polystyrene.

Investigator	n	λ,μm	n(0.6328)[a]
Boundy and Boyer			
bulk value			1.588
Heller and Pugh			
0.132–0.295 μm	1.602±0.008	0.5461	1.594
Smart and Willis			
0.132–0.295 μm	1.581	0.589	1.577
Marx and Mulholland			
D=0.460 μm[b]	1.603±0.029	0.4416	1.579
D=0.600 μm	1.599±0.013	0.4416	1.575
D=0.914 μm	1.612±0.004	0.4416	1.588
D=1.101 μm	1.619±0.002	0.4416	1.595
McRae			
D=0.600 μm[b]	1.63±0.019	0.5145	1.618
D=0.794 μm	1.58±0.008	0.5145	1.569
D=1.011 μm	1.57±0.012	0.5145	1.559
Davis and Ravindran			
D=11.9 and 5.7 μm			1.575
Bottiger, Voss, and Fry			
D=1.112 μm	1.615	0.4416	1.590
Phillips, Wyatt, and Berkman			
D=1.099 μm[b]	1.59±0.001	0.5145	1.578

[a]The refractive index has been extrapolated to λ=0.6328 using the equation $n = A + B/\lambda^2$.

[b]The values of D are the values obtained by Dow Chemical Co. using transmission electron microscopy.

All the other values in the table correspond to light-scattering measurements of single particles levitated in air. We consider Marx and Mulholland's value [14] of 1.588 for the nominal 0.914 μm particles to be the best of the single-particle measurements in regard to SRM 1690, since the measurements were made on the SRM particles and great care was taken with regard to angle calibration and data analysis. The low value obtained by McRae [11] might have resulted from an error in the calibration of the angle encoder. We observed an apparent size-dependence of the refractive index similar to that reported by McRae when our angle calibration was off by about 3°. The measurements of Davis and Ravindran [12] were done on much larger polystyrene spheres (5.7 and 11.9 μm) and the quality of the data appears to be lower than that of the other studies. The poorer data may have resulted from a slight asphericity or inhomogeneity in the particles. We take as our range of uncertainty in refractive index 1.577 to 1.595, which encompasses all the values in table 6 except the values of Davis and Ravindran, McRae, and Marx and Mulholland's value for the 0.600-μm particle size which had a large uncertainty.

To estimate the effect of this uncertainty on D_n, we repeated the data analysis for experiment A3 using the two extreme values of n. The value 1.577 leads to a slightly increased value of D_n, 0.899, while the larger value of 1.595 leads to a slightly reduced mean diameter of 0.893 μm. So the contribution to the uncertainty from this effect, δ_n, equals $\pm$0.003.

The effect of multiple scattering on the results was estimated by performing measurements at two concentrations. According to the criterion established by Napper and Ottewill [24], multiple-scattering effects become insignificant for the ratios of the average distance between particles, l, and the particle diameter, D, greater than 100. For concentrations of 7.0×10^5 and 3.5×10^6 particles/cm^3, we find that l/D is 125 and 70 respectively. From analyzing the light-scattering data for these two cases, we obtain 0.894 μm at the lower concentration and 0.890 μm at the higher concentration. We estimate δ_m as +0.001 μm allowing for a slight residual effect even though the criterion given above is satisfied for the 10 samples analyzed.

The effect of the finite acceptance angle of the photometer was determined by computer simulation in which a slit width integration was performed over the theoretically-predicted intensity pattern for D_n=0.900

and $\sigma_P=0.010$ μm. The "data" were then analyzed by the same procedure with the intensity weighted by $\sin^4(\theta/2)$, and the resulting values of D_n and σ_P were 0.900 and 0.011 μm respectively. So we find δ_θ to be at most 0.0005 μm. If the intensities were analyzed directly without the angular weighting function, the values of D_n and σ_P, 0.899 and 0.015, changed more as a result of the finite acceptance angle than the values obtained using the intensity weighted by the angular function. We also used computer simulation to estimate the error associated with a slight misalignment at zero angle, about 0.07°, and found δ_D to be 0.0004 μm.

Without a beam stop, on the order of 4% of the laser beam is reflected from the glass-air interface back into the cell. This would lead to some fraction of the light reaching the detector having been scattered through the supplement of the scattering angle. We obtain an increase of 0.002 μm size without the beam stop and estimate an error, δ_R, of at most +0.001 μm due to residual reflection.

As discussed in section 5, about 1.5% of the particles is in the form of agglomerated doublets. Bottiger et al. [13], having measured all 16 components of the Mueller matrix for a doublet of 1.112 μm polystyrene spheres, find that the peaks and valleys in the scattering pattern appear at the same angles as for the single sphere but that the amplitudes are smaller. We have no quantitative estimate of this agglomeration error, δ_A, but we intuitively expect it to be less than 0.001 μm.

Estimating the total uncertainty in the same manner as in subsection 2.4, we obtain an expression for U_T shown below together with estimates of the different terms,

$$U_T=R+|\delta_n|+|\delta_m|+|\delta_\theta|+|\delta_D|+|\theta_R|+|\delta_A|.$$
$$0.0005\ 0.003\ 0.001\ 0.0005\ 0.0004\ 0.001\ 0.001$$

Using these estimates, we obtain $U_T=0.007$ μm with a number-average size, D_n, of 0.895 μm. The uncertainty is lower than for the single-particle measurement because of the much smaller random component of error, 0.0005 μm compared to 0.007 μm.

While the average size can be determined quite accurately by scattering from a suspension, this is not the case for the standard deviation of the size distribution, σ_P. Our best estimate of σ_P based on light scattering is 0.029 μm while, as discussed in section 5, the value obtained by electron microscopy is about 0.0095 μm. We suspect that the major cause of the discrepancy is the contribution of scattered light from off-size particles and agglomerated doublets. The off-size particles are excluded from the determination of σ_P by electron microscopy and the doublets are treated as pairs of individual spheres.

4. Optical Array Sizing

Array sizing by optical microscopy provides an independent measure of D_n since the technique is based on geometrical optics rather than diffraction theory. This is one of the oldest techniques for the measurement of average size of micrometer-sized particles. Perrin [25] used this technique in his study of Brownian motion, from which Avogadro's number was first determined. Its ability to produce accurate values for the average diameter results from a combination of a highly accurate length standard for optical microscopy and the fact that monosize polystyrene spheres can form close-packed, two-dimensional hexagonal arrays. The microscopic image of a row of micrometer-size spheres consists of a string of circular images blurred by diffraction as indicated in figure 8; however, the center of the sphere can be pinpointed with considerable accuracy. In fact, when rows of, say, 10 spheres are used, the potential exists for finding the average size of 1 μm spheres to a resolution of about 1% of the sphere diameter. Our methods for preparing the arrays and performing the measurements are similar to those described by Kubitschek [26].

4.1 Formation of Two-Dimensional Arrays

To minimize non-volatile residue, the particles were "washed" with 18-megohm-centimeter deionized water filtered with a 0.2 μm pore size pleated membrane filter. The washing consisted of pouring off the supernatant after allowing the particles to settle and then adding filtered, deionized water. The particle concentration was about 0.5% by mass. A drop of the particle suspension was placed at one end of a microscope slide and smeared out by means of a second slide held such that one of its long edges would wipe slowly over the first slide. The evaporating water sweeps the particles inward though it appears that surface tension is responsible for the small scale motion leading to the ordered array. In the early phase of evaporation, the particles tend to congregate in assemblies similar in shape to ice floes in a freezing ice field. As the evaporation continues, the spheres arrange themselves into well-ordered hexagonal arrays, with rows 10–50 spheres long. This ordering occurrs too rapidly to be observed by eye.

The ordered arrays extending perhaps 7 spheres in one direction and 20 in another are separated by microcracks as seen in figure 9. The cracks occur during the drying when an array field is pulled apart perhaps to relieve a stress on the array. Another type of crack, also illustrated in figure 9, is much shorter and is V-shaped. It seems to indicate intensive drying within an array

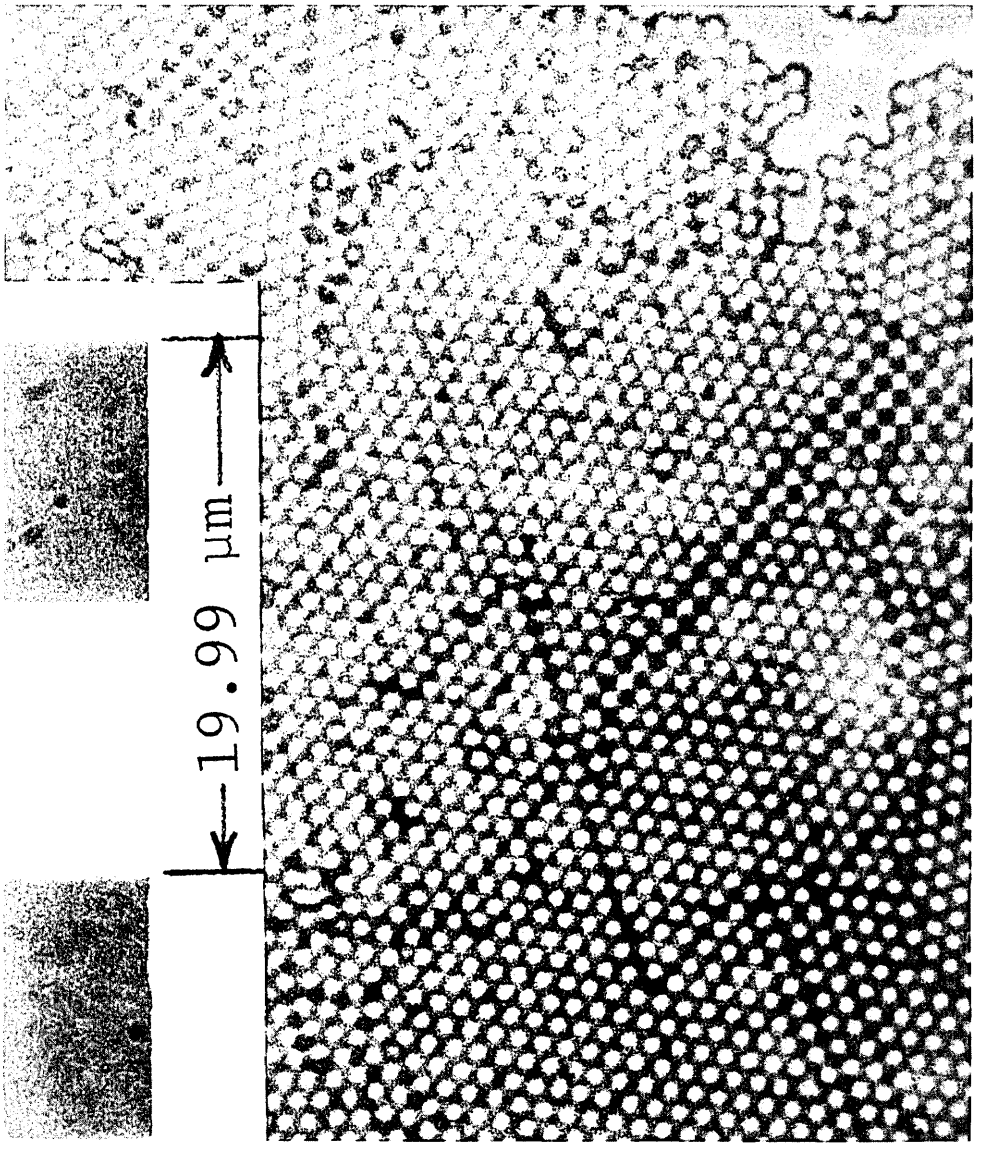

Figure 8–Hexagonal array of nominal one-μm polystyrene spheres (Standard Reference Material 1690).

field. Close inspection shows that such cracks can be detected when they are about 0.05 μm wide, and they are easily visible when the width exceeds 0.1 μm.

4.2 Measurement of Arrays

The arrays were measured by scaled microphotography rather than by microscopy with a graduated eyepiece. Microphotography has the advantage of providing a permanent record from which array defects such as microcracks can be accounted for. The image distortion in the optical train was measured to be less than 0.2%, and scale changes from repeated focusing were 0.1–0.2%. The microscope was a Zeiss Universal[1] with Polaroid attachment and with a 63×, 0.90 N.A. objective.

The micrographs, with a typical scale of 1.6 mm per μm, were measured to 0.05–0.1 mm. The magnification calibration and the image distortion were measured using a 19.990±0.005 μm linewidth spacing on SRM 474 Line Width Standard from NBS.

The arrays were prepared on six microscope slides. One to three arrays were measured on each slide for a total of 12 arrays. For each array, 15 row lengths were measured. The number-average diameter for a single row is determined by dividing the length of the row, L, by the number of spheres in the row minus one, $N-1$.

$$D_r=\frac{L}{N-1} \tag{14}$$

The -1 results from using the center-to-center row length rather than the edge-to-edge row length.

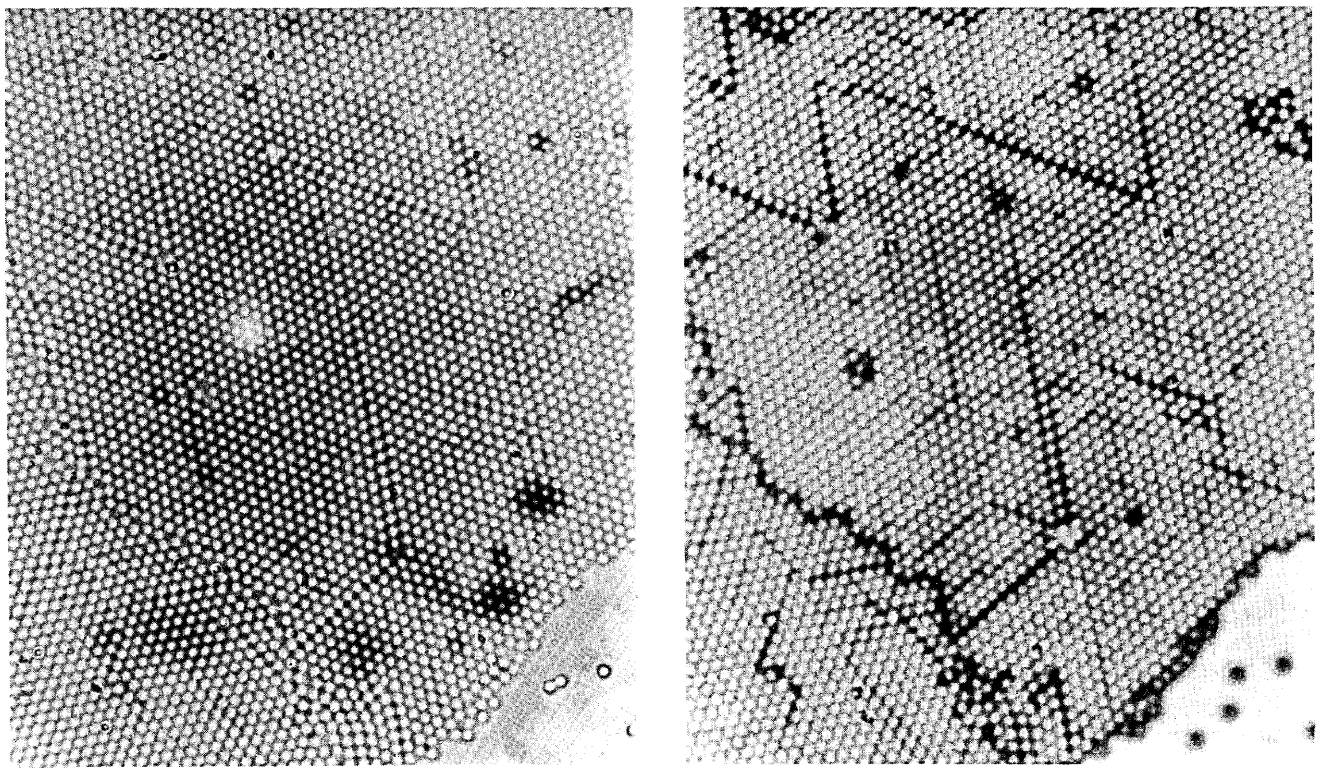

Figure 9–The same field of view is slightly defocussed for the photograph on the right to allow better visualization of the microcracks.

In our measurements the row length varied from 10 to 30 spheres.

4.3 Results

The results for two arrays are shown in table 7. Measurements along each of the three lattice directions are included. In some cases the row lengths in different directions differ by as much as 0.2 mm for an 11-sphere array leading to differences in the average diameter of 0.01 μm. The reason for this anisotropy is not clear. Kubitschek [26] attributes this effect to undetected microcracks. If the cause were a single microcrack, then it would be on the order of 0.1 to 0.2 mm and would thus have been detected. For those arrays located at the periphery of the ordered region, we found that in general the average diameters calculated from rows parallel to the edge were somewhat larger than values calculated from rows in the other two directions, suggesting looseness in that direction. The drying speed of the array also seemed to have some influence.

Table 7. Measured row lengths for two arrays.

Slide No.	Row Length Readings (mm) 0°	120°	240°	Row Average Diameter (μm) 0°	120°	240°	Orientation Average (μm)
3	28.6	29.0	29.15				
	28.8	29.0	29.15				
	28.9	28.0	29.2	0.891	0.901	0.896	0.896
	28.85	28.95	29.1				
	28.9	28.9	29.1				
6	14.55	14.55	14.7				
	14.5	14.55	14.7				
	14.5	14.5	14.7	0.898	0.898	0.908	0.901
	14.5	14.4	14.7				
	14.5	14.55	14.6				

The row-average diameter, $\bar{D}_r$, is obtained as a simple average of the values $D_r(i)$ for the R rows.

$$\bar{D}_r = \frac{\sum_{i=1}^{R} D_r(i)}{R} \tag{15}$$

The standard deviation in D_r, σ_{D_r} is given by

$$\sigma_{D_r} = \frac{\sum_{i=1}^{R} (D_r(i) - \bar{D}_r)^2}{R-1} \tag{16}$$

A summary of the values of $\bar{D}_r$ and σ_{D_r} for each of 12 arrays, which includes 240 rows, is given in table 8. The

Table 8. Array sizing results for SRM 1690.

Slide No.	Array No.	Row Length	No. of Rows	$\bar{D}_r$ μm	σ_{D_r} μm	Anisotropy μm
1	1	20	15	0.905	0.0027	0.001
1	1	20	15	0.909	0.0027	0.006
1	1	20	15	0.906	0.0037	0.003
1	1	20	15	0.905	0.0018	0.002
1	1	20	15	0.904	0.0028	0.002
1	2	15	15	0.895	0.0027	0.005
1	3	15,30	15	0.896	0.0027	0.005
2	4	20	15	0.896	0.0022	0.002
3	5	20	15	0.898	0.0049	0.011
4	6	13	15	0.886	0.0057	0.012
4	7	13	15	0.888	0.0038	0.009
4	8	13	15	0.889	0.0039	0.007
5	9	20	15	0.882	0.0029	0.004
6	10	20	15	0.898	0.0023	0.003
6	11	10	15	0.903	0.0044	0.010
6	12	10	15	0.902	0.0039	0.010
			Average:	D_n=0.898	0.0026	0.006
				σ_{D_n}=0.008		

average of all the values of $\bar{D}_r$ in table 8, defined as D_n, is 0.898 with a standard deviation among the row averages, σ_{D_n}, of 0.008 μm. The anisotropy, defined as the range in the row-averaged diameters in the three lattice directions of an array, is found to have an average value of 0.006 μm. This is comparable in magnitude to σ_{D_n}.

It is also possible to determine the standard deviation of the size distribution, σ_P, from σ_{D_n}. Assuming the spheres to be randomly distributed along a row in terms of particle size, it can be shown that the σ_P is related to σ_{D_r} by the expression,

$$\sigma_P=\sqrt{N-1}\,\sigma_{D_r}, \tag{17}$$

where N is the number of spheres in a row.

In arriving at this result, one makes use of the fact that the variance of the sum of random variables (the row length) is the sum of the variances of the individual random variables (sphere diameter). The resulting value, 0.013 μm, has a statistical uncertainty of about ±0.003 μm and is somewhat larger than the value obtained by electron microscopy, 0.0095 μm.

4.4 Error Analysis

While the experimental technique of optical array sizing is relatively simple compared to light-scattering measurements, there are more potential sources of uncertainty, both random and systematic. The random component of the total uncertainty is related to the standard deviation of the average diameters for the arrays measured, σ_{D_n}. We estimate the magnitude of the various components of the random error including image distortion, readout of microphotographs, local motion in the photographic material, and anisotropy. These are combined and compared with σ_{D_n}. There are also a number of systematic errors arising from the finite width of the size distribution, microcracks, solute impurities, and shape distortion.

Image distortion results in the length scale changing over the photographic field of view. Because of axial symmetry of the optical train, it needs to be measured in relation to one plane containing the optical axis. The Standard Reference Material 474 Line Width Standard was used as a two-line resolution target.

A series of 150 measurements was made, covering five photographs, each with 10 areas and each area being measured three times. The result was a scale factor of 0.619±0.001 μm/mm (− at center, + at edge). Using one scale value for the entire field of view introduces an image distortion error, σ_1, no greater than 0.002 μm.

Row lengths were measured to 0.05–0.1 mm (0.03–0.06 μm) using a film scale. The rows contained 10–20 spheres; thus the error contribution to the average diameter value (1.0 μm nominal) was 0.003 to 0.006 μm. In practice the film readout error, σ_2, was held below 0.005 μm.

It is known that slight motion can occur in photographic materials primarily as a result of uneven drying. In the Polaroid material used here, there was no detectable motion at the 0.05 mm level. The error contribution, σ_3, is thus less than 0.003 μm for 20-sphere rows.

The anisotropy in the array will also manifest itself as a component of the random error, σ_4. We estimate this effect as half the range in the average anisotropy, 0.003 μm.

We obtain a combined estimate of all the sigmas by using the formula

$$\sigma_t^2=\sum_{i=1}^{4}\sigma_i^2. \tag{18}$$

In using this standard formula, we are assuming the errors to be independent. The resulting value of σ_t, 0.007 μm, is comparable to σ_{D_n} so our error budget accounts for the observed value of the random error. The random component of the overall uncertainty based on 16 sets of measurements is found to be 0.0044 μm based on the formula

$$R=t_{15}(0.025)\frac{\sigma_{D_n}}{\sqrt{16}}. \tag{19}$$

It is thought that the mean distance between particle centers in monodisperse arrays, such as those shown in figure 8, is greater than the mean particle diameter be-

cause many smaller particles fail to be in contact with all of their neighbors. Thus, gaps in the array add to the length of a line of particles, causing an overestimate of their true mean diameter. For hexagonal arrays formed from machined washers of known size, Kubitschek [27] found that the overestimate ΔD for particles with standard deviation σ_P was given by

$$\Delta D = 0.46\sigma_P. \tag{20}$$

For our case, σ_P obtained from electron microscopy is 0.0095 μm, so the resulting systematic error, δ_W, is -0.0044 μm. We have chosen to treat this effect as a systematic error rather than correcting for it, because there has been no direct verification of eq (20) for micrometer-size spheres.

A second source of systematic error arises from microcracks. When a row is measured across one or two undetected cracks, one can expect an error contribution to the average diameter of about 0.01 μm for rows 10 spheres long, and less for longer rows. We take as our error estimate, δ_C, a value of -0.005 μm.

The presence of impurities in the polystyrene suspensions is another source of error. Assuming that the emulsifier and inorganic impurities form a uniform coating around the spheres when the water evaporates, one finds the following expression for the thickness, t, of the coating

$$t = \frac{C_1 D}{6C}, \tag{21}$$

where C is the volume concentration of the polystyrene and C_1 the concentration of the non-volatile impurities. For our case the non-volatile impurity concentration was about two orders of magnitude lower than the volume concentration of the polystyrene spheres, and the maximum resulting error is about 0.003 μm.

An attempt was made to detect this effect by using one sample of the stock solution and a different one in which the original solute impurity content had been reduced by an order of magnitude by settling, decanting, and addition of filtered, deionized water. The measured diameter for the second sample was slightly less, by 0.004 ± 0.003 μm. Therefore, all reported measurements were performed on samples with reduced impurity content. We estimate the error resulting from residual non-volatile impurity of washed particles, δ_I, as 0.001 μm.

Two other potential systematic errors include the effect of unequal-size spheres on a flat substrate and the effect of curved rows. If we have a row of spheres of unequal diameters, the centers of the spheres will not be on a straight line and the row length will be less than the sum of the diameters. If the size distribution is not too broad ($\sigma_P/D < 0.03$), the error in the calculated average diameter, $\sigma_P^2/2D^2$, is small (less than 0.001 μm) compared to other errors.

Occasionally arrays will exhibit curved or wavy rows. For typical curvatures, replacing the arc by the chord introduces only a small error (on the order of 0.001 μm) in the measured diameter. However, we found that curved rows are sometimes as much as 1% longer than the corresponding straight rows found in the same array. This suggests the presence of slack in the curved rows, and therefore such rows were omitted from our measurements.

It is possible that spheres in contact flatten slightly. We made an attempt to measure the average size of isolated spheres and arrays of spheres with a transmission electron microscope, but we were not able to prepare arrays on TEM grids. There were instances of particles in contact as in figure 10, and from measuring

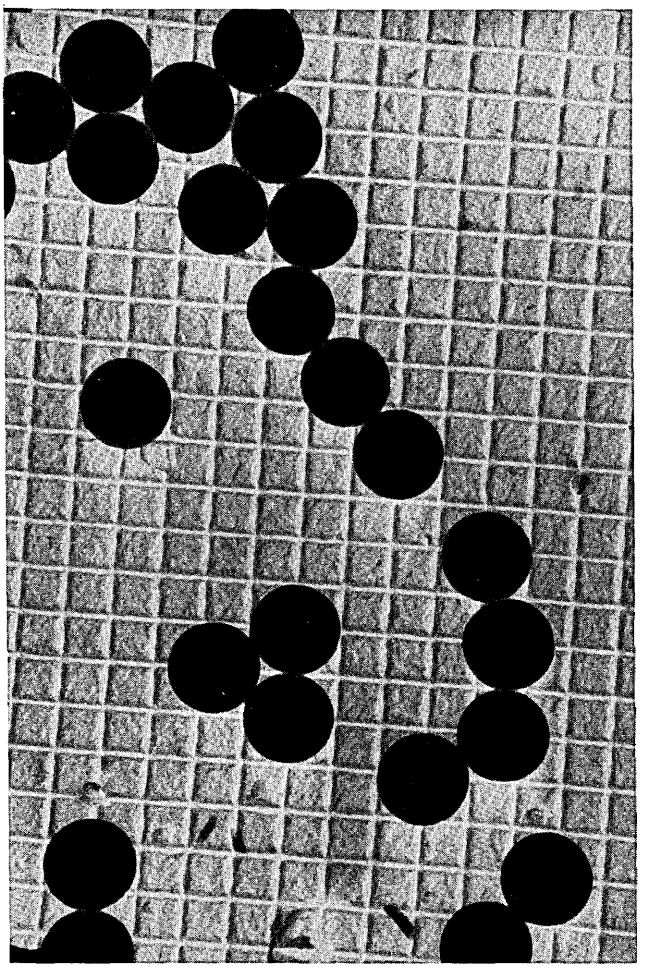

Figure 10–Electron micrograph of nominal one-μm polystyrene spheres (SRM 1690) at a magnification of 10,000×. The spacing for the diffraction grating lines is 0.46 μm.

such particles we found that the flattening effect is less than 0.005 μm. More quantitative measurements are necessary to refine δ_F.

As in the error analyses in the previous sections, we obtain the combined uncertainty from the sum of the random error, R, and the absolute values of the systematic errors,

$$U_T = R + |\delta_W| + |\delta_C| + |\delta_I| + |\delta_F|$$

We obtain a value of 0.020 for U_T with the overall average value for D_n of 0.898 μm.

5. Measurements of Size Distribution/Concentration

We have used transmission electron microscopy, flow-through electrical-sensing zone counter measurements, and optical microscopy to obtain more detailed information about the size distribution. Using these techniques, we measure σ_P, the standard deviation of the size distribution, the fraction of off-size particles, and the fraction of agglomerated doublets. Our only direct measure of number concentration was obtained with electrical sensing zone counter measurements.

5.1 Transmission Electron Microscopy

The sample was prepared for electron microscopy by evaporating a small drop of diluted suspension of the spheres on a diffraction grating replica mounted on a TEM grid. Three grids were prepared from one SRM 1690 vial. The grids were coated with approximately 20 nm of carbon and then examined with a JEOL 200CX electron microscope[1] at an accelerating potential of 100 KV and at a nominal 10,000× magnification. The particle size was measured directly from the negative using a 7× magnifier with an accurate millimeter scale reticule. A series of concentric circles on the reticule enabled quick location of the sphere diameter. A typical micrograph is shown in figure 10.

As mentioned in the introduction, we had hoped to make an accurate determination of the average particle size from the TEM measurements. However, we found significant variability in the commercially available grating replicas in regard to the line spacing even among those from the same supplier. We also found variations as much as 3% in the line spacing in different regions of the same grating. So from our assessment, transmission electron microscopy is not competitive with the light scattering and array sizing measurements for accurate particle size measurement without a suitable calibration artifact.

However, the high resolution of the TEM makes it suitable for the measurement of the standard deviation of the narrow size distribution. The size distribution typically consists of a very sharp central peak plus broadly distributed off-size particles. The inclusion of the off-size particles in the data analysis will greatly broaden the apparent value of σ_P. In one case σ_P changed from 0.031 to 0.011 as a result of removing three off-size particles from a sample of 102 particles. It is, therefore, important to have a systematic procedure for rejecting off-size particles. We used a discordancy test [28] based on the sample kurtosis as the test statistic,

$$\text{sample kurtosis} = \frac{N\sum_{i=1}^{N}(D_i - D_n)^4}{\left(\sum_{i=1}^{N}(D_i - D_n)^2\right)^2}. \quad (22)$$

If the sample kurtosis exceeds a value of about 3.77 for a 100-sphere sample, then one or more spheres are off-size at the 5% level of discordancy. The spheres with diameters farthest from the average size are eliminated consecutively until the sample kurtosis reaches the appropriate value. The particles at the edge of the field of view were eliminated because of evidence of magnification distortion in this region.

Using a common magnification for all the micrographs resulted in a smaller value of σ_P than the value obtained using a magnification for each photograph derived from the line spacing on the diffraction grating replica. The smaller value of σ_P is the better value because experimental errors only tend to increase σ_P. The constancy of the magnification was to be expected, since all the micrographs were taken at one magnification setting over a period of a few hours. We obtained values of 0.0083 μm and 0.0106 μm for σ_P based on samples of 59 and 99 particles. We take the mean value of 0.0095 as our estimate of σ_P.

The major source of uncertainty in σ_P is statistical in origin. The sample variance has a χ^2 distribution, and for a sample size of 100 there is an uncertainty of about ±13% at the 95% confidence level. The size distribution is represented as a histogram in figure 11.

Other information obtained from TEM includes the asphericity of the particles and the fraction of "new" particles. The asphericity, Δ_s, is defined as

$$\Delta_s = \left(\frac{D_{max} - D_{min}}{\bar{D}}\right) \times 100\%. \quad (23)$$

The diameter measurements were made every 45° for particles located near the center of the field of view. The asphericity is small, 0.6%±0.3%, with large uncertainty because of the resolution limit of the TEM.

We found a total of eight particles with diameters less than 0.5 μm out of some 1350 particles (0.6%). As ex-

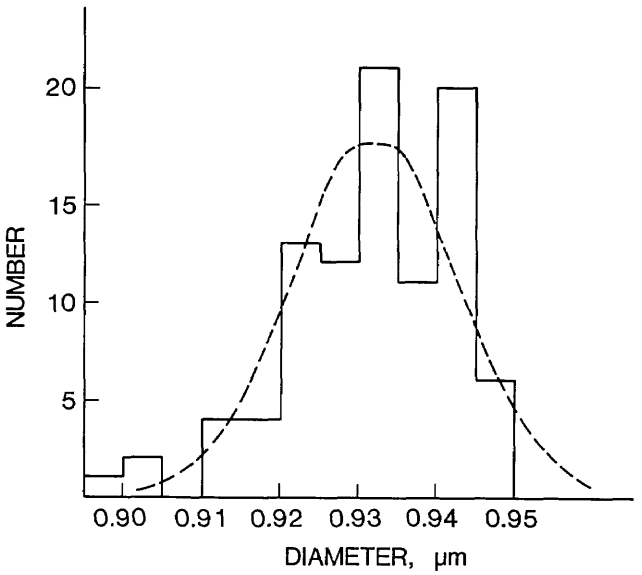

Figure 11–Size distribution of nominal one-μm polystyrene spheres (with off-size particles excluded) obtained by transmission electron microscopy. The dashed curve is the normal distribution with D_n (0.932 μm) and σ_P (0.0106 μm) obtained from the experimental data.

plained in the Appendix, it is possible to nucleate a new population of particles in the process of using seed particles to produce larger particles. We believe that this nucleation process is responsible for the small off-size spheres.

5.2 Electrical Sensing Zone–Counter Measurements

We used the Coulter ZB Counter with Coulter Channelyzer Pulse Sizer[1] to measure the fraction of doublets, the fraction of large off-size particles, and the number concentration, and to estimate the variability of D_n in the SRM 1690 samples. To apply this technique, the particles must be prepared in an electrolyte solution at a concentration of about 1% by mass. The technique consists of measuring the electrical current due to the electrolyte flowing through an orifice; in our case, 30- and 19-μm diameter orifices were used. As a particle flows through the orifice, the current is reduced by an amount approximately proportional to the volume of the particle [29].

For our application, we used nominal 0.9- and 2-μm size polystyrene spheres for a particle size calibration of the instrument, and then used the Coulter Counter to measure the concentration and size distribution. The Coulter Counter is not an absolute sizing instrument.

It was found that if the polystyrene spheres were directly diluted with electrolyte, then about 10% agglomerated doublets resulted from the combined effects of high particle concentration and the reduction in electrostatic repulsion between the particles. The agglomerated doublets were minimized by first diluting with filtered, deionized water (dilution factor 2.5×10^3) and then diluting by another factor of 10 with the electrolyte solution. The percentage of doublets was found to be $1.5\pm0.4\%$ of the total population for fresh samples, compared to about 1% obtained by visual microscopy of the suspended particles diluted without electrolyte. Based on the limited sample size, there does not appear to be any significant difference in the fraction of doublets between the sample diluted without electrolyte and the fresh samples diluted with electrolyte at the last step.

By changing the electronic settings of the Coulter Counter, it was possible to estimate the percentage of large single particles with diameters in the range of 2–6 μm. The observed count was on the order of 200 out of a total population of about 235,000 particles, which corresponds to slightly less than 0.1%.

Based on the measured number-concentration of two diluted samples for particles in the 0.6 to 1.4 μm size range, we obtain number concentrations of the undiluted samples of 1.18 and 1.45×10^{10} particles/cm^3. These values agree well with a calculated value of 1.25×10^{10} particles/cm^3 based on a concentration of 0.5% by mass of the polystyrene spheres, a particle density of 1.052 g/cm^3, and a particle size of 0.9 μm.

Diluted samples were prepared from each of 10 SRM vials and two portions of each sample were sized with the Coulter Counter using the 30-μm-diameter orifice. A typical size distribution based on sizing about 85,000 particles is given in figure 12. A complete listing of the

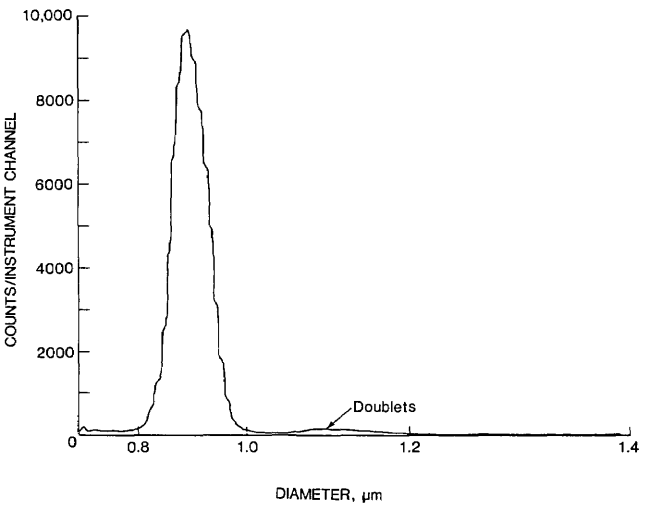

Figure 12–Size distribution of SRM 1690 obtained by a Coulter Counter for aperture current, amplification, and lower threshold settings of 1/3, 1/2, and 100 respectively. The instrument output is linear with respect to particle volume and consequently appears stretched when plotted versus particle diameter.

average particle size, D_n, and the standard deviation of the central peak are given for each sample in table 9. The standard deviation associated with 10 independent determinations of D_n has a value of 0.0027 μm. This value is approximately three times greater than the value obtained by light scattering and is due to instrumental noise rather than sample-to-sample variability. Even when measurements are made on the same sample such as F1 to F4, variations in D_n as large as 0.005 μm are observed.

Table 9. D_n and σ_P for Coulter Counter measurements of SRM 1690.

	Portion 1		Portion 2	
Sample	D_n, μm	σ_P, μm	D_n, μm	σ_P, μm
A	0.9226	0.0370	0.9239	0.0336
B	0.9225	0.0380	0.9240	0.0344
C	0.9266	0.0351	0.9286	0.0349
D	0.9226	0.0336	0.9240	0.0339
E	0.9264	0.0351	0.9251	0.0357
F1[a]	0.9308	0.0392	0.9302	0.0332
F2			0.9251	0.0329
F3			0.9246	0.0326
F4			0.9245	0.0325
G	0.9245	0.0328	0.9247	0.0356
H	0.9231	0.0333	0.9222	0.0338
I	0.9223	0.0338	0.9236	0.0340
J	0.9226	0.0323	0.9228	0.0311

[a]The numerals refer to repeat measurements of the same sample.

The average value of the standard deviation of the size distribution, 0.033 μm, for the central peak based on Coulter Counter measurements is more than a factor of three greater than the value obtained by electron microscopy. The primary cause of this broadening is the variation in the electrical pulse resulting from different particle trajectories through the orifice. The amplitude-time history of the electrical pulse for a particle moving near the aperture wall is different from that of a particle moving near the centerline. Thom [30] demonstrated this effect on a model system with plastic washers and Spielman and Goren [31] demonstrated that the resolution of the Coulter Counter could be improved by hydrodynamically focusing the particles through the center of the orifice. The Coulter Counter we used did not have hydrodynamic focusing, but it did have a pulse analyzer for rejecting counts in part due to particles with atypical trajectories.

6. Summary

The values of D_n and the associated uncertainty for three techniques are: 0.895±0.007 μm for light scattering from particles suspended in water, 0.900±0.012 μm for single-particle light-scattering measurements, and 0.898±0.020 μm for optical array sizing. For each technique there is a consistency test in addition to a quantitative error analysis. For the single-particle light-scattering measurements, the particle diameter obtained for the incident light polarized in the vertical direction (0.903 μm) agreed well with the diameter obtained for light polarized in the horizontal direction (0.898 μm). For light scattering from a particle suspension, the particle diameter obtained with two different laser sources, He-Ne (0.633 μm) and He-Cd (0.442 μm) differed by only 0.001 μm. In the case of array sizing, six independent samples were prepared and the variation in the average particle diameter, 0.882 to 0.903 μm, was less than the overall uncertainty.

We use 0.895 μm as the certified value because of the lower uncertainty associated with light scattering from a suspension. Another advantage of this value is that the measurements characterize the particles in the same form as provided in the SRM 1690, this is, in suspension rather than as a dried sample where there is the possibility of a coating of non-volatile impurities on the surface. It is reassuring that the variability among the three values of D_n is less than the uncertainty associated with any one technique. We expect that our estimates of uncertainty are, if anything, conservative. The value obtained by Dow Chemical Co. for D_n by TEM, 0.914 μm, is about 2% greater than our certified value.

In table 10 we summarize all the information regarding the size distribution obtained by our measurements. Only for D_n and the index of refraction have detailed error analyses been made. The different features of the global size distribution extending from 0.1 to 6 μm are indicated qualitatively in figure 13.

A wide range of values is found for the standard deviation of the size distribution, σ_P, extending from

Table 10. Summary of results for SRM 1690.

D_n,μm	0.895±0.007[a] light scat. from suspension (LSS) 0.900±0.012 single part. scattering (SPS) 0.898±0.020 opt. array sizing (OAS)	
σ_P,μm	0.0095±0.002 TEM, 0.010 SPS, 0.013 OAS, 0.029 LSS, 0.033 Coulter Counter	
% doublets	1.5±0.4	Coulter Counter
% large off-size particles	0.1	Coulter Counter
% "new" particles	0.6±0.2	TEM
% asphericity	0.6±0.3	TEM
number concentration	$1.3\pm0.2\times10^{10}$ part/cm^3	Coulter
index of refraction	1.612±0.009	single particle scattering
sample variability	0.0005 μm	light scat. from suspension
	0.0009 μm	Coulter Counter

[a]The first value in each case is the best estimate.

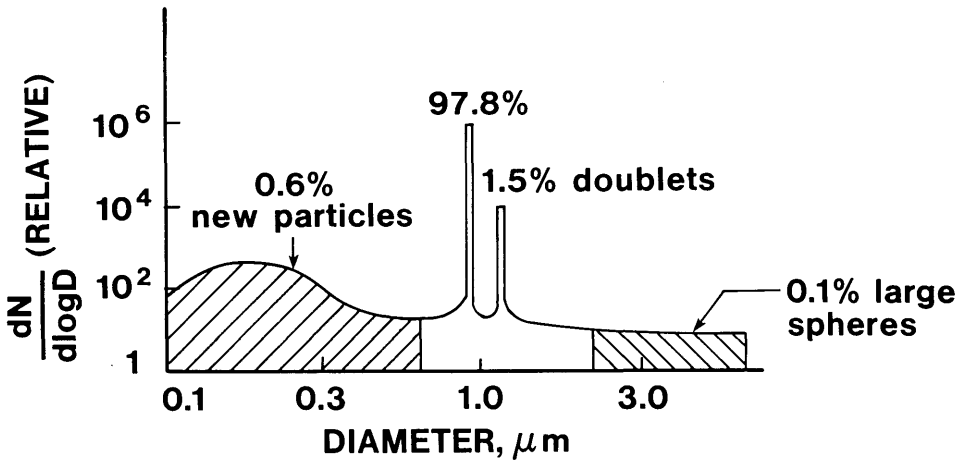

Figure 13–Global size distribution.

0.0095 μm to 0.033 μm. This is because each instrument has a sigma associated with repeat measurements of the same objects, σ_r, and measured values of σ_P given in table 10 represent a combined effect of the σ of the true size distribution and σ_r. The single-particle scattering measurement has the smallest σ_r, 0.002 μm, but the statistical uncertainty due to the small number of particles measured (eight) limits the accuracy of σ_P. The best estimate of σ comes from TEM with a slightly larger σ_r, about 0.003–0.004 μm, compared to the single particle measurements, but this is offset by the improved statistics from a much larger sample size (100). The large values of σ_r for the other instruments result from the dependence of the electrical pulse on the particle trajectory through the orifice for the Coulter Counter, the presence of doublets and off-size particles for light-scattering measurements of a particle suspension, and array nonuniformities for the case of optical array sizing.

Each measurement method requires a slightly different sample preparation. A necessity in almost all cases is particle free water for dilution. We found 18 megohm-cm deionized water passed through a 0.2 μm pore size filter to be adequate for our measurements. Clean glassware is a necessity for diluting the samples and a clean optical cell free of water marks is required to obtain good light scattering data. As described in section 3, we used both detergent and hot, concentrated nitric acid for cleaning our glassware. In the case of diluting a sample, especially if an electrolyte is used, there is always the possibility of promoting agglomeration through the reduction in the electrostatic repulsion between the particles. We found that even for a 1% by weight solution of sodium chloride little agglomeration occurred in an hour for a particle concentration of about 10^6 part/cm^3 if the electrolyte were introduced only at the final dilution stage as described in subsection 5.2.

7. Concluding Remarks

Our measurements have resulted in a particle size standard with an uncertainty in particle diameter of about 0.8%. Modest improvements in sizing accuracy, say a twofold reduction in uncertainty, may be possible with the existing techniques. About half the total uncertainty in the scattering measurements for suspensions is associated with the uncertainty in the refractive index. The refractive index of liquids is known to an uncertainty of a few parts in 10^5, while the uncertainty in the refractive index of the polystyrene spheres is a few parts in 10^3. It is possible that at least a tenfold reduction in the uncertainty in the refractive index of the spheres could be achieved by index matching the spheres with a liquid. A second improvement would be to remove the agglomerated doublets by sedimentation before performing the scattering measurements.

An accurate value of the refractive index of the polystyrene spheres would also improve the sizing capabilities of single particle scattering measurements since there would be only one unknown parameter, the particle diameter, to be determined from the scattering measurements. We have found that the sizing resolution improves by a factor of two to three if the refractive index is fixed when performing the data analysis. The single greatest source of uncertainty arises from the small number of particles sized (eight); this component of the error could be cut in half if 40 particles were sized.

Half of the uncertainty for optical array sizing results from smaller particles not touching neighboring particles and from slight flattening of the spheres on contact. Hartman [32] has demonstrated that it is possible to make square arrays of particles, where, unlike in hexagonal arrays, every particle is in contact with its neighbors. A systematic analysis of such arrays is possible but would be time-consuming because of the rela-

tively rare occurrence of square arrays. A quantitative analysis of flattening could be made by transmission electron microscopy if arrays could be prepared on TEM grids.

Major improvements in sizing accuracy, say a tenfold reduction in uncertainty, will require a more detailed characterization of the particle structure. Specific structural information of interest includes particle shape, especially in regard to deviation from sphericity, particle inhomogeneity in regard to a variable index of refraction within the particle, and the surface structure both for particles in suspension where an electrical double layer exists and in aerosol form where nonvolatile impurities coat the surface. The pertinent structural information must also be included in the light scattering theory for determining particle size from scattering intensity as a function of angle. Of course, if particles could be made with a high degree of sphericity and low inhomogeneity within the particle, the analysis would be simplified.

Ultimately it is planned to develop particle size standards over the diameter range of 0.1 to 100 μm. For such a wide range, a variety of techniques will be used. One promising instrument for larger particle sizes involves optical interferometry coupled to an electron microscope. One of us (G.G. Hembree) has developed such an instrument with a piezoelectric stage, the displacement of which is monitored interferometrically with an uncertainty on the order of 0.02 μm. Another technique for larger particles consists of the measurement of resonances in the polarization ratio of scattered light. Lettieri et al. [33] measured the diameter of droplets in the size range 6 to 12 μm to a resolution of 0.003 μm using this technique.

Work is currently in progress to develop a nominal 0.3 μm particle size standard. In this case, quasielastic scattering is being used in conjunction with transmission electron microscopy with the magnification calibration based on the 0.895 μm spheres (SRM 1690).

References

[1] Swyt, D. A. A look at techniques for the dimensional calibration of standard microscopic particles. Natl. Bur. Stand. (U.S.) Spec. Publ. 260-85 (1983).

[2] Phillips, D. T.; P. J. Wyatt and R. M. Berkman. Measurement of the Lorenz-Mie scattering of a single particle: polystyrene latex. J. Colloid Interface Sci. **34**: 159 (1970).

[3] Rowell, R. L.; R. S. Larinato, J. W. Parsons, J. R. Ford, K. H. Langley, J. R. Stone, T. R. Marshall, C. S. Parmenter, M. Seaver and E. B. Bradford. Polystyrene latex particle size by electron microscopy and light scattering. J. Colloid Interface Sci. **69**(3): 595-595 (1979).

[4] Bierhuizen, H. W. J., and G. A. Ferron. Determination of the diameter of two monodisperse lattices by the free fall method and the length of particle arrays. J. Aerosol Sci. **6**: 19-21 (1975).

[5] Gulari, Es.; Er. Gulari, Y. Tsunashima, and B. Chu. Photon correlation spectroscopy of particle distributions. J. Chem. Phys. **70**: 3965-3972 (1979).

[6] Bonse, J., and M. Hart. Small angle x-ray scattering by spherical particles of polystyrene and polyvinyltoluene. J. Phys. **189**: 151 (1966).

[7] Davidson, J. A.; C. W. Macosko and E. A. Collins. Latex particle size analysis I. flow microscopy. J. Colloid Interface Sci. **25**: 381-388 (1967).

[8] van den Hul, H. J., and J. W. Vanderhoff. "Clean" monodisperse latexes as model colloids, chapter 1 in Polymer Colloids. R. M. Fitch, ed. New York, NY: Plenum Press (1971) pp. 1-27.

[9] Wyatt, P. J., and D. T. Phillips. A new instrument for the study of individual aerosol particles. J. Colloid Interface Sci. **39**(1): 125-135 (1972).

[10] Cooke, D. D., and M. Kerker. Particle size distribution of colloidal suspensions by light scattering based upon single particle counts—polystyrene latex. J. Colloid Interface Sci. **42**(1): 150-155 (1973).

[11] McRae, D. D. The refractive index of individual cigarette smoke droplets. J. Colloid Interface Sci. **87**: 117-123 (1982).

[12] Davis, E. J., and P. Ravindran. Single particle light scattering measurements using the electrodynamic balance. Aerosol Sci. and Tech. **1**: 337-350 (1982).

[13] Bottiger, J. R.; E. S. Fry and R. C. Thompson. Phase matrix measurements for electromagnetic scattering by sphere aggregates in light scattering by irregularly shaped particles. D. W. Shuerman, ed: New York: Plenum Press (1980) pp. 280-290.

[14] Marx, E., and G. W. Mulholland. Size and refractive index determination of single polystyrene spheres. J. Res. Natl. Bur. Stand. (U.S.) **88**: 321-338 (1983).

[15] Mie, G. A contribution to the optics of turbid media, especially colloidal metallic suspensions. Ann. Physik **25**: 337-445 (1908).

[16] Born, M., and E. Wolf. Principles of optics. Oxford: Pergamon Press (1980).

[17] Kerker, M. The scattering of light and other electromagnetic radiation. New York: Academic Press (1969).

[18] Wims, A. M., and M. E. Myers, Jr. An automated, laser light-scattering photometer (0.1 to 170° range) with a single photon counting system. J. Colloid Interface Sci. **39**(3): 447-461 (1972).

[19] Matheson, L. A., and J. L. Saunderson. Optical and electrical properties of polystyrene, chapter 11 in Styrene: its polymers, copolymers, and derivatives, R. H. Boundy and R. F. Boyer, ed. New York, NY: Reinhold Publishing Corp. (1952) 524.

[20] Tilton, T. W., and J. K. Taylor. Refractive index and dispersion of distilled water for visible radiation of temperatures 0 to 60° C. J. Res. Natl. Bur. Stand. (U.S.) **20**: 419 (1938).

[21] Starkie, D. Brit. Plastics **19**: 46 (1946).

[22] Smart, C. and E. Willis. Determination of refractive indices of polystyrene latices by light scattering. J. Colloid Interface Sci. **25**: 577-583 (1967).

[23] Heller, W. and T. L. Pugh. Experimental investigations on the effect of light scattering upon the refractive index of colloidal paticles. J. Colloid Interface Sci. **12**: 299-307 (1957).

[24] Napper, D. H., and R. H. Ottewill. Multiple scattering effects in polystyrene latex dispersions. J. Colloid Interface Sci. **19**: 72-80 (1964).

[25] Perrin, M. J. Brownian movement and molecular reality, An-

nales de Chimie et de Physique, 8me series, (1909) translated by F. Soddy. London: Taylor and Francis (1910).
[26] Kubitschek, H. E. Array method of sizing monodisperse particles, in Ultrafine particles, W. E. Kuhn, ed. Wiley (1961) p. 438.
[27] Kubitschek, H. E. Optical calibration of some monodisperse polystyrene latexes in arrays. Nature **192**: 1148–1150 (1961).
[28] Barnett, V., and T. Lewis. Outliers in statistical data. New York: Wiley (1978) p. 101.
[29] Allen, T. Particle Size measurements. London: Chapman and Hall (1975).
[30] Thom, von R. Vergleichende untersuchungen zur elecktronischen zillvolumen-analyse, AEG-Telefunken report, Ulm, Germany, (around 1970).
[31] Spielman, L. and S. L. Goren. Improving resolution in Coulter counting by hydrodynamic focusing. J. Colloid Interface Sci. **26**: 175–182 (1968).
[32] Hartman, A. W. Experimental confirmation of the Kubitschek effect, Journal of Powder Technology, in press.
[33] Lettieri, T. R.; W. D. Jenkins and D. A. Swyt. Sizing of individual optically levitated evaporating droplets by measurement of resonances in the polarization ratio. Appl. Opt. **20**: 2799–2805 (1981).
[34] Blackley, D. C. Emulsion polymerisation theory and practice. New York: Wiley (1975).
[35] Verwey, E. J. W., and J. Th. G. Overbeek. Theory of stability of lyophobic colloids. New York: Elsevier (1948).

APPENDIX
Preparation and Stability of Polystyrene Sphere Suspensions

Preparation—The procedure used by Dow Chemical Co. to produce monosize polystyrene spheres is known as emulsion polymerization. A brief description of the general process is provided here, though the specific emulsifying agent and chemical initiator used by Dow are confidential. A more detailed description of emulsion polymerization is given by Blackley [34].

Emulsion polymerization involves four components: water, styrene monomer, an emulsifying agent, and a free radical initiator. A typical emulsifying agent is sodium lauryl sulfate. The emulsifier will permit the dispersion of the stirred monomer phase into a stable system of micrometer-size droplets. At a sufficiently high concentration of emulsifier, hydrated aggregates called micelles, made up of 50 to 100 molecules of emulsifier, will form. The concentration of micelles is approximately six orders of magnitude greater than that of the monomer droplets.

The polymerization reaction begins when the free radical initiator is heated to sufficiently high temperature to dissociate into radical ions. This is around 50 °C for persulfate anions. The sulfate radical anions attack the styrene dissolved in the aqueous phase to form new ion radicals. The polymer chain begins growing by the addition of more styrene molecules to the radicals in the aqueous phase. The polymer-containing radicals soon enter the micelles where propagation of the chain is continued by attack on the monomer within the micelle. The growth of the polymer chain is supported by the rapid diffusion of the styrene from the droplets into the growing micelles. This growth is terminated by reaction with a second free radical. At this point the chain polymer may have reached a molecular weight on the order of 10^6. Later the chain growth is reinitiated by another radical, and this process will continue until most of the styrene is consumed.

While the polymer growth is a chain process, the intermolecular forces and surface tension lead to a spherical shape analogous to a ball of string. The narrowness of the size distribution results from the uniformity of styrene concentration throughout the reactor and the growth time being long compared to the initiation time. The concentration of the initiator and emulsifier are also important for obtaining a narrow size distribution. Too much emulsifier can lead to new particle formation. This is especially true when small polystyrene spheres are used as seed particles for growing larger ones. The growth of 1-μm-diameter spheres for SRM 1690 required the use of seed particles, and there was evidence of a new generation of small particles.

Stability—The electrostatic charge on the surface of the particles, created by the outward pointing ionic endgroups, is crucial to the stability of the suspension. Changes in the surface layer can lead to agglomeration of the spheres. Dilution and the addition of electrolyte, required for some of the measurement techniques, can affect the stability of the suspension. The Verwey-Overbeek theory [35] describes the stability of colloidal suspensions in terms of the electrostatic forces of repulsion between colloidal particles and London-van der Waals forces of attraction. The electrostatic repulsion arises from the surface charge; for example, from the adsorbed emulsifier ions. The repulsion is greatest at the point of contact between the electrical double layers on the two particles. This is on the order of a nanometer from the polymeric surface, since the ionic portion of

the emulsifier is directed away from the sphere. At greater distances between the particles' centers, the repulsion drops off exponentially. The magnitude of the repulsion depends on the surface particle charge and electrolyte concentration. The London-van der Waals forces are greatest close to the particle surface (a few tenths of a nanometer from the polymeric surface) and are not strongly affected by the surface charge of electrolyte concentration. Of course, there are very strong repulsive forces as the polymeric molecules of two spheres come in contact.

The sum of these three forces leads to a potential with a minimum at short distances, a repulsive barrier due to electrostatic repulsion at greater distances, and possibly a second minimum at relatively large distances, resulting from the longer range of the London-van der Waals forces. If the particle has sufficient energy to penetrate the electrostatic barrier of another particle, the two particles will stay together in an aggregate. An increase in the electrolyte concentration or a decrease in the surface charge density caused by diluting the suspension with electrolyte will lower the repulsive barrier and may lead to agglomeration. Such an effect was a concern in the electrical-sensing zone counter measurments as discussed in subsection 5.2, since the particle suspension was diluted with electrolyte.

Journal of Research of the National Bureau of Standards
Volume 90, Number 1, January-February 1985

Stable Law Densities and Linear Relaxation Phenomena

Menachem Dishon
National Bureau of Standards, Gaithersburg, MD 20899

George H. Weiss
National Institutes of Health, Bethesda, MD 20205

and

John T. Bendler
General Electric Corporate Research & Development, Schenectady, NY 12301

Accepted: November 27, 1984

Stable law distributions occur in the description of the linear dielectric behavior of polymers, the motion of carriers in semi-conductors, the statistical behavior of neurons, and many other phenomena. No accurate tables of these distributions or algorithms for estimating the parameters in these relaxation models exist. In this paper we present tables of the functions

$$Q_\alpha(z)=\frac{1}{\pi}\int_0^\infty e^{-u^\alpha}\cos(zu)du$$

$$V_\alpha(z)=\frac{1}{\pi}\int_0^\infty e^{-u^\alpha}\sin(zu)du$$

together with related functional properties of $zQ_\alpha(z)$. These are useful in the estimation of the parameters in relaxation models for polymers and related materials. Values of the integral $Q_\alpha(z)$ are given for $\alpha=0.01$, 0.02(0.02)0.1(0.1)1.0(0.2)2.0 and those of $V_\alpha(z)$ are given for $\alpha=0.0(0.01)0.1(0.1)2.0$. A variety of methods was used to obtain six place accuracy. The tables can be used to sequentially estimate the three parameters appearing in the Williams-Watts model of relaxation. An illustration of this method applied to data in the literature is given.

1. Introduction

Stable law distributions and functionals of these distributions play an important role in a variety of scientific areas. They originated in a study of observation errors by Cauchy [1][1], and many of their mathematical properties were elucidated by Lévy [2], and Khintchine and Lévy [3]. Applications of stable laws have appeared in the context of models for the broadening of spectral lines [4], fluctuations in stock market prices [5], statistical properties of neuronal activity [6], the motion of carriers through amorphous semiconductors [7], as well as in a variety of chemical physics problems [8]. Integrals of stable law densities have appeared in still another area of application: the theory of mechanical and electrical relaxation processes. The suggestion that relaxation processes in some electrical and mechanical systems could be described in terms of stable distributions can be traced back to experiments by Weber [9,10] and the Kohlrausches, father [11] and son [12]. Considerable recent interest in relaxation processes describable

About the Authors: Menachem Dishon, an applied mathematician, served as a guest worker in NBS' Scientific Computing Division. He has returned to his post as acting chief scientist, Ministry of Defense, Hakirya, Tel-Aviv, Israel. George H. Weiss is an applied mathematician and John T. Bendler is a physicist.

[1]Bracketed figures indicate literature references.

in terms of stable laws has been inspired by experiments performed by Williams and Watts on polymers [13,14]. Many other examples of such applications to polymers and glasses occur in the literature, cf., for example, the work of Moynihan, Boesch, and Laberge [15] and Bendler [16]. The marriage between the mathematics of stable processes and the theory of dielectric relaxation processes has recently been proposed by Schlesinger and Montroll [17] who used the methodology of continuous time random walks [18] to try to model the underlying physical processes.

The relaxation of linear systems can be characterized by a frequency dependent dielectric constant or the appropriate mechanical analogue. This constant is generally expressible as

$$\frac{\epsilon(\omega)-\epsilon(\infty)}{\epsilon(0)-\epsilon(\infty)}=\epsilon_n'(\omega)-i\epsilon_n''(\omega)=-\int_0^\infty e^{-i\omega t}\frac{d\varphi}{dt}\,dt \quad (1)$$

where $\phi(t)$ is the relaxation function which characterizes the particular material properties and $\epsilon_n'(\omega)$ and $\epsilon_n''(\omega)$ are the components of the normalized dielectric constant. It is found that for many polymers and glasses $\phi(t)$ can, to a good approximation, be chosen to have the form

$$\phi(t)=\exp[-(t/\tau)^\alpha] \quad (2)$$

where τ and α are constants that depend on the material. Data on polymers and glasses generally lead to α values in the range 0.2 to 0.8. Equations (1) and (2) together imply that, for $z=\omega\tau$,

$$\epsilon_n'(\omega)=1-z\int_0^\infty e^{-u^\alpha}\sin(zu)du=1-\pi z V_\alpha(z)$$

$$\epsilon_n''(\omega)=z\int_0^\infty e^{-u^\alpha}\cos(zu)du=\pi z Q_\alpha(z) \quad (3)$$

where $Q_\alpha(z)$ and $V_\alpha(z)$ are the standard integrals

$$Q_\alpha(z)=\frac{1}{\pi}\int_0^\infty e^{-u^\alpha}\cos(zu)du$$

$$V_\alpha(z)=\frac{1}{\pi}\int_0^\infty e^{-u^\alpha}\sin(zu)du. \quad (4)$$

The function $Q_\alpha(z)$ can be identified as a representation of a stable law density. In a recent paper Montroll and Bendler have presented a number of approximations to the function $Q_\alpha(z)$ for values of α useful for polymer applications [19]. Because $Q_\alpha(z)$ can be identified with a stable density they were able to check their results against Holt and Crow's tables [20] for $\alpha=1/4$, 1/2, and 3/4. However, these tables are given to four places in fixed arithmetic. The variety of methods used in generating the tables has resulted in a lack of uniform accuracy.

Because of the wide range of applications of the functions $Q_\alpha(z)$ and $V_\alpha(z)$, and because there appear to be no accurate tabulations against which approximations can be checked, we present here tables of these functions for $\alpha=0.01,0.02(0.02)0.1(0.1)1.0(0.2)2.0$ for $Q_\alpha(z)$, and for $\alpha=0.0(0.01)0.1(0.1)2.0$ for $V_\alpha(z)$, accurate to six places in floating point.

2. Numerical Methods

Three methods were used to evaluate $Q_\alpha(z)$ and $V_\alpha(z)$ to 10 significant figures, which were truncated and rounded to six figures for the present tables. The first is the evaluation of a convergent series representation, the second is the evaluation of a divergent series, and the third is numerical integration in the region in which the divergent series does not yield the required accuracy at all, and the convergent series requires use of an unreasonably large number of terms. For $Q_\alpha(z)$ the following series converges for $0<\alpha<1$

$$Q_\alpha(z)=\frac{1}{\pi}\sum_{n=1}^\infty(-1)^{n+1}\frac{\Gamma(1+n\alpha)}{n!z^{1+n\alpha}}\sin\left(\frac{\pi n\alpha}{2}\right). \quad (5)$$

This series diverges when $1<\alpha<2$, but it is an asymptotic series, [21,22], and can be profitably used in this range for computation at sufficiently large values of z. The corresponding series that converges in $1<\alpha<2$, but diverges when $0<\alpha<1$, is

$$Q_\alpha(z)=\frac{1}{\pi\alpha}\sum_{n=1}^\infty(-1)^{n+1}\frac{\Gamma\left(\frac{2n-1}{\alpha}\right)}{(2n-2)!}z^{2(n-1)}. \quad (6)$$

Similar series can be derived for $V_\alpha(z)$. These are

$$V_\alpha(z)=\frac{1}{\pi}\sum_{n=0}^\infty(-1)^n\frac{\Gamma(1+n\alpha)}{n!z^{1+n\alpha}}\cos\left(\frac{\pi n\alpha}{2}\right) \quad (7)$$

which converges for $0<\alpha<1$ and diverges when $1<\alpha<2$, and

$$V_\alpha(z)=\frac{1}{\pi\alpha}\sum_{n=1}^\infty(-1)^{n+1}\frac{\Gamma\left(\frac{2n}{\alpha}\right)}{(2n-1)!}z^{2n-1} \quad (8)$$

which diverges in $0<\alpha<1$ and coverges in $1<\alpha<2$. When the appropriate series from eqs (5-8) requires a large number of terms to provide accurate results it is convenient to make the substitution $u=\tan\theta$ in eq (4) to find the following integral representations:

$$Q_\alpha(z)=\frac{1}{\pi}\int_0^{\pi/2} e^{-\tan^\alpha\theta}\cos(z\tan\theta)\frac{d\theta}{\cos^2\theta} \tag{9}$$

$$V_\alpha(z)=\frac{1}{\pi}\int_0^{\pi/2} e^{-\tan^\alpha\theta}\sin(z\tan\theta)\frac{d\theta}{\cos^2\theta}$$

which may be evaluated numerically.

Checks on the numerical calculations can be made for a few values of α for which both $Q_\alpha(z)$ and $V_\alpha(z)$ can be expressed in terms of known functions. For $\alpha=1/2$ one finds

$$Q_{1/2}(z)=2\pi\rho^3\left\{\left[\tfrac{1}{2}-C(\rho)\right]\cos\left(\frac{\pi\rho^2}{2}\right)+\left[\tfrac{1}{2}-S(\rho)\right]\sin\left(\frac{\pi\rho^2}{2}\right)\right\} \tag{10}$$

where

$$\rho=(2\pi z)^{-1/2}$$

$$C(\rho)=\int_0^\rho\cos\left(\frac{\pi t^2}{2}\right)dt,\quad S(\rho)=\int_0^\rho\sin\left(\frac{\pi t^2}{2}\right)dt \tag{11}$$

in terms of Fresnel integrals. The conjugate function, $V_{1/2}(z)$, can also be written in terms of ρ as

$$V_{1/2}(z)=2\rho^2\left[1-\pi\rho\left\{\left[\tfrac{1}{2}-S(\rho)\right]\cos\left(\frac{\pi\rho^2}{2}\right)-\left[\tfrac{1}{2}-C(\rho)\right]\sin\left(\frac{\pi\rho^2}{2}\right)\right\}\right]. \tag{12}$$

The functions in curly brackets in the expressions for $Q_{1/2}(z)$ and $V_{1/2}(z)$ are tabulated in Abramowitz and Stegun [23]. One can also verify the following special cases:

$$Q_1(z)=\frac{1}{\pi(1+z^2)},\quad V_1(z)=zQ_1(z)$$

$$Q_2(z)=(4\pi)^{-1/2}\exp(-z^2/4),$$

$$V_2(z)=\pi^{-1}\exp(-z^2/4)\int_0^{z/2}\exp(t^2)dt \tag{13}$$

the expression for $V_2(z)$ being proportional to Dawson's integral of argument $z/2$ [23]. In addition, Zolotarev [24] has found the value of $Q_{2/3}(z)$ in terms of Whittaker functions, but we have not evaluated his expression.

3. Computational Notes

All of the computations were performed in double precision in FORTRAN 77 on a Perkin-Elmer 3230 computer. Each complete set of tables, $Q_\alpha(z)$ and $V_\alpha(z)$, took between 1 and 1.5 minutes of CPU time. Tables 1 and 2 indicate when the appropriate series was used for computing $Q_\alpha(z)$ and $V_\alpha(z)$, respectively, as well as when numerical integration was required. Two points should be noted with respect to the two tables: 1) table entries for the critical values of z will change somewhat if other than six-digit accuracy is required, and 2) entries for critical z in tables 1 and 2 assume only restricted values, namely those values of z that appear in tables 3 and 4 (positioned at the end of this paper because of their length), where the $Q_\alpha(z)$ and $V_\alpha(z)$ are tabulated. Note that for some values of α the critical z values produce a range of overlap (for example, for $\alpha=1.9$ in table 2); in these cases there is no need for numerical integration. But in other instances there is a gap between the critical values of z for use of the respective series, which may simply be due to the fact that no values of z are tabulated in the intermediate range. Hence, in these instances the calculation of $Q_\alpha(z)$ or $V_\alpha(z)$ for intermediate values of z may or may not require numerical integration. Since double precision was used in the calculations, some care

Table 1. Critical values of z for the use of eqs (5) and (6) or numerical integration to evaluate $Q_\alpha(z)$.

α	Use eq (6) for $z\leqslant$	Use eq (5) for $z\geqslant$	Use numerical integration for $z=$
$\leqslant$0.3	—	0.001	—
0.4	0.002	0.004	0.003
0.5	0.01	0.02	—
0.6	0.05	0.10	—
0.7	0.1	0.15	—
0.8	0.25	0.35	0.30
0.9	0.50	0.65	0.55,0.60
1.1	1.0	2.0	1.5
1.2	2.0	2.5	—
1.3	3.0	3.5	—
1.4	4.0	4.0	—
1.5	4.5	5.0	—
1.6	5.5	5.5	—
1.7	6.0	6.5	—
1.8	6.5	7.5	7.0
1.9	6.0	8.5	6.5–8.0

Table 2. Critical values of z for the use of eqs (7) and (8)or numerical integration to evaluate $V_\alpha(z)$.

α	Use eq (8) for $z\leqslant$	Use eq (7) for $z\geqslant$	Use numerical integration for $z=$
$\leqslant 0.3$	—	0.001	—
0.4	0.001	0.01	0.002-0.005
0.5	0.01	0.025	0.015,0.02
0.6	0.045	0.06	0.05,0.055
0.7	0.1	0.15	—
0.8	0.25	0.35	0.3
0.9	0.5	0.65	0.55,0.6
1.1	1.0	2.0	1.5
1.2	2.0	2.5	—
1.3	2.5	3.0	—
1.4	3.5	4.0	—
1.5	5.0	5.5	—
1.6	5.5	6.5	—
1.7	6.5	6.0	—
1.8	7.5	7.5	—
1.9	8.0	7.5	—
2.0	8.5	8.0	—

was required in the calculation of gamma function. We used the formula

$$\frac{1}{\Gamma(y+1)}=\sum_{n=0}^{2\alpha} a_n y^n \tag{14}$$

for $x=y+1\leqslant 3.21$, and

$$\Gamma(x)=(2\pi)^{1/2}x^{x-1/2}e^{-x}\sum_{n=0}^{\infty} c_n x^n \tag{15}$$

for $x\geqslant 3.21$. The coefficients $\{a_n\}$ and $\{c_n\}$ appearing in these formulae are to be found in the book by Luke [25]. The accuracy of formula [14] increases as $x\to 0$, while the accuracy of formula (15) increases as $x\to\infty$. For $x=3.21$, both formulas yield the same accuracy.

When the series of eqs (5-8) were used to evaluate $Q_\alpha(z)$ or $V_\alpha(z)$, the number of terms used was a maximum of 150, which occurred near the switchover region for the two series. Most entries in the tables never required the evaluation of more than 20 terms. The numerical integrations of eq (9) were performed using Simpson's extended rule with a step size of $\pi/40{,}000$.

4. Application to Polymer Physics

The expressions in eq (3) allow us to estimate the three parameters that characterize polymers whose dielectric properties are described by eq (2) which is the Williams-Watts relaxation function. Although it appears that all three parameters must be fit simultaneously, we will show that a small extension of tables 3 and 4 allows one to estimate the parameters separately. Since the most frequently measured property from which it is possible to determine the parameters α, τ, and $A=\epsilon(0)-1$ is the dielectric loss function, i.e., $\epsilon''(\omega)$, we restrict our discussion to this function. As can be seen from eq (3), the dielectric loss function is proportional to $g_\alpha(z)=zQ_\alpha(z)$. This function is unimodal as a function of z as illustrated in figure 1. Several parameters can be defined that characterize the shape and properties of $g_\alpha(z)$. These include $z_m(\alpha)$, the value of z at which $g_\alpha(z)$ is maximized,

$$M(\alpha)=\max_z g_\alpha(z)=g_\alpha(z_m(\alpha)) \tag{16}$$

the height of the peak, and for $\theta<1$ two sets of abscissas, $\{z_l(\theta,\alpha)\}$, $\{z_t(\theta,\alpha)\}$. These are, respectively, the values of z on the leading and trailing edges of $g_\alpha(z)$ at which

$$g_\alpha(z)=\theta M(\alpha). \tag{17}$$

These parameters are all illustrated in figure 1. For later

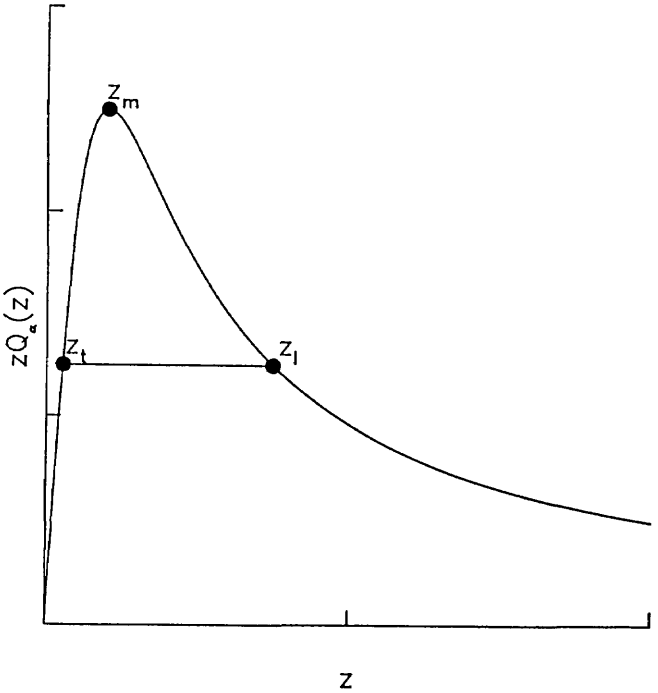

Figure 1-A typical curve of $g_\alpha(z)=zQ_\alpha(z)$ together with distinguished points useful for parameter estimation. The point z_m is the maximum, and $z_l(\theta,\alpha)$ and $z_t(\theta,\alpha)$ are the two solutions to $g_\alpha(z)=\theta M(\alpha)$. In the figure θ was taken equal to 1/2.

reference we give values of $z_m(\alpha)$ and $M(\alpha)$ in table 5 for $\alpha=0.05(0.05)1.00$. Table 6 contains values of

$$f(\theta,\alpha)=\ln[z_l(\theta,\alpha)/z_m(\alpha)] \tag{18}$$

for $\alpha=0.05(0.05)1.00$ and $\theta=0.1(0.1)0.9$ which will be used for data analysis, as will be explained in further detail below. The values of α cover the physically interesting range (0.2, 0.8) which has so far been found in polymers.

Table 5. Values of $z_m(\alpha)$ and the maximum $M(\alpha)$ for $\alpha=0.05(0.05)1.00$.

α	$z_m(\alpha)$	$M(\alpha)$
0.05	0.5741	0.9188(−2)
0.10	0.5885	0.1833(−1)
0.15	0.6041	0.2738(−1)
0.20	0.6207	0.3632(−1)
0.25	0.6380	0.4513(−1)
0.30	0.6561	0.5380(−1)
0.35	0.6751	0.6233(−1)
0.40	0.6948	0.7071(−1)
0.45	0.7154	0.7896(−1)
0.50	0.7370	0.8705(−1)
0.55	0.7595	0.9501(−1)
0.60	0.7830	0.1028(0)
0.65	0.8075	0.1105(0)
0.70	0.8329	0.1180(0)
0.75	0.8592	0.1253(0)
0.80	0.8863	0.1325(0)
0.85	0.9142	0.1394(0)
0.90	0.9425	0.1462(0)
0.95	0.9712	0.1528(0)
1.00	1.0000	0.1592(0)

The procedure for parameter estimation involves three successive steps. Since τ, α, and A are initially unknown one can get an estimate of α independent of τ and A by first estimating the peak height, $z_m(\alpha)$, from the data and then solving for α from eq (18). Since $z=2\pi f\tau$, the parameter τ drops out of eq (18) when the ratio of z's is taken. Although it appears that there are many independent estimates of α, each of which corresponds to a different θ, the data may not be equally useful at all values of θ. At high frequencies the underlying physical assumption that the system has a single degree of freedom may be poor approximation. In particular, the data at θ values less than 0.5 may not fit the Williams-Watts model as well as data for $\theta>0.5$. When a satisfactory value of α is determined, using eq (18), we may find τ from the relation

$$\hat{\tau}=z_m(\hat{\alpha})/(2\pi f_m) \tag{19}$$

where f_m is the frequency in Hz at which the peak maximum occurs. Finally, since an estimate of the peak height will generally be available, the estimate of the parameter A can be found from

$$\hat{A}=\max_f \epsilon_n''(2\pi f_m\hat{\tau})/M(\hat{\alpha}) \tag{20}$$

where relevant values of $M(\alpha)$ are given in table 5.

Table 6. Values of the function $f(\theta,\alpha)=\ln[z_l(\theta,\alpha)/z_m(\alpha)]$.

α	$\theta=0.1$	$\theta=0.2$	$\theta=0.3$	$\theta=0.4$	$\theta=0.5$	$\theta=0.6$	$\theta=0.7$	$\theta=0.8$	$\theta=0.9$
0.05	6.5303(1)	5.0611(1)	4.1593(1)	3.4833(1)	2.9237(1)	2.4287(1)	1.9654(1)	1.5039(1)	9.9471(0)
0.10	3.2670(1)	2.5323(1)	2.0813(1)	1.7432(1)	1.4633(1)	1.2157(1)	9.8394(0)	7.5297(0)	4.9815(0)
0.15	2.1793(1)	1.6895(1)	1.3888(1)	1.1633(1)	9.7667(0)	8.1152(0)	6.5691(0)	5.0280(0)	3.3273(0)
0.20	1.6353(1)	1.2679(1)	1.0424(1)	8.7325(0)	7.3322(0)	6.0932(0)	4.9332(0)	3.7766(0)	2.4999(0)
0.25	1.3085(1)	1.0146(1)	8.3420(0)	6.9892(0)	5.8690(0)	4.8778(0)	3.9497(0)	3.0244(0)	2.0025(0)
0.30	1.0902(1)	8.4535(0)	6.9504(0)	5.8235(0)	4.8905(0)	4.0649(0)	3.2919(0)	2.5210(0)	1.6697(0)
0.35	9.3382(0)	7.2399(0)	5.9523(0)	4.9871(0)	4.1881(0)	3.4812(0)	2.8195(0)	2.1596(0)	1.4308(0)
0.40	8.1600(0)	6.3250(0)	5.1993(0)	4.3558(0)	3.6578(0)	3.0405(0)	2.4627(0)	1.8866(0)	1.2502(0)
0.45	7.2385(0)	5.6087(0)	4.6095(0)	3.8611(0)	3.2421(0)	2.6948(0)	2.1827(0)	1.6724(0)	1.1086(0)
0.50	6.4962(0)	5.0310(0)	4.1333(0)	3.4615(0)	2.9061(0)	2.4154(0)	1.9565(0)	1.4993(0)	9.9427(−1)
0.55	5.8838(0)	4.5537(0)	3.7397(0)	3.1309(0)	2.6282(0)	2.1843(0)	1.7694(0)	1.3561(0)	8.9980(−1)
0.60	5.3686(0)	4.1517(0)	3.4078(0)	2.8521(0)	2.3937(0)	1.9893(0)	1.6116(0)	1.2355(0)	8.2024(−1)
0.65	4.9280(0)	3.8075(0)	3.1235(0)	2.6133(0)	2.1919(0)	1.8223(0)	1.4765(0)	1.1324(0)	7.5236(−1)
0.70	4.5459(0)	3.5084(0)	2.8764(0)	2.4057(0)	2.0183(0)	1.6774(0)	1.3594(0)	1.0431(0)	6.9377(−1)
0.75	4.2106(0)	3.2459(0)	2.6594(0)	2.2235(0)	1.8653(0)	1.5504(0)	1.2570(0)	9.6523(−1)	6.4276(−1)
0.80	3.9134(0)	3.0129(0)	2.4669(0)	2.0620(0)	1.7298(0)	1.4382(0)	1.1667(0)	8.9674(−1)	5.9811(−1)
0.85	3.6477(0)	2.8047(0)	2.2951(0)	1.9180(0)	1.6093(0)	1.3385(0)	1.0867(0)	8.3625(−1)	5.5887(−1)
0.90	3.4082(0)	2.6170(0)	2.1403(0)	1.7886(0)	1.5012(0)	1.2496(0)	1.0155(0)	7.8269(−1)	5.2431(−1)
0.95	3.1911(0)	2.4470(0)	2.0006(0)	1.6721(0)	1.4042(0)	1.1699(0)	9.5210(−1)	7.3521(−1)	4.9389(−1)
1.00	2.9932(0)	2.2924(0)	1.8738(0)	1.5668(0)	1.3170(0)	1.0986(0)	8.9559(−1)	6.9315(−1)	4.6715(−1)

This estimation procedure was applied to dielectric loss data of Sasabe and Moynihan [26] on polyvinyl acetate at 66.7 °C. The relevant data are the following:

	$\log_{10} f$	$\epsilon''(f)$	θ
1.	2.701	0.964	
2.	2.854	0.980	
3.	3.033	0.948	
4.	3.187	0.884	0.901
5.	3.560	0.665	0.678
6.	3.701	0.587	0.599
7.	3.857	0.510	0.520

The first three data points were used to estimate the peak location and height. These were found to be

$$\log_{10} \hat{f}_m = 2.839 \qquad \hat{\epsilon}''(\max) = 0.981$$

following which the values of θ shown in data set were calculated. Equations (18–20) were then used to estimate α, τ, and A for the last four data points. The resulting estimates are the following:

	α	$\hat{\tau}$(s)	$\hat{A}$
4.	0.62	1.83(−4)	9.54
5.	0.60	1.81(−4)	9.54
6.	0.60	1.81(−4)	9.54
7.	0.60	1.81(−4)	9.54

These results should be contrasted with the estimates by Sasabe and Moynihan, $\hat{\alpha} = 0.59$ and $\hat{\tau} = 1.97 \times 10^{-4}$ s for the same set of data. The fitting procedure used by them required approximations suggested by Moynihan, Boesch, and Laberge [15], but these are of uncertain accuracy over the entire range of α because no accurate tables were available to check them.

References

[1] Cauchy, A. Ouevres Complètes, 1 ser. **12**, Sur les rèsultats moyens d'observations de même nature, et sur les resultats les probables, 94–104; Sur la probabilité des erreurs qui affectent des résultats moyens d'observations de même nature, 104–114. Gauthier-Villars, Paris (1900).

[2] Lévy, P. Theorie des erreurs. La loi de Gauss et les lois exceptionelles. Bull. Societe Math. France **52**, 49–85 (1924).

[3] Khintchine, A. Ya, and P. Lévy. Sur les lois stables. Compt. Rend. Acad. Sci. Paris **202**, 374–376 (1936).

[4] Holstmark, J. Über die Verbreiterung von Spektrallinien. Ann. der Phys. **58**, 577–630 (1919).

[5] Mandelbrot, B. B. The variation of certain speculative prices. J. Bus. Univ. Chic. **36**, 394–419 (1963).

[6] Gerstein, G. L., and B. B. Mandelbrot. Random walk models for the spike activity of a single neuron. Biophys. J. **4**, 41–68 (1964).

[7] Scher, H. and E. W. Montroll. Anomalous transit-time dispersion in amorphous solids. Phys. Rev. **B12**, 2455–2477 (1975).

[8] Shlesinger, M. F. Electron scavenging in glasses. J. Chem. Phys. **70**, 4813–4818 (1979).

[9] Weber, W. Über die Elastizität der Seidenfäden. Pogg. Ann. der Phys. **4**, 247–261 (1835).

[10] Weber, W. Über die Elastizität fester Körper. Pogg. Ann. der Phys. **24**, 1–18 (1841).

[11] Kohlrausch, R. Theorie des Elektrischen Rückstandes in der Leidener Flasche. Pogg. Ann. der Phys. und Chemie. **91**, 179–214 (1854).

[12] Kohlrausch, F. Ueber die elastische Nachwirkung bei der Torsion, Pogg. Ann. der Phys. und Chemie. **119**, 337-338 (1863).

[13] Williams, G., and D. C. Watts. Non-symmetrical dielectric relaxation behaviour arising from a simple empirical decay function. Trans. Far. Soc. **66**, 80–85 (1970).

[14] Williams, G., and D. C. Watts. Further considerations of non symmetrical dielectric behaviour arising from a simple empirical decay function. Trans. Far. Soc. **67**, 1323–1335 (1971).

[15] Moynihan, C. T.; L. P. Boesch and N. L. Laberge. Decay function for the electric field relaxation in vitreous ionic conductors. Phys. and Chem. of Glasses **14**, 122–125 (1973).

[16] Bendler, J. T. Internal molecular motions and the elastic constants of polymer glasses. Macromol. **15**, 1325–1328 (1982).

[17] Shlesinger, M. F., and E. W. Montroll. On the Williams-Watts function of dielectric relaxation. Proc. Natl. Acad. Sci. USA **81**, 1280–1283 (1984).

[18] Montroll, E. W., and G. H. Weiss. Random walks on lattices. II. J. Math. Phys. **6**, 167–181 (1965).

[19] Montroll, E. W., and J. T. Bendler. On Levy (or stable) distributions and the Williams-Watts model of dielectric relaxation. J. Stat. Phys. **34**, 129–162 (1984).

[20] Holt, D. R., and E. L. Crow. Tables and Graphs of the Stable Probability Density Functions. J. Res. Natl. Bur. Stand. **77B**, 143–198 (1973).

[21] Bergström, H. On some expansions of stable distribution functions. Ark. Mat. **2**, 375–378 (1952).

[22] Feller, W. *An Introduction to Probability Theory and its Applications.* Vol. II 2nd ed. (John Wiley, New York) 1971.

[23] Abramowitz, M., and I. A. Stegun. *Handbook of Mathematical Functions.* AMS **55**, (Government Printing Office, Washington, DC) 1970.

[24] Zolotarev, V. M. (in Russian) Expression of the density of a stable distribution with exponent α greater than one by means of a frequency with exponent $1/\alpha$. Dokl. Akad. Nauk. USSR **98**, 735–738 (1954). English translation in Selected Trans. Math. Stat. and Prob., Inst. Math. Stat. and Am. Math. Soc. **1**, 163–167 (1961).

[25] Luke, T. L. *Mathematical Functions and Their Approximations.* (Academic Press, New York), 1975.

[26] Sasabe, H. and C. T. Moynihan. Structural relaxation in Poly (vinyl acetate). J. Poly. Sci. Phys. **16**, 1447–1457 (1978).

Table 3. Function $Q_\alpha(Z)$ for Alpha =

Z =	0.010	0.020	0.040	0.060	0.080
0.000	0.29707D+158	0.968111D+64	0.493737D+25	0.437462D+14	0.544482D+09
0.001	0.183556D+01	0.364749D+01	0.709933D+31	0.101454D+02	0.125852D+02
0.002	0.918171D+00	0.182697D+01	0.357643D+01	0.516536D+01	0.651078D+01
0.003	0.612253D+00	0.121911D+01	0.239372D+01	0.347610D+01	0.441802D+01
0.004	0.459259D+00	0.914900D+00	0.179997D+01	0.262323D+01	0.335214D+01
0.005	0.367447D+00	0.732252D+00	0.144273D+01	0.210809D+01	0.270446D+01
0.010	0.183781D+00	0.366591D+00	0.725210D+00	0.105734D+01	0.138416D+01
0.015	0.122540D+00	0.244552D+00	0.484776D+00	0.715060D+00	0.933610D+00
0.020	0.919143D-01	0.183490D+00	0.364210D+00	0.539213D+00	0.705432D+00
0.025	0.735368D-01	0.146836D+00	0.291727D+00	0.432612D+00	0.567339D+00
0.030	0.612841D-01	0.122391D+00	0.243335D+00	0.361300D+00	0.474687D+00
0.035	0.525316D-01	0.104926D+00	0.208729D+00	0.310225D+00	0.408175D+00
0.040	0.459668D-01	0.918237D-01	0.182750D+00	0.271834D+00	0.358086D+00
0.045	0.408607D-01	0.816192D-01	0.162590D+00	0.241919D+00	0.318995D+00
0.050	0.367756D-01	0.734760D-01	0.146340D+00	0.217949D+00	0.287631D+00
0.055	0.334331D-01	0.668026D-01	0.133087D+00	0.198310D+00	0.261905D+00
0.060	0.306476D-01	0.612407D-01	0.122038D+00	0.181925D+00	0.240418D+00
0.065	0.282906D-01	0.565340D-01	0.112683D+00	0.168046D+00	0.222201D+00
0.070	0.262703D-01	0.524992D-01	0.104662D+00	0.156137D+00	0.206559D+00
0.075	0.245193D-01	0.490021D-01	0.977079D-01	0.145808D+00	0.192981D+00
0.080	0.229871D-01	0.459419D-01	0.916208D-01	0.136763D+00	0.181082D+00
0.085	0.216352D-01	0.432415D-01	0.862482D-01	0.128776D+00	0.170570D+00
0.090	0.204336D-01	0.408409D-01	0.814711D-01	0.121671D+00	0.161214D+00
0.095	0.193582D-01	0.386933D-01	0.771983D-01	0.115311D+00	0.152833D+00
0.100	0.183905D-01	0.367597D-01	0.733470D-01	0.109583D+00	0.145283D+00
0.150	0.122611D-01	0.245126D-01	0.489484D-01	0.732284D-01	0.972716D-01
0.200	0.919612D-02	0.183870D-01	0.367319D-01	0.549921D-01	0.731243D-01
0.250	0.735705D-02	0.147108D-01	0.293956D-01	0.440281D-01	0.585823D-01
0.300	0.613095D-02	0.122597D-01	0.245016D-01	0.367084D-01	0.488627D-01
0.350	0.525515D-02	0.105087D-01	0.210044D-01	0.314745D-01	0.419071D-01
0.400	0.459828D-02	0.919528D-02	0.183805D-01	0.275460D-01	0.366827D-01
0.450	0.408737D-02	0.817369D-02	0.163391D-01	0.244886D-01	0.326147D-01
0.500	0.367864D-02	0.735638D-02	0.147057D-01	0.220413D-01	0.293574D-01
0.550	0.334422D-02	0.668764D-02	0.133690D-01	0.200382D-01	0.266902D-01
0.600	0.306554D-02	0.613033D-02	0.122549D-01	0.183684D-01	0.244662D-01
0.650	0.282972D-02	0.565875D-02	0.113121D-01	0.169551D-01	0.225834D-01
0.700	0.262760D-02	0.525453D-02	0.105039D-01	0.157433D-01	0.209689D-01
0.750	0.245242D-02	0.490419D-02	0.980335D-02	0.146930D-01	0.195691D-01
0.800	0.229914D-02	0.459764D-02	0.919036D-02	0.137737D-01	0.183439D-01
0.850	0.216389D-02	0.432715D-02	0.864944D-02	0.129625D-01	0.172625D-01
0.900	0.204367D-02	0.408672D-02	0.816860D-02	0.122413D-01	0.163011D-01
0.950	0.193610D-02	0.387158D-02	0.773836D-02	0.115960D-01	0.154408D-01
1.000	0.183929D-02	0.367796D-02	0.735112D-02	0.110152D-01	0.146663D-01
1.500	0.122616D-02	0.245167D-02	0.489836D-02	0.733557D-02	0.975934D-02
2.000	0.919588D-03	0.183852D-02	0.367194D-02	0.549564D-02	0.730551D-02
2.500	0.735648D-03	0.147044D-02	0.293616D-02	0.439193D-02	0.583381D-02
3.000	0.613022D-03	0.122539D-02	0.244872D-02	0.365638D-02	0.485329D-02
3.500	0.525434D-03	0.105023D-02	0.209547D-02	0.313119D-02	0.415341D-02
4.000	0.459743D-03	0.918857D-03	0.183282D-02	0.273747D-02	0.362889D-02
4.500	0.408651D-03	0.816686D-03	0.162859D-02	0.243137D-02	0.322124D-02
5.000	0.367778D-03	0.734953D-03	0.146523D-02	0.218660D-02	0.289535D-02
5.500	0.334336D-03	0.668084D-03	0.133159D-02	0.198641D-02	0.262892D-02
6.000	0.306469D-03	0.612362D-03	0.122025D-02	0.181965D-02	0.240704D-02
6.500	0.282889D-03	0.565214D-03	0.112646D-02	0.167861D-02	0.221944D-02
7.000	0.262678D-03	0.524804D-03	0.104534D-02	0.155776D-02	0.205874D-02
7.500	0.245162D-03	0.489784D-03	0.975387D-03	0.145306D-02	0.191955D-02
8.000	0.229835D-03	0.459142D-03	0.914192D-03	0.136149D-02	0.179886D-02
8.500	0.216312D-03	0.432107D-03	0.860204D-03	0.128071D-02	0.169254D-02
9.000	0.204291D-03	0.408076D-03	0.812224D-03	0.120894D-02	0.159520D-02
9.500	0.193535D-03	0.386575D-03	0.769300D-03	0.114474D-02	0.150995D-02
10.000	0.183857D-03	0.367226D-03	0.730674D-03	0.108698D-02	0.143327D-02
15.000	0.122555D-03	0.244699D-03	0.486206D-03	0.721716D-03	0.948853D-03
20.000	0.919083D-04	0.183454D-03	0.364120D-03	0.539568D-03	0.707773D-03
25.000	0.735207D-04	0.146717D-03	0.291094D-03	0.430519D-03	0.563674D-03
30.000	0.612630D-04	0.122231D-03	0.242199D-03	0.357957D-03	0.467921D-03
35.000	0.525079D-04	0.104744D-03	0.207498D-03	0.306213D-03	0.399721D-03
40.000	0.459419D-04	0.916316D-04	0.181333D-03	0.267462D-03	0.348703D-03
45.000	0.408352D-04	0.814344D-04	0.161065D-03	0.237363D-03	0.309113D-03
50.000	0.367590D-04	0.732779D-04	0.144860D-03	0.213314D-03	0.277509D-03
55.000	0.334077D-04	0.666053D-04	0.131608D-03	0.193659D-03	0.251702D-03
60.000	0.306225D-04	0.610455D-04	0.120570D-03	0.177298D-03	0.230235D-03
65.000	0.282659D-04	0.563416D-04	0.111234D-03	0.163468D-03	0.212101D-03
70.000	0.262460D-04	0.523101D-04	0.103236D-03	0.151624D-03	0.196583D-03
75.000	0.244955D-04	0.488165D-04	0.963056D-04	0.141369D-03	0.183155D-03
80.000	0.229638D-04	0.457600D-04	0.902459D-04	0.132403D-03	0.171421D-03
85.000	0.216123D-04	0.430633D-04	0.849002D-04	0.124498D-03	0.161083D-03
90.000	0.204111D-04	0.406664D-04	0.801502D-04	0.117477D-03	0.151905D-03
95.000	0.193363D-04	0.385220D-04	0.759016D-04	0.111199D-03	0.143703D-03
100.000	0.183690D-04	0.365923D-04	0.720790D-04	0.105553D-03	0.136330D-03
150.000	0.122434D-04	0.243747D-04	0.479025D-04	0.699005D-04	0.898690D-04

FUNCTION Q(ALPHA,Z) FOR

Z =	ALPHA = 0.010	0.020	0.040	0.060	0.080
200.000	0.918108D-05	0.182696D-04	0.358426D-04	0.521642D-04	0.668379D-04
250.000	0.734391D-05	0.146084D-04	0.286198D-04	0.415640D-04	0.531109D-04
300.000	0.611926D-05	0.121685D-04	0.238118D-04	0.345200D-04	0.440295D-04
350.000	0.524458D-05	0.104263D-04	0.203820D-04	0.295023D-04	0.375386D-04
400.000	0.458862D-05	0.912004D-05	0.178125D-04	0.257481D-04	0.327053D-04
450.000	0.407847D-05	0.810434D-05	0.158160D-04	0.228345D-04	0.289596D-04
500.000	0.367037D-05	0.729197D-05	0.142203D-04	0.205081D-04	0.259728D-04
550.000	0.333649D-05	0.662745D-05	0.129158D-04	0.186080D-04	0.235364D-04
600.000	0.305827D-05	0.607379D-05	0.118295D-04	0.170272D-04	0.215116D-04
650.000	0.282287D-05	0.560541D-05	0.109111D-04	0.156917D-04	0.198026D-04
700.000	0.262110D-05	0.520400D-05	0.101243D-04	0.145485D-04	0.183413D-04
750.000	0.244624D-05	0.485618D-05	0.944885D-05	0.135591D-04	0.170776D-04
800.000	0.229325D-05	0.455187D-05	0.884698D-05	0.126944D-04	0.159742D-04
850.000	0.215826D-05	0.428341D-05	0.832147D-05	0.119323D-04	0.150026D-04
900.000	0.203827D-05	0.404481D-05	0.785461D-05	0.112557D-04	0.141405D-04
950.000	0.193092D-05	0.383136D-05	0.743709D-05	0.106510D-04	0.133705D-04
1000.000	0.183431D-05	0.363927D-05	0.706151D-05	0.101072D-04	0.126787D-04
1500.000	0.122251D-05	0.242338D-05	0.468756D-05	0.667811D-05	0.832817D-05
2000.000	0.916676D-06	0.181599D-05	0.350460D-05	0.497576D-05	0.617870D-05
2500.000	0.733211D-06	0.145180D-05	0.279664D-05	0.395986D-05	0.490359D-05

Z =	ALPHA = 0.100	0.200	0.300	0.400	0.500
0.000	0.115508D+07	0.381972D+02	0.294772D+01	0.105786D+01	0.636629D+00
0.001	0.142455D+02	0.104414D+02	0.283285D+01	0.105712D+01	0.636582D+00
0.002	0.753831D+01	0.703477D+01	0.255043D+01	0.105549D+01	0.636457D+00
0.003	0.517482D+01	0.545474D+01	0.249887D+01	0.105147D+01	0.636277D+00
0.004	0.395595D+01	0.450920D+01	0.104686D+01	0.636011D+00	
0.005	0.320902D+01	0.386919D+01	0.222929D+01	0.104129D+01	0.635671D+00
0.010	0.166695D+01	0.233747D+01	0.177569D+01	0.100404D+01	0.632891D+00
0.015	0.113262D+01	0.170846D+01	0.149144D+01	0.959876D+00	0.628461D+00
0.020	0.859765D+00	0.135720D+01	0.129346D+01	0.914986D+00	0.622621D+00
0.025	0.693723D+00	0.113051D+01	0.114610D+01	0.871837D+00	0.615530D+00
0.030	0.581867D+00	0.971153D+00	0.103137D+01	0.831333D+00	0.607733D+00
0.035	0.501314D+00	0.852550D+00	0.939074D+00	0.793705D+00	0.599147D+00
0.040	0.440497D+00	0.760607D+00	0.862969D+00	0.758899D+00	0.590055D+00
0.045	0.392931D+00	0.687108D+00	0.798979D+00	0.726740D+00	0.580615D+00
0.050	0.354698D+00	0.626928D+00	0.744319D+00	0.697013D+00	0.570950D+00
0.055	0.323288D+00	0.576695D+00	0.697018D+00	0.669495D+00	0.561161D+00
0.060	0.297018D+00	0.534097D+00	0.655634D+00	0.643978D+00	0.551328D+00
0.065	0.274719D+00	0.497493D+00	0.619087D+00	0.620269D+00	0.541517D+00
0.070	0.255550D+00	0.465684D+00	0.586550D+00	0.598191D+00	0.531776D+00
0.075	0.238894D+00	0.437773D+00	0.557378D+00	0.577591D+00	0.522144D+00
0.080	0.224286D+00	0.413076D+00	0.531061D+00	0.558328D+00	0.512652D+00
0.085	0.211369D+00	0.391062D+00	0.507187D+00	0.540279D+00	0.503320D+00
0.090	0.199864D+00	0.371311D+00	0.485422D+00	0.523335D+00	0.494165D+00
0.095	0.189552D+00	0.353487D+00	0.465492D+00	0.507399D+00	0.485202D+00
0.100	0.180255D+00	0.337318D+00	0.447169D+00	0.492385D+00	0.476436D+00
0.150	0.120995D+00	0.231804D+00	0.321416D+00	0.379292D+00	0.399882D+00
0.200	0.910846D-01	0.176720D+00	0.251009D+00	0.307622D+00	0.341135D+00
0.250	0.730320D-01	0.142782D+00	0.205784D+00	0.258114D+00	0.295645D+00
0.300	0.609477D-01	0.119743D+00	0.174216D+00	0.221854D+00	0.259732D+00
0.350	0.522901D-01	0.103069D+00	0.150909D+00	0.194182D+00	0.230816D+00
0.400	0.457820D-01	0.904374D-01	0.132989D+00	0.172362D+00	0.207120D+00
0.450	0.407110D-01	0.805360D-01	0.118780D+00	0.154730D+00	0.187399D+00
0.500	0.366482D-01	0.725653D-01	0.107239D+00	0.140193D+00	0.170762D+00
0.550	0.333202D-01	0.660109D-01	0.976787D-01	0.128009D+00	0.156563D+00
0.600	0.305442D-01	0.605261D-01	0.896316D-01	0.117655D+00	0.144323D+00
0.650	0.281333D-01	0.558692D-01	0.827659D-01	0.108752D+00	0.133666D+00
0.700	0.261769D-01	0.518661D-01	0.768403D-01	0.101019D+00	0.124322D+00
0.750	0.244283D-01	0.483883D-01	0.716751D-01	0.942425D-01	0.116068D+00
0.800	0.228976D-01	0.453390D-01	0.671337D-01	0.882576D-01	0.108729D+00
0.850	0.215463D-01	0.426439D-01	0.631102D-01	0.829356D-01	0.102166D+00
0.900	0.203448D-01	0.402447D-01	0.595214D-01	0.781739D-01	0.962676D-01
0.950	0.192695D-01	0.380955D-01	0.563012D-01	0.738900D-01	0.909399D-01
1.000	0.183014D-01	0.361591D-01	0.533959D-01	0.700168D-01	0.861071D-01
1.500	0.121662D-01	0.238627D-01	0.348803D-01	0.451942D-01	0.548740D-01
2.000	0.909801D-02	0.177094D-01	0.256048D-01	0.327352D-01	0.391429D-01
2.500	0.725825D-02	0.140270D-01	0.200718D-01	0.253359D-01	0.298515D-01
3.000	0.603292D-02	0.116814D-01	0.165765D-01	0.207425D-01	0.243992D-01
3.500	0.515865D-02	0.984209D-02	0.138266D-01	0.170627D-01	0.199852D-01
4.000	0.450370D-02	0.854340D-02	0.119048D-01	0.145454D-01	0.165257D-01
4.500	0.399489D-02	0.753782D-02	0.104244D-01	0.126201D-01	0.141709D-01
5.000	0.358830D-02	0.673690D-02	0.925140D-02	0.111048D-01	0.123487D-01
5.500	0.325602D-02	0.608441D-02	0.830650D-02	0.988444D-02	0.108928D-01
6.000	0.297942D-02	0.554294D-02	0.751515D-02	0.888284D-02	0.970694D-02
6.500	0.274563D-02	0.508663D-02	0.685636D-02	0.804766D-02	0.872521D-02
7.000	0.254545D-02	0.469705D-02	0.629637D-02	0.734180D-02	0.790118D-02

FUNCTION Q(ALPHA,Z) FOR

Z = \ ALPHA =	0.100	0.200	0.300	0.400	0.500
7.500	0.2372130-02	0.4360690-02	0.5814950-02	0.6738280-02	0.7201220-02
8.000	0.2220630-02	0.4067470-02	0.5396980-02	0.6217050-02	0.6600450-02
8.500	0.2087080-02	0.3809660-02	0.5030940-02	0.5762880-02	0.6080308-02
9.000	0.1968480-02	0.3581290-02	0.4707940-02	0.5364030-02	0.5625690-02
9.500	0.1852460-02	0.3377650-02	0.4420960-02	0.5011320-02	0.5226040-02
10.000	0.1746130-02	0.3194970-02	0.4164430-02	0.4697450-02	0.4872260-02
15.000	0.1165700-02	0.2054380-02	0.2686960-02	0.2803350-02	0.2782990-02
20.000	0.8671160-03	0.1498590-02	0.1838790-02	0.1934350-02	0.1859990-02
25.000	0.6890070-03	0.1171990-02	0.1408390-02	0.1447090-02	0.1357010-02
30.000	0.5708570-03	0.9580410-03	0.1131380-02	0.1139970-02	0.1047180-02
35.000	0.4868310-03	0.8075380-03	0.9394340-03	0.9308820-03	0.8402720-03
40.000	0.4240550-03	0.6961780-03	0.7992700-03	0.7805260-03	0.6939210-03
45.000	0.3754020-03	0.6106130-03	0.6923290-03	0.6678800-03	0.5858530-03
50.000	0.3366040-03	0.5429140-03	0.6095010-03	0.5807570-03	0.5033420-03
55.000	0.3049540-03	0.4880850-03	0.5426610-03	0.5116350-03	0.4386350-03
60.000	0.2786520-03	0.4428220-03	0.4879690-03	0.4556400-03	0.3867690-03
65.000	0.2564540-03	0.4048560-03	0.4462660-03	0.4094840-03	0.3444280-03
70.000	0.2374730-03	0.3725800-03	0.4104810-03	0.3708740-03	0.3093250-03
75.000	0.2210600-03	0.3443220-03	0.3793310-03	0.3381660-03	0.2798340-03
80.000	0.2067290-03	0.3207100-03	0.3430170-03	0.3101540-03	0.2547710-03
85.000	0.1941110-03	0.2995810-03	0.3183880-03	0.2859310-03	0.2332570-03
90.000	0.1829170-03	0.2809230-03	0.2967680-03	0.2648080-03	0.2146230-03
95.000	0.1729190-03	0.2643320-03	0.2776520-03	0.2462480-03	0.1983550-03
100.000	0.1639380-03	0.2494900-03	0.2606420-03	0.2298310-03	0.1843540-03
150.000	0.1074800-03	0.1577930-03	0.1578440-03	0.1329540-03	0.1016850-03
200.000	0.7961400-04	0.1138500-03	0.1190384-03	0.8999700-04	0.6663290-04
250.000	0.6305980-04	0.8832160-04	0.8356400-04	0.6642950-04	0.4796660-04
300.000	0.5211320-04	0.7174250-04	0.6652770-04	0.5180520-04	0.3666180-04
350.000	0.4434830-04	0.6015980-04	0.5434010-04	0.4196750-04	0.2918580-04
400.000	0.3855980-04	0.5163780-04	0.4638150-04	0.3496040-04	0.2395480-04
450.000	0.3408190-04	0.4512150-04	0.4000260-04	0.2975190-04	0.2012160-04
500.000	0.3051690-04	0.3998730-04	0.3503500-04	0.2575030-04	0.1721350-04
550.000	0.2761290-04	0.3586440-04	0.3107250-04	0.2259370-04	0.1494540-04
600.000	0.2520280-04	0.3243550-04	0.2784510-04	0.2004930-04	0.1313580-04
650.000	0.2317110-04	0.2953470-04	0.2517100-04	0.1796120-04	0.1166470-04
700.000	0.2143580-04	0.2716750-04	0.2293230-04	0.1622140-04	0.1044950-04
750.000	0.1993680-04	0.2509390-04	0.2101020-04	0.1475270-04	0.9431840-05
800.000	0.1862920-04	0.2329660-04	0.1936460-04	0.1349900-04	0.8569540-05
850.000	0.1747880-04	0.2172500-04	0.1793560-04	0.1241800-04	0.7831260-05
900.000	0.1645910-04	0.2033980-04	0.1668450-04	0.1147790-04	0.7193380-05
950.000	0.1554900-04	0.1911040-04	0.1558090-04	0.1065390-04	0.6637760-05
1000.000	0.1473210-04	0.1801230-04	0.1460120-04	0.9926760-05	0.6159250-05
1500.000	0.9611480-05	0.1127350-04	0.8730300-05	0.5672510-05	0.3363390-05
2000.000	0.7095710-05	0.8077800-05	0.6055690-05	0.3810820-05	0.2193650-05
2500.000	0.5606070-05	0.6234560-05	0.4557570-05	0.2798040-05	0.1573460-05

FUNCTION Q(ALPHA,Z) FOR

Z = \ ALPHA =	0.600	0.700	0.800	0.900	1.000
0.000	0.4789210+00	0.4029240+00	0.3606460+00	0.3349200+00	0.3183100+00
0.001	0.4789150+00	0.4029220+00	0.3606450+00	0.3349200+00	0.3183100+00
0.002	0.4788960+00	0.4029160+00	0.3606430+00	0.3349190+00	0.3183090+00
0.003	0.4788640+00	0.4029060+00	0.3606380+00	0.3349160+00	0.3183070+00
0.004	0.4783190+00	0.4028930+00	0.3606320+00	0.3349130+00	0.3183050+00
0.005	0.4787620+00	0.4028750+00	0.3606240+00	0.3349080+00	0.3183020+00
0.010	0.4782870+00	0.4027270+00	0.3605580+00	0.3348710+00	0.3182780+00
0.015	0.4775000+00	0.4024810+00	0.3604480+00	0.3348100+00	0.3182380+00
0.020	0.4764090+00	0.4021370+00	0.3602950+00	0.3347240+00	0.3181830+00
0.025	0.4750250+00	0.4016960+00	0.3600970+00	0.3346140+00	0.3181110+00
0.030	0.4733610+00	0.4011610+00	0.3598570+00	0.3344790+00	0.3180240+00
0.035	0.4714310+00	0.4005310+00	0.3595730+00	0.3343200+00	0.3179200+00
0.040	0.4692510+00	0.3998080+00	0.3592460+00	0.3341370+00	0.3178010+00
0.045	0.4668380+00	0.3989950+00	0.3588770+00	0.3339290+00	0.3176670+00
0.050	0.4642100+00	0.3980940+00	0.3584650+00	0.3336980+00	0.3175160+00
0.055	0.4613840+00	0.3971060+00	0.3580120+00	0.3334420+00	0.3173500+00
0.060	0.4583780+00	0.3960340+00	0.3575170+00	0.3331630+00	0.3171680+00
0.065	0.4552090+00	0.3948810+00	0.3569820+00	0.3328600+00	0.3169710+00
0.070	0.4518950+00	0.3936490+00	0.3564070+00	0.3325330+00	0.3167580+00
0.075	0.4484510+00	0.3923400+00	0.3557910+00	0.3321830+00	0.3165290+00
0.080	0.4448920+00	0.3909590+00	0.3551370+00	0.3318100+00	0.3162850+00
0.085	0.4412330+00	0.3895070+00	0.3544440+00	0.3314140+00	0.3160270+00
0.090	0.4374880+00	0.3879880+00	0.3537130+00	0.3309960+00	0.3157520+00
0.095	0.4336680+00	0.3864040+00	0.3529450+00	0.3305540+00	0.3154630+00
0.100	0.4297870+00	0.3847590+00	0.3521410+00	0.3300900+00	0.3151580+00

FUNCTION Q(ALPHA,Z) FOR

Z = \ ALPHA =	0.600	0.700	0.800	0.900	1.000
0.150	0.3895710+00	0.3655850+00	0.3422650+00	0.3242760+00	0.3113060+00
0.200	0.3507330+00	0.3433510+00	0.3296510+00	0.3165250+00	0.3060670+00
0.250	0.3157610+00	0.3201770+00	0.3151630+00	0.3071670+00	0.2995850+00
0.300	0.2851140+00	0.2974110+00	0.2995940+00	0.2965580+00	0.2920270+00
0.350	0.2585100+00	0.2758060+00	0.2835920+00	0.2850540+00	0.2835720+00
0.400	0.2355450+00	0.2557200+00	0.2676510+00	0.2729800+00	0.2744050+00
0.450	0.2154150+00	0.2372690+00	0.2521160+00	0.2606240+00	0.2647070+00
0.500	0.1979380+00	0.2204400+00	0.2372150+00	0.2482240+00	0.2546480+00
0.550	0.1826190+00	0.2051450+00	0.2230830+00	0.2359710+00	0.2443840+00
0.600	0.1691230+00	0.1912670+00	0.2097880+00	0.2240110+00	0.2340510+00
0.650	0.1571740+00	0.1786770+00	0.1973510+00	0.2124500+00	0.2237680+00
0.700	0.1465420+00	0.1672470+00	0.1857640+00	0.2013590+00	0.2135310+00
0.750	0.1370390+00	0.1568580+00	0.1749960+00	0.1907850+00	0.2037180+00
0.800	0.1285060+00	0.1473980+00	0.1650260+00	0.1807510+00	0.1940910+00
0.850	0.1208130+00	0.1387690+00	0.1557460+00	0.1712650+00	0.1847950+00
0.900	0.1138510+00	0.1308820+00	0.1471660+00	0.1623220+00	0.1758620+00
0.950	0.1075260+00	0.1236580+00	0.1392160+00	0.1539100+00	0.1673110+00
1.000	0.1017620+00	0.1170270+00	0.1318460+00	0.1460090+00	0.1591550+00
1.500	0.6403270-01	0.7279940-01	0.8130340-01	0.8965840-01	0.9794150-01
2.000	0.4491150-01	0.5014100-01	0.5591760-01	0.6240870-01	0.6966200-01
2.500	0.3368820-01	0.3682880-01	0.3965750-01	0.4195650-01	0.4390480-01
3.000	0.2644930-01	0.2855420-01	0.3004220-01	0.3112790-01	0.3183100-01
3.500	0.2146320-01	0.2277460-01	0.2359470-01	0.2399120-01	0.2402340-01
4.000	0.1785860-01	0.1868440-01	0.1905990-01	0.1905350-01	0.1872410-01
4.500	0.1515390-01	0.1565220-01	0.1574450-01	0.1550030-01	0.1497930-01
5.000	0.1306370-01	0.1333560-01	0.1324430-01	0.1286000-01	0.1224270-01
5.500	0.1140940-01	0.1152160-01	0.1131900-01	0.1084500-01	0.1018390-01
6.000	0.1007370-01	0.1007160-01	0.9781330-02	0.9272410-02	0.8602970-02
6.500	0.8977190-02	0.8892450-02	0.8551100-02	0.8021420-02	0.7359770-02
7.000	0.8064020-02	0.7919120-02	0.7545540-02	0.7009820-02	0.6366220-02
7.500	0.7294120-02	0.7105320-02	0.6712450-02	0.6180060-02	0.5560000-02
8.000	0.6638060-02	0.6447220-02	0.6071470-02	0.5569910-02	0.4997080-02
8.500	0.6073500-02	0.5829590-02	0.5422480-02	0.4912180-02	0.4345530-02
9.000	0.5583730-02	0.5323340-02	0.4916680-02	0.4421410-02	0.3881830-02
9.500	0.5155590-02	0.4883750-02	0.4480640-02	0.4001540-02	0.3488330-02
10.000	0.4778790-02	0.4499340-02	0.4101910-02	0.3639500-02	0.3151580-02
15.000	0.2605870-02	0.2338030-02	0.2108510-02	0.1711510-02	0.1408450-02
20.000	0.1634630-02	0.1460910-02	0.1224730-02	0.9982820-03	0.7937900-03
25.000	0.1197700-02	0.1011800-02	0.8262730-03	0.6561730-03	0.5084820-03
30.000	0.9049430-03	0.7484270-03	0.5984080-03	0.4653860-03	0.3532850-03
35.000	0.7133190-03	0.5795210-03	0.4552420-03	0.3479280-03	0.2696330-03
40.000	0.5803790-03	0.4664860-03	0.3596810-03	0.2703690-03	0.1988190-03
45.000	0.4831510-03	0.3813780-03	0.2911880-03	0.2164070-03	0.1571120-03
50.000	0.4101170-03	0.3198710-03	0.2413620-03	0.1773100-03	0.1272730-03
55.000	0.3535170-03	0.2727660-03	0.2036450-03	0.1480530-03	0.1051920-03
60.000	0.3086330-03	0.2358090-03	0.1743640-03	0.1255720-03	0.8839490-04
65.000	0.2723510-03	0.2062240-03	0.1511470-03	0.1079140-03	0.7532180-04
70.000	0.2425410-03	0.1821330-03	0.1324080-03	0.9378290-04	0.6494790-04
75.000	0.2177050-03	0.1622290-03	0.1170500-03	0.8229360-04	0.5657840-04
80.000	0.1967640-03	0.1455730-03	0.1042190-03	0.7282190-04	0.4972810-04
85.000	0.1789170-03	0.1314810-03	0.9357990-04	0.6491880-04	0.4405060-04
90.000	0.1635650-03	0.1194410-03	0.8448650-04	0.5825380-04	0.3929270-04
95.000	0.1502500-03	0.1089630-03	0.7669400-04	0.5257950-04	0.3525590-04
100.000	0.1386140-03	0.1000490-03	0.6996660-04	0.4770760-04	0.3182780-04
150.000	0.7318840-04	0.5053430-04	0.3383900-04	0.2211190-04	0.1414650-04
200.000	0.4645710-04	0.3109550-04	0.2019850-04	0.1281020-04	0.7957550-05
250.000	0.3263350-04	0.2132670-04	0.1353250-04	0.8387180-05	0.5092880-05
300.000	0.2444420-04	0.1566770-04	0.9754330-05	0.5933350-05	0.3536740-05
350.000	0.1914170-04	0.1207010-04	0.7395150-05	0.4427870-05	0.2598430-05
400.000	0.1548540-04	0.9627830-05	0.5817780-05	0.3436210-05	0.1989420-05
450.000	0.1284320-04	0.7886690-05	0.4708320-05	0.2747550-05	0.1571890-05
500.000	0.1086330-04	0.6597450-05	0.3895850-05	0.2249320-05	0.1273230-05
550.000	0.9335900-05	0.5613520-05	0.3282470-05	0.1876900-05	0.1052250-05
600.000	0.8129450-05	0.4843830-05	0.2807190-05	0.1591020-05	0.8841920-06
650.000	0.7157510-05	0.4229240-05	0.2430960-05	0.1366640-05	0.7533940-06
700.000	0.6361360-05	0.3729890-05	0.2127710-05	0.1187200-05	0.6696110-06
750.000	0.5699820-05	0.3319090-05	0.1879480-05	0.1041390-05	0.5658830-06
800.000	0.5143300-05	0.2974110-05	0.1673550-05	0.9212510-06	0.4973580-06
850.000	0.4670040-05	0.2683500-05	0.1500700-05	0.8210480-06	0.4405670-06
900.000	0.4263730-05	0.2435550-05	0.1354110-05	0.7365760-06	0.3929750-06
950.000	0.3911930-05	0.2222110-05	0.1228640-05	0.6646850-06	0.3526980-06
1000.000	0.3605000-05	0.2036920-05	0.1120370-05	0.6029790-06	0.3183100-06
1500.000	0.1889050-05	0.1023650-05	0.5402890-06	0.2791270-06	0.1414710-06
2000.000	0.1193890-05	0.6281320-06	0.3220020-06	0.1616050-06	0.7957750-07
2500.000	0.8362220-06	0.4300260-06	0.2155250-06	0.1057670-06	0.5092960-07

FUNCTION Q(ALPHA,Z) FOR

Z =	ALPHA = 1.200	1.400	1.600	1.800	2.000
0.000	0.299420D+00	0.290115D+00	0.285388D+00	0.283069D+00	0.282095D+00
0.001	0.299420D+00	0.290115D+00	0.285388D+00	0.283069D+00	0.282095D+00
0.002	0.299419D+00	0.290115D+00	0.285388D+00	0.283068D+00	0.282095D+00
0.003	0.299418D+00	0.290114D+00	0.285388D+00	0.283068D+00	0.282094D+00
0.004	0.299417D+00	0.290113D+00	0.285387D+00	0.283067D+00	0.282094D+00
0.005	0.299416D+00	0.290112D+00	0.285386D+00	0.283067D+00	0.282093D+00
0.010	0.299402D+00	0.290103D+00	0.285379D+00	0.283061D+00	0.282088D+00
0.015	0.299380D+00	0.290088D+00	0.285367D+00	0.283051D+00	0.282079D+00
0.020	0.299350D+00	0.290066D+00	0.285351D+00	0.283037D+00	0.282067D+00
0.025	0.299310D+00	0.290039D+00	0.285329D+00	0.283019D+00	0.282051D+00
0.030	0.299261D+00	0.290006D+00	0.285303D+00	0.282997D+00	0.282031D+00
0.035	0.299204D+00	0.289966D+00	0.285272D+00	0.282971D+00	0.282008D+00
0.040	0.299138D+00	0.289921D+00	0.285237D+00	0.282941D+00	0.281982D+00
0.045	0.299063D+00	0.289869D+00	0.285196D+00	0.282907D+00	0.281952D+00
0.050	0.298980D+00	0.289811D+00	0.285151D+00	0.282869D+00	0.281919D+00
0.055	0.298887D+00	0.289748D+00	0.285102D+00	0.282827D+00	0.281882D+00
0.060	0.298786D+00	0.289678D+00	0.285047D+00	0.282782D+00	0.281841D+00
0.065	0.298677D+00	0.289602D+00	0.284988D+00	0.282732D+00	0.281797D+00
0.070	0.298558D+00	0.289520D+00	0.284924D+00	0.282678D+00	0.281749D+00
0.075	0.298431D+00	0.289433D+00	0.284856D+00	0.282620D+00	0.281698D+00
0.080	0.298295D+00	0.289339D+00	0.284782D+00	0.282558D+00	0.281644D+00
0.085	0.298150D+00	0.289239D+00	0.284704D+00	0.282493D+00	0.281586D+00
0.090	0.297997D+00	0.289133D+00	0.284621D+00	0.282423D+00	0.281524D+00
0.095	0.297836D+00	0.289021D+00	0.284534D+00	0.282349D+00	0.281459D+00
0.100	0.297665D+00	0.288903D+00	0.284442D+00	0.282272D+00	0.281390D+00
0.150	0.295494D+00	0.287398D+00	0.283264D+00	0.281279D+00	0.280512D+00
0.200	0.292497D+00	0.285308D+00	0.281625D+00	0.279895D+00	0.279288D+00
0.250	0.288713D+00	0.282651D+00	0.279533D+00	0.278127D+00	0.277721D+00
0.300	0.284194D+00	0.279448D+00	0.277002D+00	0.275982D+00	0.275819D+00
0.350	0.278995D+00	0.275725D+00	0.274046D+00	0.273470D+00	0.273587D+00
0.400	0.273183D+00	0.271512D+00	0.270681D+00	0.270603D+00	0.271034D+00
0.450	0.266825D+00	0.266842D+00	0.266926D+00	0.267392D+00	0.268169D+00
0.500	0.259996D+00	0.261749D+00	0.262803D+00	0.263352D+00	0.265004D+00
0.550	0.252767D+00	0.256272D+00	0.258334D+00	0.259998D+00	0.261548D+00
0.600	0.245214D+00	0.250450D+00	0.253543D+00	0.255847D+00	0.257815D+00
0.650	0.237407D+00	0.244324D+00	0.248455D+00	0.251416D+00	0.253818D+00
0.700	0.229418D+00	0.237934D+00	0.243096D+00	0.246723D+00	0.249571D+00
0.750	0.221311D+00	0.231321D+00	0.237493D+00	0.241788D+00	0.245088D+00
0.800	0.213148D+00	0.224528D+00	0.231675D+00	0.236631D+00	0.240385D+00
0.850	0.204984D+00	0.217592D+00	0.225667D+00	0.231271D+00	0.235478D+00
0.900	0.196870D+00	0.210555D+00	0.219499D+00	0.225731D+00	0.230383D+00
0.950	0.188851D+00	0.203452D+00	0.213198D+00	0.220029D+00	0.225117D+00
1.000	0.180965D+00	0.196318D+00	0.206790D+00	0.214189D+00	0.219696D+00
1.500	0.114249D+00	0.129382D+00	0.142241D+00	0.152571D+00	0.160733D+00
2.000	0.719201D-01	0.802981D-01	0.887359D-01	0.967010D-01	0.103777D+00
2.500	0.470641D-01	0.497747D-01	0.526014D-01	0.557683D-01	0.591303D-01
3.000	0.323096D-01	0.319048D-01	0.310651D-01	0.302443D-01	0.297326D-01
3.500	0.231885D-01	0.214113D-01	0.189550D-01	0.161071D-01	0.131937D-01
4.000	0.172848D-01	0.150374D-01	0.121722D-01	0.882803D-02	0.516675D-02
4.500	0.132964D-01	0.109920D-01	0.824870D-02	0.516265D-02	0.178558D-02
5.000	0.104989D-01	0.831050D-02	0.586515D-02	0.326530D-02	0.544571D-03
5.500	0.847258D-02	0.646192D-02	0.434048D-02	0.221880D-02	0.146569D-03
6.000	0.696380D-02	0.514343D-02	0.331833D-02	0.159574D-02	0.348133D-04
6.500	0.581359D-02	0.417516D-02	0.250495D-02	0.119763D-02	0.729726D-05
7.000	0.491871D-02	0.344607D-02	0.208996D-02	0.928247D-03	0.134986D-05
7.500	0.421007D-02	0.288513D-02	0.170752D-02	0.737662D-03	0.220358D-06
8.000	0.364018D-02	0.244545D-02	0.141665D-02	0.598060D-03	0.317456D-07
8.500	0.317560D-02	0.209515D-02	0.119088D-02	0.492930D-03	0.403600D-08
9.000	0.279228D-02	0.181206D-02	0.101254D-02	0.411943D-03	0.452826D-09
9.500	0.247260D-02	0.158038D-02	0.869517D-03	0.348362D-03	0.448359D-10
10.000	0.220341D-02	0.138863D-02	0.753272D-03	0.297634D-03	0.391772D-11
15.000	0.888687D-03	0.505729D-03	0.248297D-03	0.891810D-04	0.105034D-24
20.000	0.468085D-03	0.249446D-03	0.114975D-03	0.388750D-04	0.104941D-43
25.000	0.285107D-03	0.144722D-03	0.636496D-04	0.205676D-04	0.390735D-68
30.000	0.190293D-03	0.929221D-04	0.393627D-04	0.122630D-04	0.542171D-98
35.000	0.135259D-03	0.639522D-04	0.262542D-04	0.793166D-05	
40.000	0.100663D-03	0.462964D-04	0.184998D-04	0.544252D-05	
45.000	0.775364D-04	0.348294D-04	0.135915D-04	0.390608D-05	
50.000	0.614736D-04	0.270078D-04	0.103187D-04	0.290411D-05	
55.000	0.498056D-04	0.214607D-04	0.804426D-05	0.222155D-05	
60.000	0.411015D-04	0.173999D-04	0.640954D-05	0.173977D-05	
65.000	0.344464D-04	0.143479D-04	0.520136D-05	0.138957D-05	
70.000	0.292507D-04	0.120025D-04	0.428714D-05	0.112859D-05	
75.000	0.251215D-04	0.101655D-04	0.358130D-05	0.929939D-06	
80.000	0.217888D-04	0.870283D-05	0.302676D-05	0.775928D-06	
85.000	0.190625D-04	0.752145D-05	0.258442D-05	0.654594D-06	
90.000	0.168056D-04	0.655507D-05	0.222682D-05	0.557644D-06	
95.000	0.149174D-04	0.575564D-05	0.193427D-05	0.479200D-06	
100.000	0.133228D-04	0.508764D-05	0.169237D-05	0.415014D-06	
150.000	0.545311D-05	0.191971D-05	0.588956D-06	0.133222D-06	

FUNCTION Q(ALPHA,Z) FOR

Z =	ALPHA = 1.200	1.400	1.600	1.800	2.000
200.000	0.289415D-05	0.961824D-06	0.278618D-06	0.595097D-07	
250.000	0.177081D-05	0.562803D-06	0.155928D-06	0.318538D-07	
300.000	0.118544D-05	0.363267D-06	0.970472D-07	0.191165D-07	
350.000	0.844367D-06	0.250894D-06	0.649944D-07	0.124145D-07	
400.000	0.629364D-06	0.182081D-06	0.459268D-07	0.854150D-08	
450.000	0.485658D-06	0.137235D-06	0.338101D-07	0.614177D-08	
500.000	0.385155D-06	0.106567D-06	0.257075D-07	0.457260D-08	
550.000	0.312283D-06	0.847732D-07	0.200644D-07	0.350152D-08	
600.000	0.257867D-06	0.687939D-07	0.160017D-07	0.274437D-08	
650.000	0.216224D-06	0.567685D-07	0.129950D-07	0.219333D-08	
700.000	0.183690D-06	0.475175D-07	0.107174D-07	0.178231D-08	
750.000	0.157817D-06	0.402655D-07	0.895735D-08	0.146921D-08	
800.000	0.136925D-06	0.344370D-07	0.757356D-08	0.122631D-08	
850.000	0.119826D-06	0.298167D-07	0.646905D-08	0.103485D-08	
900.000	0.105665D-06	0.259942D-07	0.557566D-08	0.881801D-09	
950.000	0.938135D-07	0.228306D-07	0.484443D-08	0.757918D-09	
1000.000	0.838014D-07	0.201860D-07	0.423956D-08	0.656518D-09	
1500.000	0.343412D-07	0.762788D-08	0.147730D-08	0.210952D-09	
2000.000	0.182362D-07	0.382419D-08	0.599234D-09	0.942656D-10	
2500.000	0.111615D-07	0.223846D-08	0.391430D-09	0.504666D-10	

Table 4. Function $V_{\alpha}(Z)$ for

Z =	Alpha= 0.000	0.010	0.020	0.030	0.040
0.000	INFINITY	0.000000D+00	0.000000D+00	0.000000D+00	0.000000D+00
0.001	0.117100D+03	0.109691D+03	0.102311D+03	0.949897D+02	0.877571D+02
0.002	0.585498D+02	0.552508D+02	0.519615D+02	0.486922D+02	0.454534D+02
0.003	0.390332D+02	0.369919D+02	0.349556D+02	0.329298D+02	0.309199D+02
0.004	0.292749D+02	0.278280D+02	0.263843D+02	0.249470D+02	0.235197D+02
0.005	0.234199D+02	0.223146D+02	0.212115D+02	0.201128D+02	0.190208D+02
0.010	0.117100D+02	0.112384D+02	0.107675D+02	0.102978D+02	0.983008D+01
0.015	0.780664D+01	0.752390D+01	0.724143D+01	0.695955D+01	0.667854D+01
0.020	0.585498D+01	0.565976D+01	0.546469D+01	0.526993D+01	0.507565D+01
0.025	0.468399D+01	0.453825D+01	0.439261D+01	0.424716D+01	0.410200D+01
0.030	0.390332D+01	0.378899D+01	0.367472D+01	0.356057D+01	0.344660D+01
0.035	0.334570D+01	0.325286D+01	0.316006D+01	0.306734D+01	0.297474D+01
0.040	0.292749D+01	0.285016D+01	0.277286D+01	0.269561D+01	0.261845D+01
0.045	0.260221D+01	0.253654D+01	0.247089D+01	0.240527D+01	0.233971D+01
0.050	0.234199D+01	0.228535D+01	0.222873D+01	0.217213D+01	0.211557D+01
0.055	0.212908D+01	0.207962D+01	0.203017D+01	0.198074D+01	0.193133D+01
0.060	0.195166D+01	0.190802D+01	0.186438D+01	0.182076D+01	0.177715D+01
0.065	0.180153D+01	0.176269D+01	0.172385D+01	0.168502D+01	0.164620D+01
0.070	0.167285D+01	0.163802D+01	0.160320D+01	0.156837D+01	0.153356D+01
0.075	0.156133D+01	0.152990D+01	0.149847D+01	0.146704D+01	0.143562D+01
0.080	0.146375D+01	0.143522D+01	0.140670D+01	0.137818D+01	0.134966D+01
0.085	0.137764D+01	0.135163D+01	0.132563D+01	0.129961D+01	0.127360D+01
0.090	0.130111D+01	0.127729D+01	0.125347D+01	0.122964D+01	0.120581D+01
0.095	0.123263D+01	0.121073D+01	0.118883D+01	0.116692D+01	0.114501D+01
0.100	0.117100D+01	0.115079D+01	0.113059D+01	0.111038D+01	0.109016D+01
0.150	0.780664D+00	0.770360D+00	0.760053D+00	0.749740D+00	0.739419D+00
0.200	0.585498D+00	0.579454D+00	0.573408D+00	0.567357D+00	0.561299D+00
0.250	0.468399D+00	0.464609D+00	0.460817D+00	0.457021D+00	0.453220D+00
0.300	0.390332D+00	0.387886D+00	0.385437D+00	0.382986D+00	0.380531D+00
0.350	0.334570D+00	0.332989D+00	0.331406D+00	0.329822D+00	0.328233D+00
0.400	0.292749D+00	0.291756D+00	0.290763D+00	0.289767D+00	0.288768D+00
0.450	0.260221D+00	0.259645D+00	0.259069D+00	0.258490D+00	0.257910D+00
0.500	0.234199D+00	0.233928D+00	0.233655D+00	0.233382D+00	0.233106D+00
0.550	0.212908D+00	0.212864D+00	0.212820D+00	0.212774D+00	0.212727D+00
0.600	0.195166D+00	0.195296D+00	0.195425D+00	0.195553D+00	0.195680D+00
0.650	0.180153D+00	0.180417D+00	0.180680D+00	0.180943D+00	0.181205D+00
0.700	0.167285D+00	0.167654D+00	0.168023D+00	0.168391D+00	0.168758D+00
0.750	0.156133D+00	0.156585D+00	0.157037D+00	0.157488D+00	0.157938D+00
0.800	0.146375D+00	0.146893D+00	0.147411D+00	0.147928D+00	0.148445D+00
0.850	0.137764D+00	0.138336D+00	0.138907D+00	0.139477D+00	0.140047D+00

FUNCTION V(ALPHA,Z) FOR

Z =	ALPHA = 0.000	0.010	0.020	0.030	0.040
0.900	0.130111D+00	0.130725D+00	0.131338D+00	0.131952D+00	0.132565D+00
0.950	0.123263D+00	0.123911D+00	0.124559D+00	0.125207D+00	0.125854D+00
1.000	0.117100D+00	0.117776D+00	0.118451D+00	0.119127D+00	0.119802D+00
1.500	0.780664D-01	0.788336D-01	0.796006D-01	0.803676D-01	0.811343D-01
2.000	0.585498D-01	0.592936D-01	0.600373D-01	0.607809D-01	0.615242D-01
2.500	0.468399D-01	0.475394D-01	0.482389D-01	0.489381D-01	0.496371D-01
3.000	0.390332D-01	0.396873D-01	0.403413D-01	0.409951D-01	0.416485D-01
3.500	0.334570D-01	0.340693D-01	0.346814D-01	0.352932D-01	0.359047D-01
4.000	0.292749D-01	0.298497D-01	0.304243D-01	0.309987D-01	0.315726D-01
4.500	0.260221D-01	0.265637D-01	0.271051D-01	0.276462D-01	0.281868D-01
5.000	0.234199D-01	0.239320D-01	0.244439D-01	0.249555D-01	0.254666D-01
5.500	0.212908D-01	0.217767D-01	0.222623D-01	0.227476D-01	0.232323D-01
6.000	0.195166D-01	0.199789D-01	0.204410D-01	0.209028D-01	0.213640D-01
6.500	0.180153D-01	0.184565D-01	0.188975D-01	0.193380D-01	0.197781D-01
7.000	0.167285D-01	0.171506D-01	0.175724D-01	0.179939D-01	0.184147D-01
7.500	0.156133D-01	0.160180D-01	0.164224D-01	0.168265D-01	0.172300D-01
8.000	0.146375D-01	0.150263D-01	0.154149D-01	0.158031D-01	0.161907D-01
8.500	0.137764D-01	0.141507D-01	0.145248D-01	0.148985D-01	0.152716D-01
9.000	0.130111D-01	0.133720D-01	0.137328D-01	0.140931D-01	0.144527D-01
9.500	0.123263D-01	0.126749D-01	0.130233D-01	0.133712D-01	0.137186D-01
10.000	0.117100D-01	0.120472D-01	0.123841D-01	0.127206D-01	0.130565D-01
15.000	0.780664D-02	0.806307D-02	0.831928D-02	0.857503D-02	0.883012D-02
20.000	0.585498D-02	0.606414D-02	0.627307D-02	0.648156D-02	0.668940D-02
25.000	0.468399D-02	0.486176D-02	0.503931D-02	0.521643D-02	0.539292D-02
30.000	0.390332D-02	0.405858D-02	0.421362D-02	0.436825D-02	0.452226D-02
35.000	0.334570D-02	0.348393D-02	0.362196D-02	0.375958D-02	0.389661D-02
40.000	0.292749D-02	0.305235D-02	0.317700D-02	0.330127D-02	0.342497D-02
45.000	0.260221D-02	0.271626D-02	0.283011D-02	0.294359D-02	0.305651D-02
50.000	0.234199D-02	0.244710D-02	0.255202D-02	0.265657D-02	0.276059D-02
55.000	0.212908D-02	0.222666D-02	0.232406D-02	0.242110D-02	0.251763D-02
60.000	0.195166D-02	0.204280D-02	0.213377D-02	0.222439D-02	0.231451D-02
65.000	0.180153D-02	0.188711D-02	0.197251D-02	0.205757D-02	0.214215D-02
70.000	0.167285D-02	0.175355D-02	0.183408D-02	0.191429D-02	0.199401D-02
75.000	0.156133D-02	0.163772D-02	0.171396D-02	0.178987D-02	0.186532D-02
80.000	0.146375D-02	0.153631D-02	0.160871D-02	0.168081D-02	0.175245D-02
85.000	0.137764D-02	0.144677D-02	0.151575D-02	0.158442D-02	0.165264D-02
90.000	0.130111D-02	0.136714D-02	0.143302D-02	0.149860D-02	0.156375D-02
95.000	0.123263D-02	0.129585D-02	0.135892D-02	0.142170D-02	0.148406D-02
100.000	0.117100D-02	0.123166D-02	0.129217D-02	0.135240D-02	0.141221D-02
150.000	0.780664D-03	0.824266D-03	0.867744D-03	0.910983D-03	0.953874D-03
200.000	0.585498D-03	0.619881D-03	0.654156D-03	0.688222D-03	0.721984D-03
250.000	0.468399D-03	0.496948D-03	0.525401D-03	0.553667D-03	0.581661D-03
300.000	0.390332D-03	0.414834D-03	0.439247D-03	0.463490D-03	0.487486D-03
350.000	0.334570D-03	0.356087D-03	0.377521D-03	0.398799D-03	0.419848D-03
400.000	0.292749D-03	0.311966D-03	0.331107D-03	0.350101D-03	0.368884D-03
450.000	0.260221D-03	0.277609D-03	0.294925D-03	0.312104D-03	0.329085D-03
500.000	0.234199D-03	0.250094D-03	0.265922D-03	0.281620D-03	0.297131D-03
550.000	0.212908D-03	0.227561D-03	0.242150D-03	0.256615D-03	0.270904D-03
600.000	0.195166D-03	0.208767D-03	0.222307D-03	0.235730D-03	0.248985D-03
650.000	0.180153D-03	0.192852D-03	0.205492D-03	0.218021D-03	0.230389D-03
700.000	0.167285D-03	0.179200D-03	0.191060D-03	0.202812D-03	0.214411D-03
750.000	0.156133D-03	0.167361D-03	0.178536D-03	0.189608D-03	0.200532D-03
800.000	0.146375D-03	0.156995D-03	0.167564D-03	0.178035D-03	0.188363D-03
850.000	0.137764D-03	0.147844D-03	0.157873D-03	0.167807D-03	0.177604D-03
900.000	0.130111D-03	0.139704D-03	0.149250D-03	0.158703D-03	0.168023D-03
950.000	0.123263D-03	0.132418D-03	0.141526D-03	0.150545D-03	0.159436D-03
1000.000	0.117100D-03	0.125857D-03	0.134569D-03	0.143194D-03	0.151695D-03
1500.000	0.780664D-04	0.842202D-04	0.903386D-04	0.963895D-04	0.102344D-03
2000.000	0.585498D-04	0.633330D-04	0.680868D-04	0.727842D-04	0.774014D-04
2500.000	0.468399D-04	0.507706D-04	0.546758D-04	0.585322D-04	0.623192D-04

FUNCTION V(ALPHA,Z) FOR

Z =	ALPHA = 0.050	0.060	0.070	0.080	0.090
0.000	0.000000D+00	0.000000D+00	0.000000D+00	0.000000D+00	0.000000D+00
0.001	0.806454D+02	0.736872D+02	0.669151D+02	0.603620D+02	0.540601D+02
0.002	0.422560D+02	0.391113D+02	0.360304D+02	0.330249D+02	0.301063D+02
0.003	0.289316D+02	0.269706D+02	0.250428D+02	0.231544D+02	0.213115D+02
0.004	0.221057D+02	0.207086D+02	0.193322D+02	0.179802D+02	0.166565D+02
0.005	0.179380D+02	0.168668D+02	0.158097D+02	0.147692D+02	0.137482D+02
0.010	0.936497D+01	0.890318D+01	0.844543D+01	0.799246D+01	0.754503D+01
0.015	0.639871D+01	0.612037D+01	0.584384D+01	0.556946D+01	0.529757D+01
0.020	0.488201D+01	0.468918D+01	0.449733D+01	0.430664D+01	0.411730D+01
0.025	0.395722D+01	0.381292D+01	0.366921D+01	0.352620D+01	0.338400D+01

FUNCTION V(ALPHA,Z) FOR

Z =	ALPHA = 0.050	0.060	0.070	0.080	0.090
0.030	0.333288D+01	0.321947D+01	0.310643D+01	0.299383D+01	0.288175D+01
0.035	0.286230D+01	0.279006D+01	0.269808D+01	0.260638D+01	0.251503D+01
0.040	0.254139D+01	0.246448D+01	0.238773D+01	0.231117D+01	0.223485D+01
0.045	0.227423D+01	0.220884D+01	0.214356D+01	0.207842D+01	0.201343D+01
0.050	0.205906D+01	0.200261D+01	0.194624D+01	0.188997D+01	0.183380D+01
0.055	0.188195D+01	0.183262D+01	0.178335D+01	0.173413D+01	0.168498D+01
0.060	0.173357D+01	0.169001D+01	0.164649D+01	0.160301D+01	0.155957D+01
0.065	0.160739D+01	0.156860D+01	0.152983D+01	0.149108D+01	0.145236D+01
0.070	0.149875D+01	0.146395D+01	0.142915D+01	0.139437D+01	0.135961D+01
0.075	0.140419D+01	0.137277D+01	0.134135D+01	0.130994D+01	0.127853D+01
0.080	0.132114D+01	0.129261D+01	0.126408D+01	0.123555D+01	0.120701D+01
0.085	0.124758D+01	0.122156D+01	0.119553D+01	0.116949D+01	0.114344D+01
0.090	0.118198D+01	0.115814D+01	0.113428D+01	0.111042D+01	0.108654D+01
0.095	0.112309D+01	0.110116D+01	0.107922D+01	0.105726D+01	0.103529D+01
0.100	0.106993D+01	0.104969D+01	0.102944D+01	0.100917D+01	0.988880D+00
0.150	0.729086D+00	0.718738D+00	0.708371D+00	0.697984D+00	0.687571D+00
0.200	0.555231D+00	0.549150D+00	0.543055D+00	0.536941D+00	0.530807D+00
0.250	0.449411D+00	0.445592D+00	0.441761D+00	0.437916D+00	0.434055D+00
0.300	0.378069D+00	0.375599D+00	0.373120D+00	0.370630D+00	0.368128D+00
0.350	0.326640D+00	0.325040D+00	0.323433D+00	0.321817D+00	0.320191D+00
0.400	0.287766D+00	0.286758D+00	0.285745D+00	0.284725D+00	0.283696D+00
0.450	0.257326D+00	0.256738D+00	0.256145D+00	0.255547D+00	0.254942D+00
0.500	0.232828D+00	0.232547D+00	0.232262D+00	0.231972D+00	0.231676D+00
0.550	0.212678D+00	0.212626D+00	0.212570D+00	0.212511D+00	0.212448D+00
0.600	0.195805D+00	0.195927D+00	0.196048D+00	0.196164D+00	0.196278D+00
0.650	0.181465D+00	0.181723D+00	0.181978D+00	0.182232D+00	0.182482D+00
0.700	0.169123D+00	0.169487D+00	0.169850D+00	0.170209D+00	0.170567D+00
0.750	0.158388D+00	0.158835D+00	0.159282D+00	0.159726D+00	0.160168D+00
0.800	0.148961D+00	0.149476D+00	0.149989D+00	0.150501D+00	0.151011D+00
0.850	0.140617D+00	0.141185D+00	0.141752D+00	0.142318D+00	0.142882D+00
0.900	0.133177D+00	0.133788D+00	0.134398D+00	0.135007D+00	0.135615D+00
0.950	0.126501D+00	0.127147D+00	0.127792D+00	0.128436D+00	0.129078D+00
1.000	0.120476D+00	0.121150D+00	0.121823D+00	0.122495D+00	0.123166D+00
1.500	0.819007D-01	0.826668D-01	0.834325D-01	0.841977D-01	0.849624D-01
2.000	0.622672D-01	0.630099D-01	0.637522D-01	0.644939D-01	0.652351D-01
2.500	0.503357D-01	0.510339D-01	0.517315D-01	0.524285D-01	0.531248D-01
3.000	0.423015D-01	0.429540D-01	0.436058D-01	0.442568D-01	0.449070D-01
3.500	0.365156D-01	0.371259D-01	0.377355D-01	0.383442D-01	0.389519D-01
4.000	0.321460D-01	0.327186D-01	0.332904D-01	0.338612D-01	0.344310D-01
4.500	0.287268D-01	0.292660D-01	0.298044D-01	0.303416D-01	0.308777D-01
5.000	0.259770D-01	0.264865D-01	0.269951D-01	0.275026D-01	0.280089D-01
5.500	0.237164D-01	0.241995D-01	0.246817D-01	0.251627D-01	0.256423D-01
6.000	0.218244D-01	0.222840D-01	0.227425D-01	0.231998D-01	0.236557D-01
6.500	0.202173D-01	0.206556D-01	0.210928D-01	0.215288D-01	0.219633D-01
7.000	0.188348D-01	0.192539D-01	0.196719D-01	0.200886D-01	0.205038D-01
7.500	0.176326D-01	0.180343D-01	0.184349D-01	0.188341D-01	0.192318D-01
8.000	0.165775D-01	0.169633D-01	0.173479D-01	0.177311D-01	0.181129D-01
8.500	0.156438D-01	0.160150D-01	0.163850D-01	0.167537D-01	0.171208D-01
9.000	0.148116D-01	0.151694D-01	0.155260D-01	0.158812D-01	0.162349D-01
9.500	0.140651D-01	0.144105D-01	0.147547D-01	0.150976D-01	0.154388D-01
10.000	0.133916D-01	0.137256D-01	0.140583D-01	0.143897D-01	0.147195D-01
15.000	0.908435D-02	0.933751D-02	0.958941D-02	0.983989D-02	0.100888D-01
20.000	0.689639D-02	0.710234D-02	0.730706D-02	0.751038D-02	0.771215D-02
25.000	0.556859D-02	0.574325D-02	0.591672D-02	0.608885D-02	0.625948D-02
30.000	0.467548D-02	0.482773D-02	0.497883D-02	0.512865D-02	0.527702D-02
35.000	0.403287D-02	0.416920D-02	0.430243D-02	0.443541D-02	0.456702D-02
40.000	0.354793D-02	0.366998D-02	0.379097D-02	0.391077D-02	0.402924D-02
45.000	0.316872D-02	0.328005D-02	0.339037D-02	0.349953D-02	0.360741D-02
50.000	0.286392D-02	0.296640D-02	0.306789D-02	0.316827D-02	0.326742D-02
55.000	0.261348D-02	0.270851D-02	0.280259D-02	0.289559D-02	0.298740D-02
60.000	0.240398D-02	0.249265D-02	0.258039D-02	0.266710D-02	0.275264D-02
65.000	0.222609D-02	0.230926D-02	0.239153D-02	0.247279D-02	0.255293D-02
70.000	0.207312D-02	0.215148D-02	0.222897D-02	0.230547D-02	0.238089D-02
75.000	0.194016D-02	0.201427D-02	0.208754D-02	0.215985D-02	0.223110D-02
80.000	0.182350D-02	0.189384D-02	0.196335D-02	0.203193D-02	0.209948D-02
85.000	0.172029D-02	0.178725D-02	0.135340D-02	0.191864D-02	0.198289D-02
90.000	0.162834D-02	0.169224D-02	0.175537D-02	0.181760D-02	0.187886D-02
95.000	0.154587D-02	0.160702D-02	0.166739D-02	0.172690D-02	0.178546D-02
100.000	0.147149D-02	0.153012D-02	0.158799D-02	0.164502D-02	0.170112D-02
150.000	0.996316D-03	0.103822D-02	0.107950D-02	0.112008D-02	0.115989D-02
200.000	0.755356D-03	0.788259D-03	0.820623D-03	0.852384D-03	0.883487D-03
250.000	0.609306D-03	0.636535D-03	0.663283D-03	0.689497D-03	0.715128D-03
300.000	0.511165D-03	0.534466D-03	0.557332D-03	0.579716D-03	0.601574D-03
350.000	0.440607D-03	0.461018D-03	0.481031D-03	0.500601D-03	0.519691D-03
400.000	0.387397D-03	0.405586D-03	0.423407D-03	0.440818D-03	0.457786D-03
450.000	0.345812D-03	0.362238D-03	0.378320D-03	0.394019D-03	0.409305D-03
500.000	0.312404D-03	0.327394D-03	0.342059D-03	0.356366D-03	0.370285D-03
550.000	0.284968D-03	0.298763D-03	0.312252D-03	0.325403D-03	0.338188D-03
600.000	0.262026D-03	0.274811D-03	0.287307D-03	0.299482D-03	0.311311D-03
650.000	0.242553D-03	0.254474D-03	0.266118D-03	0.277457D-03	0.288468D-03

FUNCTION V(ALPHA,Z) FOR

Z =	ALPHA = 0.050	0.060	0.070	0.080	0.090
700.000	0.225814D-03	0.236985D-03	0.247891D-03	0.258507D-03	0.268809D-03
750.000	0.211269D-03	0.221783D-03	0.232044D-03	0.242026D-03	0.251708D-03
800.000	0.198510D-03	0.208444D-03	0.218135D-03	0.227557D-03	0.236692D-03
850.000	0.187227D-03	0.196644D-03	0.205827D-03	0.214752D-03	0.223401D-03
900.000	0.177176D-03	0.186130D-03	0.194858D-03	0.203338D-03	0.211551D-03
950.000	0.168165D-03	0.176701D-03	0.185019D-03	0.193097D-03	0.200918D-03
1000.000	0.160039D-03	0.168197D-03	0.176143D-03	0.183858D-03	0.191324D-03
1500.000	0.108176D-03	0.113865D-03	0.119392D-03	0.124741D-03	0.129902D-03
2000.000	0.819174D-04	0.863145D-04	0.905779D-04	0.946957D-04	0.986584D-04
2500.000	0.660190D-04	0.696164D-04	0.730990D-04	0.764568D-04	0.796821D-04

FUNCTION V(ALPHA,Z) FOR

Z =	ALPHA = 0.100	0.200	0.300	0.400	0.500
0.000	0.000000D+00	0.000000D+00	0.000000D+00	0.000000D+00	0.000000D+00
0.001	0.480405D+02	0.815844D+01	0.338702D+00	0.190510D-01	0.381918D-02
0.002	0.272861D+02	0.661488D+01	0.537512D+00	0.378287D-01	0.763517D-02
0.003	0.195201D+02	0.568045D+01	0.561137D+00	0.561089D-01	0.114448D-01
0.004	0.153648D+02	0.503700D+01	0.742682D+00	0.737345D-01	0.152449D-01
0.005	0.127491D+02	0.455850D+01	0.798486D+00	0.906088D-01	0.190324D-01
0.010	0.710394D+01	0.323182D+01	0.906972D+00	0.162899D+00	0.376821D-01
0.015	0.502853D+01	0.258579D+01	0.915169D+00	0.217042D+00	0.556294D-01
0.020	0.392950D+01	0.218780D+01	0.896210D+00	0.257345D+00	0.726480D-01
0.025	0.324272D+01	0.191260D+01	0.868895D+00	0.287508D+00	0.886031D-01
0.030	0.277025D+01	0.170858D+01	0.839543D+00	0.310219D+00	0.1034340+00
0.035	0.242406D+01	0.155005D+01	0.810541D+00	0.327383D+00	0.1171310+00
0.040	0.215879D+01	0.142262D+01	0.782818D+00	0.340358D+00	0.1297240+00
0.045	0.194862D+01	0.131753D+01	0.756696D+00	0.350123D+00	0.1412600+00
0.050	0.177775D+01	0.122908D+01	0.732238D+00	0.357399D+00	0.1518000+00
0.055	0.163592D+01	0.115344D+01	0.709392D+00	0.362723D+00	0.1614120+00
0.060	0.151618D+01	0.108786D+01	0.688058D+00	0.366502D+00	0.1701640+00
0.065	0.141367D+01	0.103037D+01	0.668121D+00	0.369048D+00	0.1781230+00
0.070	0.132486D+01	0.979490D+00	0.649462D+00	0.370605D+00	0.1853540+00
0.075	0.124712D+01	0.934082D+00	0.631972D+00	0.371361D+00	0.1919160+00
0.080	0.117847D+01	0.893267D+00	0.615547D+00	0.371668D+00	0.1978670+00
0.085	0.111738D+01	0.856348D+00	0.600093D+00	0.371045D+00	0.2032580+00
0.090	0.106264D+01	0.822766D+00	0.585526D+00	0.370191D+00	0.2081370+00
0.095	0.101329D+01	0.792066D+00	0.571770D+00	0.368984D+00	0.2125490+00
0.100	0.968566D+00	0.763875D+00	0.558757D+00	0.367489D+00	0.2165330+00
0.150	0.677130D+00	0.570485D+00	0.458737D+00	0.344803D+00	0.2394840+00
0.200	0.524650D+00	0.461183D+00	0.392781D+00	0.319280D+00	0.2448760+00
0.250	0.430175D+00	0.389877D+00	0.345462D+00	0.295891D+00	0.2425200+00
0.300	0.365610D+00	0.339253D+00	0.309569D+00	0.275339D+00	0.2366720+00
0.350	0.318554D+00	0.301239D+00	0.281248D+00	0.257417D+00	0.2293180+00
0.400	0.282658D+00	0.271528D+00	0.258236D+00	0.241749D+00	0.2214320+00
0.450	0.254329D+00	0.247597D+00	0.239109D+00	0.227972D+00	0.2135030+00
0.500	0.231375D+00	0.227864D+00	0.222918D+00	0.215777D+00	0.2057790+00
0.550	0.212379D+00	0.211285D+00	0.209010D+00	0.204910D+00	0.1983810+00
0.600	0.195387D+00	0.197139D+00	0.196912D+00	0.195166D+00	0.1913590+00
0.650	0.182728D+00	0.184912D+00	0.186280D+00	0.186377D+00	0.1847290+00
0.700	0.170921D+00	0.174228D+00	0.176851D+00	0.178407D+00	0.1784860+00
0.750	0.160608D+00	0.164805D+00	0.168425D+00	0.171145D+00	0.1726140+00
0.800	0.151518D+00	0.156425D+00	0.160842D+00	0.164499D+00	0.1670910+00
0.850	0.143444D+00	0.148919D+00	0.153978D+00	0.158390D+00	0.1618970+00
0.900	0.136221D+00	0.142155D+00	0.147731D+00	0.152755D+00	0.1570070+00
0.950	0.129720D+00	0.136023D+00	0.142018D+00	0.147539D+00	0.1523990+00
1.000	0.123836D+00	0.130438D+00	0.136771D+00	0.142695D+00	0.1480530+00
1.500	0.857265D-01	0.933236D-01	0.100818D+00	0.108148D+00	0.1153110+00
2.000	0.659757D-01	0.733365D-01	0.805867D-01	0.876998D-01	0.9466420-01
2.500	0.538204D-01	0.607193D-01	0.674783D-01	0.740625D-01	0.8045560-01
3.000	0.455563D-01	0.519799D-01	0.582320D-01	0.642672D-01	0.7006190-01
3.500	0.395585D-01	0.455446D-01	0.513312D-01	0.568547D-01	0.6211580-01
4.000	0.349995D-01	0.405953D-01	0.459685D-01	0.510595D-01	0.5583530-01
4.500	0.314125D-01	0.366629D-01	0.416721D-01	0.463763D-01	0.5074120-01
5.000	0.285137D-01	0.334584D-01	0.381470D-01	0.425132D-01	0.4652260-01
5.500	0.261205D-01	0.307936D-01	0.351989D-01	0.392686D-01	0.4296930-01
6.000	0.241100D-01	0.285407D-01	0.326942D-01	0.365027D-01	0.3993370-01
6.500	0.223963D-01	0.266095D-01	0.305383D-01	0.341149D-01	0.3730910-01
7.000	0.209175D-01	0.249346D-01	0.286616D-01	0.320316D-01	0.3501650-01
7.500	0.196279D-01	0.234673D-01	0.270123D-01	0.301971D-01	0.3299600-01
8.000	0.184930D-01	0.221706D-01	0.255557D-01	0.285686D-01	0.3120120-01
8.500	0.174362D-01	0.210160D-01	0.242458D-01	0.271128D-01	0.2959600-01
9.000	0.165869D-01	0.199809D-01	0.230734D-01	0.258031D-01	0.2815160-01
9.500	0.157784D-01	0.190474D-01	0.220139D-01	0.246183D-01	0.2684470-01

FUNCTION V(ALPHA,Z) FOR

Z =	ALPHA = 0.100	0.200	0.300	0.400	0.500
10.000	0.150475D-01	0.182010D-01	0.210514D-01	0.235411D-01	0.2565630-01
15.000	0.103359D-01	0.126805D-01	0.147318D-01	0.164491D-01	0.1783700-01
20.000	0.791220D-02	0.979139D-02	0.113952D-01	0.126962D-01	0.1371010-01
25.000	0.642846D-02	0.800285D-02	0.931975D-02	0.103619D-01	0.1116100-01
30.000	0.542382D-02	0.678206D-02	0.789942D-02	0.876511D-02	0.9405630-02
35.000	0.469711D-02	0.589356D-02	0.686366D-02	0.760200D-02	0.8137520-02
40.000	0.414626D-02	0.521677D-02	0.607375D-02	0.671595D-02	0.7173800-02
45.000	0.371390D-02	0.468340D-02	0.545074D-02	0.601789D-02	0.6416160-02
50.000	0.336522D-02	0.425182D-02	0.494635D-02	0.545336D-02	0.5804620-02
55.000	0.307791D-02	0.389515D-02	0.452936D-02	0.498717D-02	0.5300490-02
60.000	0.283694D-02	0.359526D-02	0.417869D-02	0.459552D-02	0.4877640-02
65.000	0.263185D-02	0.333947D-02	0.387954D-02	0.426175D-02	0.4517810-02
70.000	0.245513D-02	0.311861D-02	0.362124D-02	0.397384D-02	0.4207830-02
75.000	0.230121D-02	0.292593D-02	0.339539D-02	0.372289D-02	0.3937990-02
80.000	0.216592D-02	0.275629D-02	0.319751D-02	0.350216D-02	0.3700920-02
85.000	0.204604D-02	0.260576D-02	0.302150D-02	0.330648D-02	0.3490990-02
90.000	0.193906D-02	0.247126D-02	0.286424D-02	0.313179D-02	0.3303770-02
95.000	0.184299D-02	0.235031D-02	0.272286D-02	0.297486D-02	0.3135740-02
100.000	0.175622D-02	0.224097D-02	0.259505D-02	0.283311D-02	0.2984100-02
150.000	0.119889D-02	0.153572D-02	0.177156D-02	0.192260D-02	0.2013660-02
200.000	0.913883D-03	0.117297D-02	0.134891D-02	0.145777D-02	0.1521110-02
250.000	0.740136D-03	0.951055D-03	0.109089D-02	0.117514D-02	0.1222830-02
300.000	0.622871D-03	0.800929D-03	0.918690D-03	0.984900D-03	0.1022680-02
350.000	0.538268D-03	0.692439D-03	0.790988D-03	0.846020D-03	0.8790150-03
400.000	0.474281D-03	0.610283D-03	0.695959D-03	0.744758D-03	0.7708560-03
450.000	0.424152D-03	0.545859D-03	0.621545D-03	0.664055D-03	0.6867710-03
500.000	0.383794D-03	0.493953D-03	0.561669D-03	0.599229D-03	0.6187870-03
550.000	0.350587D-03	0.451218D-03	0.512432D-03	0.546003D-03	0.5632880-03
600.000	0.322773D-03	0.415408D-03	0.471219D-03	0.501512D-03	0.5169500-03
650.000	0.299130D-03	0.384956D-03	0.436238D-03	0.463764D-03	0.4776750-03
700.000	0.278779D-03	0.358735D-03	0.406091D-03	0.431331D-03	0.4439620-03
750.000	0.261072D-03	0.335916D-03	0.379906D-03	0.403161D-03	0.4147050-03
800.000	0.245524D-03	0.315372D-03	0.356926D-03	0.378464D-03	0.3890750-03
850.000	0.231758D-03	0.298125D-03	0.336594D-03	0.356633D-03	0.3664350-03
900.000	0.219483D-03	0.282298D-03	0.318477D-03	0.337196D-03	0.3462920-03
950.000	0.208468D-03	0.268093D-03	0.302228D-03	0.319778D-03	0.3282520-03
1000.000	0.198528D-03	0.255272D-03	0.287573D-03	0.304080D-03	0.3120040-03
1500.000	0.134864D-03	0.173148D-03	0.193975D-03	0.204124D-03	0.2087740-03
2000.000	0.102459D-03	0.131354D-03	0.146573D-03	0.153745D-03	0.1569250-03
2500.000	0.827696D-04	0.105972D-03	0.117890D-03	0.123362D-03	0.1257280-03

FUNCTION V(ALPHA,Z) FOR

Z =	ALPHA = 0.600	0.700	0.800	0.900	1.000
0.000	0.000000D+00	0.000000D+00	0.000000D+00	0.000000D+00	0.000000D+00
0.001	0.147382D-02	0.800408D-03	0.528926D-03	0.394480D-03	0.3183100-03
0.002	0.294744D-02	0.160078D-02	0.105784D-02	0.788956D-03	0.6366170-03
0.003	0.442065D-02	0.240114D-02	0.158674D-02	0.1183420-02	0.9549210-03
0.004	0.589324D-02	0.320129D-02	0.211561D-02	0.1577880-02	0.1273220-02
0.005	0.736500D-02	0.400136D-02	0.264444D-02	0.1972320-02	0.1591510-02
0.010	0.1470430-01	0.799851D-02	0.528769D-02	0.3944170-02	0.3182780-02
0.015	0.2199300-01	0.119873D-01	0.792855D-02	0.5915070-02	0.4773570-02
0.020	0.2927070-01	0.159634D-01	0.1056580-01	0.7884530-02	0.6363650-02
0.025	0.3632400-01	0.199230D-01	0.1319840-01	0.9852100-02	0.7952780-02
0.030	0.4332360-01	0.238619D-01	0.1582500-01	0.1181730-01	0.9540710-02
0.035	0.5018780-01	0.277763D-01	0.1844460-01	0.1377970-01	0.1112720-01
0.040	0.5690050-01	0.316625D-01	0.2105590-01	0.1573870-01	0.1271210-01
0.045	0.6344850-01	0.355168D-01	0.2365790-01	0.1769400-01	0.1429050-01
0.050	0.6982060-01	0.393358D-01	0.2624940-01	0.1964500-01	0.1587580-01
0.055	0.7600790-01	0.431161D-01	0.2882930-01	0.2159140-01	0.1745620-01
0.060	0.8200390-01	0.468548D-01	0.3139660-01	0.2353260-01	0.1903010-01
0.065	0.8780350-01	0.505488D-01	0.3395030-01	0.2546820-01	0.2060310-01
0.070	0.9340390-01	0.541954D-01	0.3648920-01	0.2739770-01	0.2217300-01
0.075	0.9880330-01	0.577922D-01	0.3901250-01	0.2932080-01	0.2373970-01
0.080	0.1040020+00	0.613368D-01	0.4151910-01	0.3123700-01	0.2530290-01
0.085	0.1090000+00	0.648270D-01	0.4400810-01	0.3314590-01	0.2686230-01
0.090	0.1138000+00	0.682610D-01	0.4647860-01	0.3504700-01	0.2841770-01
0.095	0.1184040+00	0.716371D-01	0.4892970-01	0.3694000-01	0.2996900-01
0.100	0.1228170+00	0.749537D-01	0.5136050-01	0.3882430-01	0.3151580-01
0.150	0.1574150+00	0.1046410+00	0.7439500-01	0.5711240-01	0.4669580-01
0.200	0.1783230+00	0.1278930+00	0.9473450-01	0.7415680-01	0.6121340-01
0.250	0.1900930+00	0.1452670+00	0.1120970+00	0.8969760-01	0.7489640-01
0.300	0.1959410+00	0.1577310+00	0.1264800+00	0.1035740+00	0.8760820-01
0.350	0.1979760+00	0.1662900+00	0.1380650+00	0.1157170+00	0.9925030-01

FUNCTION V(ALPHA,Z) FOR

Z =	ALPHA = 0.600	0.700	0.800	0.900	1.000
0.400	0.197561D+00	0.171831D+00	0.147143D+00	0.126136D+00	0.109762D+00
0.450	0.195576D+00	0.175074D+00	0.154043D+00	0.134902D+00	0.119118D+00
0.500	0.192596D+00	0.176588D+00	0.159096D+00	0.142124D+00	0.127326D+00
0.550	0.189002D+00	0.176810D+00	0.162609D+00	0.147940D+00	0.134411D+00
0.600	0.185047D+00	0.176074D+00	0.164853D+00	0.152496D+00	0.140431D+00
0.650	0.180901D+00	0.174632D+00	0.166065D+00	0.155942D+00	0.145449D+00
0.700	0.176680D+00	0.172677D+00	0.166442D+00	0.158421D+00	0.149542D+00
0.750	0.172459D+00	0.170355D+00	0.166150D+00	0.160069D+00	0.152789D+00
0.800	0.168291D+00	0.167775D+00	0.165328D+00	0.161007D+00	0.155273D+00
0.850	0.164209D+00	0.165022D+00	0.164086D+00	0.161345D+00	0.157076D+00
0.900	0.160235D+00	0.162158D+00	0.162518D+00	0.161180D+00	0.158276D+00
0.950	0.156381D+00	0.159233D+00	0.160698D+00	0.160595D+00	0.158946D+00
1.000	0.152656D+00	0.156282D+00	0.158687D+00	0.159665D+00	0.159155D+00
1.500	0.122267D+00	0.128977D+00	0.135385D+00	0.141403D+00	0.146912D+00
2.000	0.101479D+00	0.108148D+00	0.114678D+00	0.121072D+00	0.127324D+00
2.500	0.866550D-01	0.926685D-01	0.985108D-01	0.104201D+00	0.109762D+00
3.000	0.756084D-01	0.809101D-01	0.859790D-01	0.908326D-01	0.954930D-01
3.500	0.670726D-01	0.717359D-01	0.761147D-01	0.802238D-01	0.840819D-01
4.000	0.602827D-01	0.644013D-01	0.681999D-01	0.716924D-01	0.749964D-01
4.500	0.547533D-01	0.584135D-01	0.617317D-01	0.647233D-01	0.674368D-01
5.000	0.501630D-01	0.534374D-01	0.563581D-01	0.589432D-01	0.612134D-01
5.500	0.462908D-01	0.492390D-01	0.518292D-01	0.540825D-01	0.560225D-01
6.000	0.429800D-01	0.456505D-01	0.479637D-01	0.499440D-01	0.516178D-01
6.500	0.401164D-01	0.425487D-01	0.446280D-01	0.463815D-01	0.478385D-01
7.000	0.376147D-01	0.398414D-01	0.417215D-01	0.432849D-01	0.445634D-01
7.500	0.354102D-01	0.374580D-01	0.391671D-01	0.405699D-01	0.417000D-01
8.000	0.334526D-01	0.353438D-01	0.369051D-01	0.381709D-01	0.391766D-01
8.500	0.317025D-01	0.334558D-01	0.348884D-01	0.360366D-01	0.369370D-01
9.000	0.301284D-01	0.317595D-01	0.330795D-01	0.341259D-01	0.349365D-01
9.500	0.287049D-01	0.302272D-01	0.314479D-01	0.324057D-01	0.331391D-01
10.000	0.274113D-01	0.288363D-01	0.299690D-01	0.308492D-01	0.315158D-01
15.000	0.189255D-01	0.197561D-01	0.203728D-01	0.208174D-01	0.211268D-01
20.000	0.144739D-01	0.150319D-01	0.154272D-01	0.156979D-01	0.158758D-01
25.000	0.117273D-01	0.121345D-01	0.124130D-01	0.125965D-01	0.127121D-01
30.000	0.986165D-02	0.101754D-01	0.103840D-01	0.105174D-01	0.105986D-01
35.000	0.851088D-02	0.876210D-02	0.892522D-02	0.902694D-02	0.908715D-02
40.000	0.748725D-02	0.769418D-02	0.782589D-02	0.790629D-02	0.795278D-02
45.000	0.668450D-02	0.685873D-02	0.696773D-02	0.703306D-02	0.707006D-02
50.000	0.603796D-02	0.618725D-02	0.627924D-02	0.633349D-02	0.636365D-02
55.000	0.550598D-02	0.563574D-02	0.571461D-02	0.576046D-02	0.578554D-02
60.000	0.506054D-02	0.517466D-02	0.524318D-02	0.528249D-02	0.530369D-02
65.000	0.468206D-02	0.478344D-02	0.484363D-02	0.487776D-02	0.489592D-02
70.000	0.435647D-02	0.444731D-02	0.450069D-02	0.453062D-02	0.454636D-02
75.000	0.407339D-02	0.415539D-02	0.420311D-02	0.422961D-02	0.424338D-02
80.000	0.382500D-02	0.389948D-02	0.394246D-02	0.396609D-02	0.397825D-02
85.000	0.360526D-02	0.367331D-02	0.371225D-02	0.373349D-02	0.374430D-02
90.000	0.340949D-02	0.347198D-02	0.350746D-02	0.352665D-02	0.353634D-02
95.000	0.323395D-02	0.329159D-02	0.332409D-02	0.334153D-02	0.335026D-02
100.000	0.307567D-02	0.312906D-02	0.315835D-02	0.317488D-02	0.318278D-02
150.000	0.206611D-02	0.209515D-02	0.211055D-02	0.211835D-02	0.212197D-02
200.000	0.155631D-02	0.157512D-02	0.158475D-02	0.158942D-02	0.159151D-02
250.000	0.124862D-02	0.126203D-02	0.126871D-02	0.127186D-02	0.127322D-02
300.000	0.104266D-02	0.105283D-02	0.105778D-02	0.106006D-02	0.106102D-02
350.000	0.895114D-03	0.903153D-03	0.906999D-03	0.908735D-03	0.909449D-03
400.000	0.784199D-03	0.790758D-03	0.793845D-03	0.795217D-03	0.795770D-03
450.000	0.697773D-03	0.703253D-03	0.705737D-03	0.706910D-03	0.707352D-03
500.000	0.628528D-03	0.633193D-03	0.635332D-03	0.636256D-03	0.636617D-03
550.000	0.571800D-03	0.575833D-03	0.577662D-03	0.578442D-03	0.578743D-03
600.000	0.524476D-03	0.528006D-03	0.529591D-03	0.530260D-03	0.530515D-03
650.000	0.484395D-03	0.487518D-03	0.488907D-03	0.489488D-03	0.489706D-03
700.000	0.450011D-03	0.452799D-03	0.454028D-03	0.454537D-03	0.454727D-03
750.000	0.420190D-03	0.422698D-03	0.423795D-03	0.424246D-03	0.424412D-03
800.000	0.394079D-03	0.396351D-03	0.397337D-03	0.397739D-03	0.397887D-03
850.000	0.371027D-03	0.373097D-03	0.373989D-03	0.374351D-03	0.374482D-03
900.000	0.350525D-03	0.352421D-03	0.353233D-03	0.353560D-03	0.353677D-03
950.000	0.332172D-03	0.333917D-03	0.334660D-03	0.334957D-03	0.335063D-03
1000.000	0.315647D-03	0.317260D-03	0.317942D-03	0.318213D-03	0.318310D-03
1500.000	0.210816D-03	0.211680D-03	0.212030D-03	0.212162D-03	0.212205D-03
2000.000	0.158278D-03	0.158833D-03	0.159050D-03	0.159129D-03	0.159155D-03
2500.000	0.126711D-03	0.127103D-03	0.127254D-03	0.127307D-03	0.127324D-03

FUNCTION V(ALPHA,Z) FOR

Z =	ALPHA = 1.100	1.200	1.300	1.400	1.500
0.000	0.000000D+00	0.000000D+00	0.000000D+00	0.000000D+00	0.000000D+00
0.001	0.270950D-03	0.239461D-03	0.217449D-03	0.201462D-03	0.189495D-03
0.002	0.541899D-03	0.478920D-03	0.434898D-03	0.402924D-03	0.378992D-03
0.003	0.812845D-03	0.718379D-03	0.652346D-03	0.604384D-03	0.568487D-03
0.004	0.108379D-02	0.957835D-03	0.869792D-03	0.805844D-03	0.757981D-03
0.005	0.135473D-02	0.119729D-02	0.108724D-02	0.100730D-02	0.947674D-03
0.010	0.270931D-02	0.239448D-02	0.217441D-02	0.201455D-02	0.189491D-02
0.015	0.406362D-02	0.359149D-02	0.326144D-02	0.302171D-02	0.284226D-02
0.020	0.541751D-02	0.478823D-02	0.434829D-02	0.402871D-02	0.378950D-02
0.025	0.677083D-02	0.598460D-02	0.543486D-02	0.503551D-02	0.473657D-02
0.030	0.812346D-02	0.718050D-02	0.652111D-02	0.604206D-02	0.568346D-02
0.035	0.947524D-02	0.837586D-02	0.760697D-02	0.704831D-02	0.663008D-02
0.040	0.108261D-01	0.957057D-02	0.869236D-02	0.805422D-02	0.757644D-02
0.045	0.121757D-01	0.107645D-01	0.977723D-02	0.905972D-02	0.852248D-02
0.050	0.135242D-01	0.119577D-01	0.108615D-01	0.100648D-01	0.946816D-02
0.055	0.148712D-01	0.131499D-01	0.119451D-01	0.110693D-01	0.1041340-01
0.060	0.162167D-01	0.143411D-01	0.130280D-01	0.120733D-01	0.113583D-01
0.065	0.175606D-01	0.155313D-01	0.141102D-01	0.130767D-01	0.123026D-01
0.070	0.189026D-01	0.167202D-01	0.151914D-01	0.140795D-01	0.132465D-01
0.075	0.202427D-01	0.179079D-01	0.162718D-01	0.150816D-01	0.141898D-01
0.080	0.215807D-01	0.190941D-01	0.173511D-01	0.160829D-01	0.151325D-01
0.085	0.229165D-01	0.202790D-01	0.184294D-01	0.170834D-01	0.1607450-01
0.090	0.242500D-01	0.214622D-01	0.195067D-01	0.180831D-01	0.170159D-01
0.095	0.255809D-01	0.226439D-01	0.205827D-01	0.190818D-01	0.179566D-01
0.100	0.259093D-01	0.238238D-01	0.215575D-01	0.200797D-01	0.188965D-01
0.150	0.400206D-01	0.355086D-01	0.323234D-01	0.299954D-01	0.282456D-01
0.200	0.527318D-01	0.469363D-01	0.427364D-01	0.397640D-01	0.374400D-01
0.250	0.649282D-01	0.579967D-01	0.530185D-01	0.493392D-01	0.465528D-01
0.300	0.765103D-01	0.686466D-01	0.629325D-01	0.586770D-01	0.554375D-01
0.350	0.873952D-01	0.788113D-01	0.724880D-01	0.677363D-01	0.640968D-01
0.400	0.975180D-01	0.884352D-01	0.816392D-01	0.764792D-01	0.724987D-01
0.450	0.1068320+00	0.974728D-01	0.903453D-01	0.848715D-01	0.806138D-01
0.500	0.1153090+00	0.1058890+00	0.985753D-01	0.928827D-01	0.884152D-01
0.550	0.1229380+00	0.1136580+00	0.1062990+00	0.1004870+00	0.958788D-01
0.600	0.129721D+00	0.120764D+00	0.1134960+00	0.1076620+00	0.1029840+00
0.650	0.1356750+00	0.127203D+00	0.1201510+00	0.1143900+00	0.1097120+00
0.700	0.1408280+00	0.1329770+00	0.1262570+00	0.1206580+00	0.1160480+00
0.750	0.1452170+00	0.1380960+00	0.1318100+00	0.1264570+00	0.1219810+00
0.800	0.1488860+00	0.1425770+00	0.1368120+00	0.1317820+00	0.1275020+00
0.850	0.151881D+00	0.146444D+00	0.141272D+00	0.136633D+00	0.132607D+00
0.900	0.1542550+00	0.149724D+00	0.1452020+00	0.141011D+00	0.137291D+00
0.950	0.1560600+00	0.1524480+00	0.1486180+00	0.1449240+00	0.1415570+00
1.000	0.157347D+00	0.1546510+00	0.1515390+00	0.1483810+00	0.1454070+00
1.500	0.1517690+00	0.1558440+00	0.1590730+00	0.1614950+00	0.1632310+00
2.000	0.133409D+00	0.139276D+00	0.144849D+00	0.150037D+00	0.154761D+00
2.500	0.1152150+00	0.1205770+00	0.1258550+00	0.1310390+00	0.1360950+00
3.000	0.999856D-01	0.1043390+00	0.1085810+00	0.1127420+00	0.1168430+00
3.500	0.8771040-01	0.911333D-01	0.943769D-01	0.974697D-01	0.1004430+00
4.000	0.778313D-01	0.805177D-01	0.829770D-01	0.852314D-01	0.873050D-01
4.500	0.698021D-01	0.719294D-01	0.738086D-01	0.754591D-01	0.768998D-01
5.000	0.631907D-01	0.648967D-01	0.663524D-01	0.675773D-01	0.685894D-01
5.500	0.576738D-01	0.590605D-01	0.602053D-01	0.611295D-01	0.618523D-01
6.000	0.530124D-01	0.541541D-01	0.550679D-01	0.557769D-01	0.563021D-01
6.500	0.490284D-01	0.499799D-01	0.507195D-01	0.512720D-01	0.516597D-01
7.000	0.455884D-01	0.463901D-01	0.469964D-01	0.474332D-01	0.477235D-01
7.500	0.425905D-01	0.432728D-01	0.437757D-01	0.441254D-01	0.443454D-01
8.000	0.399564D-01	0.405423D-01	0.409637D-01	0.412469D-01	0.414154D-01
8.500	0.376246D-01	0.381320D-01	0.384884D-01	0.387202D-01	0.388502D-01
9.000	0.355467D-01	0.359893D-01	0.362935D-01	0.364848D-01	0.365858D-01
9.500	0.336839D-01	0.340726D-01	0.343341D-01	0.344935D-01	0.345722D-01
10.000	0.320048D-01	0.323483D-01	0.325747D-01	0.327083D-01	0.327699D-01
15.000	0.213326D-01	0.214602D-01	0.215310D-01	0.215611D-01	0.215633D-01
20.000	0.159864D-01	0.160493D-01	0.160879D-01	0.160826D-01	0.160826D-01
25.000	0.127803D-01	0.128165D-01	0.128317D-01	0.128338D-01	0.128281D-01
30.000	0.106446D-01	0.106676D-01	0.106761D-01	0.106760D-01	0.106710D-01
35.000	0.912013D-02	0.913581D-02	0.914095D-02	0.914000D-02	0.913585D-02
40.000	0.797750D-02	0.798874D-02	0.799198D-02	0.799076D-02	0.798731D-02
45.000	0.708924D-02	0.709762D-02	0.709973D-02	0.709846D-02	0.709558D-02
50.000	0.637894D-02	0.638537D-02	0.638678D-02	0.638556D-02	0.638312D-02
55.000	0.579799D-02	0.580306D-02	0.580401D-02	0.580286D-02	0.580079D-02
60.000	0.531402D-02	0.531809D-02	0.531874D-02	0.531767D-02	0.531589D-02
65.000	0.490442D-02	0.490794D-02	0.490838D-02	0.490760D-02	0.490558D-02
70.000	0.455378D-02	0.455653D-02	0.455682D-02	0.455593D-02	0.455458D-02
75.000	0.424978D-02	0.425209D-02	0.425228D-02	0.425146D-02	0.425027D-02
80.000	0.398383D-02	0.398579D-02	0.398590D-02	0.398515D-02	0.398410D-02
85.000	0.374920D-02	0.375088D-02	0.375094D-02	0.375025D-02	0.374931D-02
90.000	0.354067D-02	0.354213D-02	0.354214D-02	0.354151D-02	0.354067D-02
95.000	0.335412D-02	0.335539D-02	0.335537D-02	0.335479D-02	0.335403D-02
100.000	0.318624D-02	0.318735D-02	0.318731D-02	0.318678D-02	0.318609D-02
150.000	0.212343D-02	0.212382D-02	0.212373D-02	0.212346D-02	0.212315D-02

FUNCTION V(ALPHA,Z) FOR

Z =	ALPHA = 1.100	1.200	1.300	1.400	1.500
200.000	0.1592330D-02	0.1592480D-02	0.1592410D-02	0.1592250D-02	0.1592080D-02
250.000	0.1273710D-02	0.1273810D-02	0.1273750D-02	0.1273650D-02	0.1273540D-02
300.000	0.1061360D-02	0.1061420D-02	0.1061370D-02	0.1061300D-02	0.1061220D-02
350.000	0.9096910D-03	0.9097300D-03	0.9096940D-03	0.9096390D-03	0.9095870D-03
400.000	0.7959520D-03	0.7959790D-03	0.7959490D-03	0.7959070D-03	0.7958680D-03
450.000	0.7074940D-03	0.7075130D-03	0.7074880D-03	0.7074550D-03	0.7074250D-03
500.000	0.6367310D-03	0.6367450D-03	0.6367240D-03	0.6366970D-03	0.6366730D-03
550.000	0.5788360D-03	0.5788460D-03	0.5788290D-03	0.5788070D-03	0.5787870D-03
600.000	0.5305920D-03	0.5306000D-03	0.5305850D-03	0.5305660D-03	0.5305500D-03
650.000	0.4897720D-03	0.4897780D-03	0.4897650D-03	0.4897490D-03	0.4897350D-03
700.000	0.4547830D-03	0.4547880D-03	0.4547770D-03	0.4547630D-03	0.4547510D-03
750.000	0.4244610D-03	0.4244640D-03	0.4244540D-03	0.4244420D-03	0.4244330D-03
800.000	0.3979290D-03	0.3979320D-03	0.3979230D-03	0.3979120D-03	0.3979040D-03
850.000	0.3745190D-03	0.3745210D-03	0.3745130D-03	0.3745040D-03	0.3744960D-03
900.000	0.3537100D-03	0.3537120D-03	0.3537050D-03	0.3536970D-03	0.3536900D-03
950.000	0.3350920D-03	0.3350930D-03	0.3350870D-03	0.3350800D-03	0.3350740D-03
1000.000	0.3183360D-03	0.3183370D-03	0.3183330D-03	0.3183250D-03	0.3183190D-03
1500.000	0.2122180D-03	0.2122180D-03	0.2122150D-03	0.2122120D-03	0.2122100D-03
2000.000	0.1591610D-03	0.1591610D-03	0.1591590D-03	0.1591580D-03	0.1591570D-03
2500.000	0.1273280D-03	0.1273280D-03	0.1273270D-03	0.1273260D-03	0.1273250D-03

FUNCTION V(ALPHA,Z) FOR

Z =	ALPHA = 1.600	1.700	1.800	1.900	2.000
0.000	0.0000000D+00	0.0000000D+00	0.0000000D+00	0.0000000D+00	0.0000000D+00
0.001	0.1803230D-03	0.1731530D-03	0.1674600D-03	0.1628800D-03	0.1591530D-03
0.002	0.3606460D-03	0.3463070D-03	0.3349200D-03	0.3257600D-03	0.3183100D-03
0.003	0.5409680D-03	0.5194590D-03	0.5023800D-03	0.4886390D-03	0.4774640D-03
0.004	0.7212890D-03	0.6926110D-03	0.6698390D-03	0.6515180D-03	0.6366180D-03
0.005	0.9016100D-03	0.8657620D-03	0.8372970D-03	0.8143960D-03	0.7957710D-03
0.010	0.1803190D-02	0.1731500D-02	0.1674570D-02	0.1628770D-02	0.1591520D-02
0.015	0.2704700D-02	0.2597170D-02	0.2511790D-02	0.2443100D-02	0.2387230D-02
0.020	0.3606110D-02	0.3462770D-02	0.3348940D-02	0.3257370D-02	0.3182890D-02
0.025	0.4507390D-02	0.4323250D-02	0.4185990D-02	0.4071540D-02	0.3978460D-02
0.030	0.5408500D-02	0.5193590D-02	0.5022920D-02	0.4885610D-02	0.4773930D-02
0.035	0.6309420D-02	0.6058760D-02	0.5859760D-02	0.5699540D-02	0.5569290D-02
0.040	0.7210100D-02	0.6923730D-02	0.6696310D-02	0.6513320D-02	0.6364550D-02
0.045	0.8110520D-02	0.7788480D-02	0.7532720D-02	0.7326930D-02	0.7159560D-02
0.050	0.9010640D-02	0.8652970D-02	0.8368900D-02	0.8140340D-02	0.7954430D-02
0.055	0.9910440D-02	0.9517180D-02	0.9204850D-02	0.8953530D-02	0.8749110D-02
0.060	0.1080990D-01	0.1038110D-01	0.1004050D-01	0.9766470D-02	0.9543570D-02
0.065	0.1170890D-01	0.1124460D-01	0.1087590D-01	0.1057920D-01	0.1033780D-01
0.070	0.1260750D-01	0.1210780D-01	0.1171090D-01	0.1139160D-01	0.1113180D-01
0.075	0.1350570D-01	0.1297070D-01	0.1254570D-01	0.1220360D-01	0.1192540D-01
0.080	0.1440330D-01	0.1383300D-01	0.1338000D-01	0.1301540D-01	0.1271880D-01
0.085	0.1530040D-01	0.1469500D-01	0.1421400D-01	0.1382680D-01	0.1351190D-01
0.090	0.1619700D-01	0.1555640D-01	0.1504750D-01	0.1463790D-01	0.1430460D-01
0.095	0.1709300D-01	0.1641740D-01	0.1588060D-01	0.1544850D-01	0.1509700D-01
0.100	0.1798830D-01	0.1727780D-01	0.1671320D-01	0.1625870D-01	0.1588900D-01
0.150	0.2693003D-01	0.2584650D-01	0.2500840D-01	0.2433340D-01	0.2378390D-01
0.200	0.3571430D-01	0.3433150D-01	0.3323040D-01	0.3234270D-01	0.3161960D-01
0.250	0.4439920D-01	0.4270590D-01	0.4135540D-01	0.4026540D-01	0.3937680D-01
0.300	0.5292440D-01	0.5094340D-01	0.4936040D-01	0.4808090D-01	0.4703670D-01
0.350	0.6126120D-01	0.5901880D-01	0.5722290D-01	0.5576890D-01	0.5458070D-01
0.400	0.6938180D-01	0.6690810D-01	0.6492150D-01	0.6330990D-01	0.6199120D-01
0.450	0.7726070D-01	0.7458830D-01	0.7243570D-01	0.7068540D-01	0.5925080D-01
0.500	0.8487380D-01	0.8203810D-01	0.7974600D-01	0.7787760D-01	0.7634320D-01
0.550	0.9219940D-01	0.8923760D-01	0.8683420D-01	0.8486950D-01	0.8325260D-01
0.600	0.9921780D-01	0.9616860D-01	0.9368350D-01	0.9164550D-01	0.8996450D-01
0.650	0.1059120D+00	0.1028150D+00	0.1002780D+00	0.9819100D-01	0.9646480D-01
0.700	0.1122660D+00	0.1091610D+00	0.1066050D+00	0.1044920D+00	0.1027410D+00
0.750	0.1182680D+00	0.1151950D+00	0.1126500D+00	0.1105380D+00	0.1087810D+00
0.800	0.1239080D+00	0.1209060D+00	0.1184030D+00	0.1163160D+00	0.1145740D+00
0.850	0.1291770D+00	0.1262840D+00	0.1238540D+00	0.1218170D+00	0.1201100D+00
0.900	0.1340720D+00	0.1313240D+00	0.1289970D+00	0.1270340D+00	0.1253820D+00
0.950	0.1385870D+00	0.1360190D+00	0.1338230D+00	0.1319580D+00	0.1303810D+00
1.000	0.1427240D+00	0.1403670D+00	0.1383290D+00	0.1365850D+00	0.1351020D+00
1.500	0.1644360D+00	0.1652560D+00	0.1658140D+00	0.1662000D+00	0.1664800D+00
2.000	0.1589810D+00	0.1627000D+00	0.1659530D+00	0.1687920D+00	0.1712760D+00
2.500	0.1403740D+00	0.1456210D+00	0.1499930D+00	0.1540640D+00	0.1578270D+00
3.000	0.1208940D+00	0.1248910D+00	0.1288120D+00	0.1326300D+00	0.1363160D+00
3.500	0.1033270D+00	0.1061510D+00	0.1089350D+00	0.1116890D+00	0.1144120D+00
4.000	0.8922360D-01	0.9101560D-01	0.9271070D-01	0.9433740D-01	0.9591960D-01
4.500	0.7814960D-01	0.7922830D-01	0.8015740D-01	0.8096070D-01	0.8166380D-01

FUNCTION V(ALPHA,Z) FOR

Z =	ALPHA = 1.600	1.700	1.800	1.900	2.000
5.000	0.6940550D-01	0.7004060D-01	0.7050940D-01	0.7082700D-01	0.7103980D-01
5.500	0.6239110D-01	0.6276070D-01	0.6297440D-01	0.6304330D-01	0.6297790D-01
6.000	0.5666210D-01	0.5667350D-01	0.5695040D-01	0.5690450D-01	0.5674540D-01
6.500	0.5190270D-01	0.5201860D-01	0.5202290D-01	0.5192910D-01	0.5174790D-01
7.000	0.4788810D-01	0.4794540D-01	0.4791180D-01	0.4780120D-01	0.4762600D-01
7.500	0.4445660D-01	0.4447760D-01	0.4442450D-01	0.4431160D-01	0.4415120D-01
8.000	0.4148960D-01	0.4148780D-01	0.4142550D-01	0.4131660D-01	0.4117270D-01
8.500	0.3889850D-01	0.3888230D-01	0.3881670D-01	0.3871420D-01	0.3858600D-01
9.000	0.3661560D-01	0.3659060D-01	0.3652470D-01	0.3642980D-01	0.3631550D-01
9.500	0.3458870D-01	0.3455840D-01	0.3449410D-01	0.3440670D-01	0.3430470D-01
10.000	0.3277680D-01	0.3274350D-01	0.3268180D-01	0.3260150D-01	0.3251030D-01
15.000	0.2154700D-01	0.2151960D-01	0.2148610D-01	0.2145020D-01	0.2141460D-01
20.000	0.1606930D-01	0.1605180D-01	0.1603280D-01	0.1601400D-01	0.1599630D-01
25.000	0.1281830D-01	0.1280670D-01	0.1279490D-01	0.1278370D-01	0.1277350D-01
30.000	0.1066370D-01	0.1065560D-01	0.1064770D-01	0.1064040D-01	0.1063410D-01
35.000	0.9130290D-02	0.9124410D-02	0.9118810D-02	0.9113790D-02	0.9109490D-02
40.000	0.7989290D-02	0.7984530D-02	0.7979440D-02	0.7974180D-02	0.7967730D-02
45.000	0.7092120D-02	0.7088670D-02	0.7085520D-02	0.7082810D-02	0.7080560D-02
50.000	0.6330310D-02	0.6327560D-02	0.6325100D-02	0.6323010D-02	0.6321300D-02
55.000	0.5798460D-02	0.5796240D-02	0.5794270D-02	0.5792620D-02	0.5791290D-02
60.000	0.5313940D-02	0.5312110D-02	0.5310510D-02	0.5309180D-02	0.5308120D-02
65.000	0.4904200D-02	0.4902670D-02	0.4901340D-02	0.4900260D-02	0.4899400D-02
70.000	0.4553160D-02	0.4551860D-02	0.4550750D-02	0.4549850D-02	0.4549140D-02
75.000	0.4249040D-02	0.4247930D-02	0.4246990D-02	0.4246230D-02	0.4245640D-02
80.000	0.3983030D-02	0.3982060D-02	0.3981260D-02	0.3980610D-02	0.3980120D-02
85.000	0.3748370D-02	0.3747530D-02	0.3746830D-02	0.3746280D-02	0.3745860D-02
90.000	0.3539830D-02	0.3539100D-02	0.3538490D-02	0.3538010D-02	0.3537650D-02
95.000	0.3353290D-02	0.3352640D-02	0.3352100D-02	0.3351690D-02	0.3351370D-02
100.000	0.3183940D-02	0.3183480D-02	0.3183090D-02	0.3183010D-02	0.3183740D-02
150.000	0.2122880D-02	0.2122650D-02	0.2122480D-02	0.2122350D-02	0.2122250D-02
200.000	0.1591930D-02	0.1591820D-02	0.1591730D-02	0.1591670D-02	0.1591630D-02
250.000	0.1273450D-02	0.1273390D-02	0.1273340D-02	0.1273300D-02	0.1273280D-02
300.000	0.1061170D-02	0.1061120D-02	0.1061090D-02	0.1061070D-02	0.1061060D-02
350.000	0.9095460D-03	0.9095160D-03	0.9094950D-03	0.9094810D-03	0.9094720D-03
400.000	0.7958380D-03	0.7958160D-03	0.7958010D-03	0.7957910D-03	0.7957850D-03
450.000	0.7074020D-03	0.7073850D-03	0.7073740D-03	0.7073670D-03	0.7073620D-03
500.000	0.6366550D-03	0.6366420D-03	0.6366340D-03	0.6366280D-03	0.6366250D-03
550.000	0.5787730D-03	0.5787630D-03	0.5787560D-03	0.5787520D-03	0.5787490D-03
600.000	0.5305380D-03	0.5305300D-03	0.5305250D-03	0.5305220D-03	0.5305190D-03
650.000	0.4897250D-03	0.4897190D-03	0.4897140D-03	0.4897120D-03	0.4897100D-03
700.000	0.4547430D-03	0.4547380D-03	0.4547350D-03	0.4547320D-03	0.4547300D-03
750.000	0.4244260D-03	0.4244210D-03	0.4244180D-03	0.4244160D-03	0.4244150D-03
800.000	0.3978980D-03	0.3978940D-03	0.3978910D-03	0.3978900D-03	0.3978890D-03
850.000	0.3744910D-03	0.3744880D-03	0.3744850D-03	0.3744840D-03	0.3744830D-03
900.000	0.3536850D-03	0.3536820D-03	0.3536800D-03	0.3536790D-03	0.3536790D-03
950.000	0.3350700D-03	0.3350670D-03	0.3350650D-03	0.3350640D-03	0.3350640D-03
1000.000	0.3183160D-03	0.3183130D-03	0.3183120D-03	0.3183110D-03	0.3183110D-03
1500.000	0.2122090D-03	0.2122080D-03	0.2122070D-03	0.2122070D-03	0.2122070D-03
2000.000	0.1591560D-03	0.1591550D-03	0.1591550D-03	0.1591550D-03	0.1591550D-03
2500.000	0.1273240D-03	0.1273240D-03	0.1273240D-03	0.1273240D-03	0.1273240D-03

Journal of Research of the National Bureau of Standards
Volume 90, Number 1, January–February 1985

An Automated Coupled-Column Liquid Chromatography System for Measuring Aqueous Solubilities of Hydrophobic Solutes

John W. Owens and Howard DeVoe
University of Maryland, College Park, MD 20742
and
Thomas J. Buckley and Stanley P. Wasik
National Bureau of Standards, Gaithersburg, MD 20899

Accepted: October 11, 1984

An automated apparatus is described for measuring the aqueous solubility of a sparingly soluble organic compound at many different temperatures. Water is pumped through a generator column packed with a chromatographic support coated with the organic compound, producing a saturated solution. The solute in a measured volume of this solution is extracted with an extractor column and analyzed by high performance liquid chromatography (HPLC). The temperature of the thermostat bath and the operation of the valves and the HPLC are under the control of a microcomputer. Solubility measurements of ethylbenzene obtained with this apparatus have a standard deviation at any one temperature of about 3% of the mean.

Key words: automation; ethylbenzene; HPLC; hydrophobic; liquid chromatography; microcomputer; solubility; solute; water.

Introduction

Accurate measurements of the aqueous solubilities of hydrophobic substances as functions of temperature are needed for testing theoretical models of hydrophobic effects. Over the past few years a general method for measuring aqueous solubilities of solid and liquid hydrophobic compounds has been developed at the Center for Analytical Chemistry and the Center for Chemical Physics at the National Bureau of Standards [1–4][1]. In this method, which will be called coupled-column liquid chromatography (CCLC), a saturated solution of the solute is generated by pumping water through a thermostated generator column containing the solute coated on a chromatographic support. A measured volume of the solution passes through a small extractor column filled

[1]Figures in brackets indicate literature references.

About the Authors, Paper: John W. Owens worked on this project as a graduate student at the University of Maryland and an IPA (Intergovernmental Personnel Act) summer employee at NBS. Howard DeVoe, an associate professor in the Department of Chemistry at the University of Maryland and the author to whom correspondence should be addressed, was a guest worker and IPA summer employee at NBS. Thomas J. Buckley and Stanley P. Wasik are research chemists in the NBS Center for Chemical Physics. The work presented here is taken from a thesis prepared by Mr. Owens in partial fulfillment of his M.S. degree. His efforts and those of Professor DeVoe were supported in part by

with a superficially-porous reverse phase packing where the solute is removed quantitatively. The extracted solute is eluted from the extractor column with a water-organic mobile phase onto a reverse phase analytical column where the solute is separated from impurities and its amount determined by high performance liquid chromatography (HPLC) with ultraviolet detection. The method minimizes or avoids experimental problems inherent in the usual "shake-flask" method (formation of colloidal dispersions, errors from adsorption on walls, and loss of volatile solutes to the atmosphere), and also has advantages of speed and ease of thermostating [3].

This paper describes our exploitation of an additional advantage of the CCLC method, i.e., the ease with which the solubility measurements can be automated. We have assembled an automated CCLC system in which manual control of the required sequence of valve switchings, HPLC pump settings, and integrator functions is replaced with timed control signals from a microcomputer in order to eliminate operator error. Because the automated system can run unattended overnight, the productivity of the laboratory is greatly increased. An important additional feature is automatic temperature control of the generator column, so that the solubility of a solute at many pre-selected temperatures can be measured for subsequent calculation of the enthalpy of solution through the van't Hoff method. This paper describes the construction and operation of the system and evaluation of some results obtained for ethylbenzene, a liquid solute.

2. Operation of the CCLC System

This section describes general aspects of the operation of the CCLC system that are common to both manual and automated control. Details of individual components of the system are given in section 3.

Figure 1 is a block diagram of the entire system. Water is pumped through the generator column from the generator column pump at a constant flow rate, typically 0.3 mL/min. Because of the large interfacial area and small diffusion path in the generator column, the water rapidly becomes saturated with the solute. Internal surfaces between the generator column and Valve 1 become equilibrated with the saturated solution before measurements are made, so that no further adsorption occurs here that would introduce errors by removing solute from solution.

The HPLC pump supplies a mobile phase composed of water, methanol, or a water-methanol mixture. The composition of the mobile phase and the flow rate are

Valve 1 is a two-position switching valve. In the Extract position, with interport connections shown as heavy solid lines in figure 1, the saturated aqueous solution from the generator column passes through the extractor column and out to waste (labeled W in fig. 1) and the mobile phase from the HPLC pump continues on to Valve 2. In the Analyze position of Valve 1 (heavy broken lines) the aqueous solution goes directly to waste and the mobile phase passes through the extractor column and then continues on to Valve 2. Valve 2 is a two-position switching valve that allows the mobile phase to either pass through the analytical column (connections shown by heavy solid lines) or to bypass the analytical column (heavy broken lines). The valve positions are changed by actuators that can be operated either manually (using electric switches) or by commands from the microcomputer. The generator and extractor columns, Valve 1, and interconnecting tubing are thermostated in a water bath (indicated by the dash-dot rectangle in fig. 1) whose temperature is monitored with a quartz crystal thermometer (QCT) and controlled with two heating elements (H).

The signal peak from the ultraviolet detector (D) is integrated by the integrator (I).

The sequence of operations for a typical run (one solubility measurement) is shown in figure 2. While these tedious operations could be carried out manually, automated control has the distinct advantage of eliminating procedural errors. The four main steps of the run, labeled Condition, Extract, Analyze, and Strip, are as follows:

1. **Condition.** In this step pure water from the HPLC pump displaces methanol in the extractor column in order to condition this column for extraction. Valve 2 is placed in the Bypass position to prevent pure water from entering the analytical column which contains pure methanol from the initial setup or the preceding run. (We have found that it is advantageous to avoid in this way a sudden drastic change of the mobile phase composition in the analytical column, since such changes tend in time to damage the column packing as shown by broadened peak widths.) During this step the saturated aqueous solution from the generator column is diverted to waste.

2. **Extract.** Valve 1 is placed in the Extract position, switching the saturated aqueous solution from the generator column into the extractor column where the solute is extracted. The water remaining from extraction goes to waste. The mobile phase is changed to a composition (80% methanol in this example) that will later give a convenient retention time for the solute peak during HPLC analysis. After a brief delay to allow the new composition to reach Valve 2, Valve 2 is switched

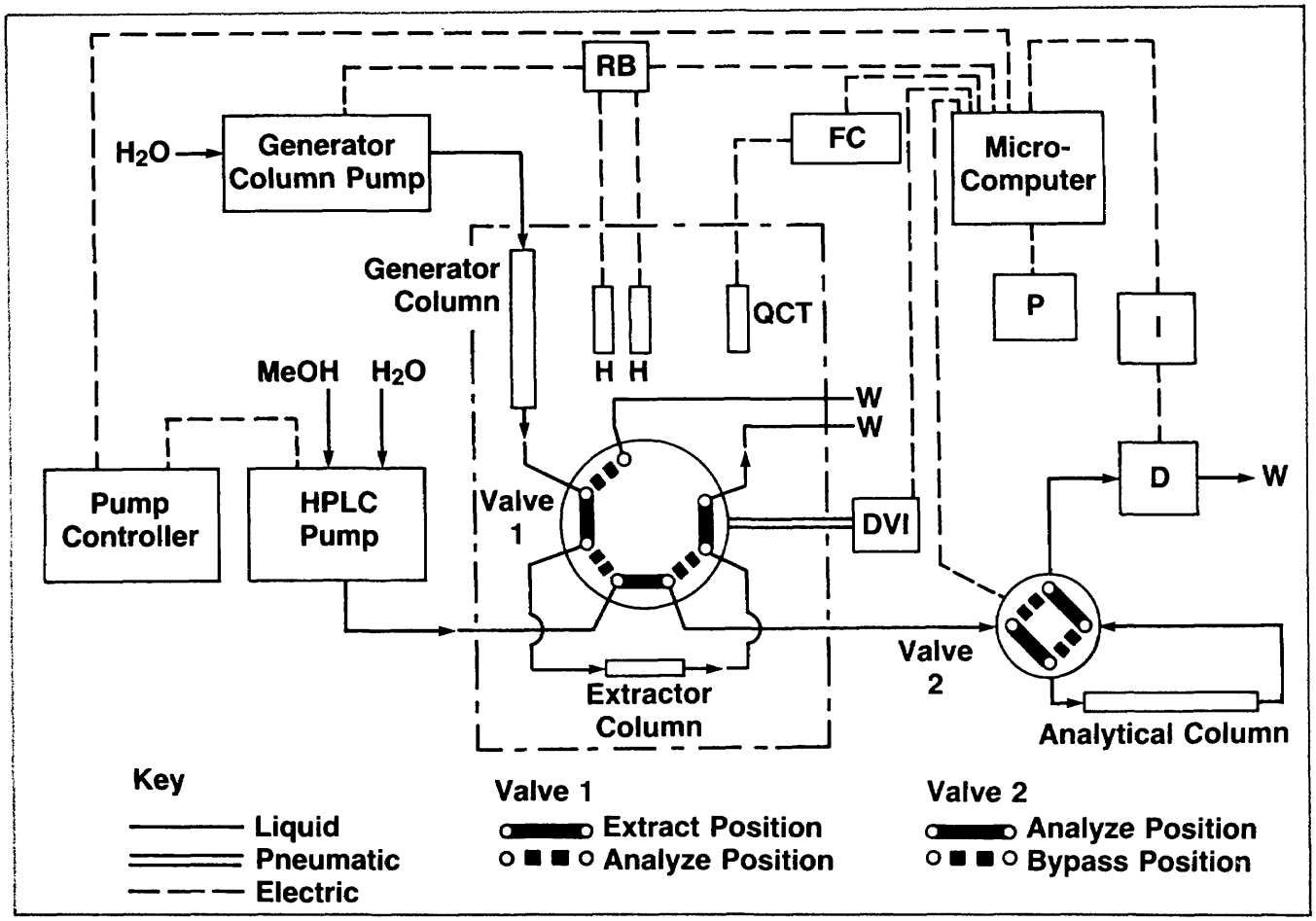

Figure 1–Block diagram of automated CCLC system. Abbreviations: D, detector; DVI, digital valve interface; FC, frequency counter; H, heater; I, integrator; MeOH, methanol; P, printer; QCT, quartz crystal thermometer; RB, relay box; W, waste. The components shown within the dash-dot rectangle are thermostated.

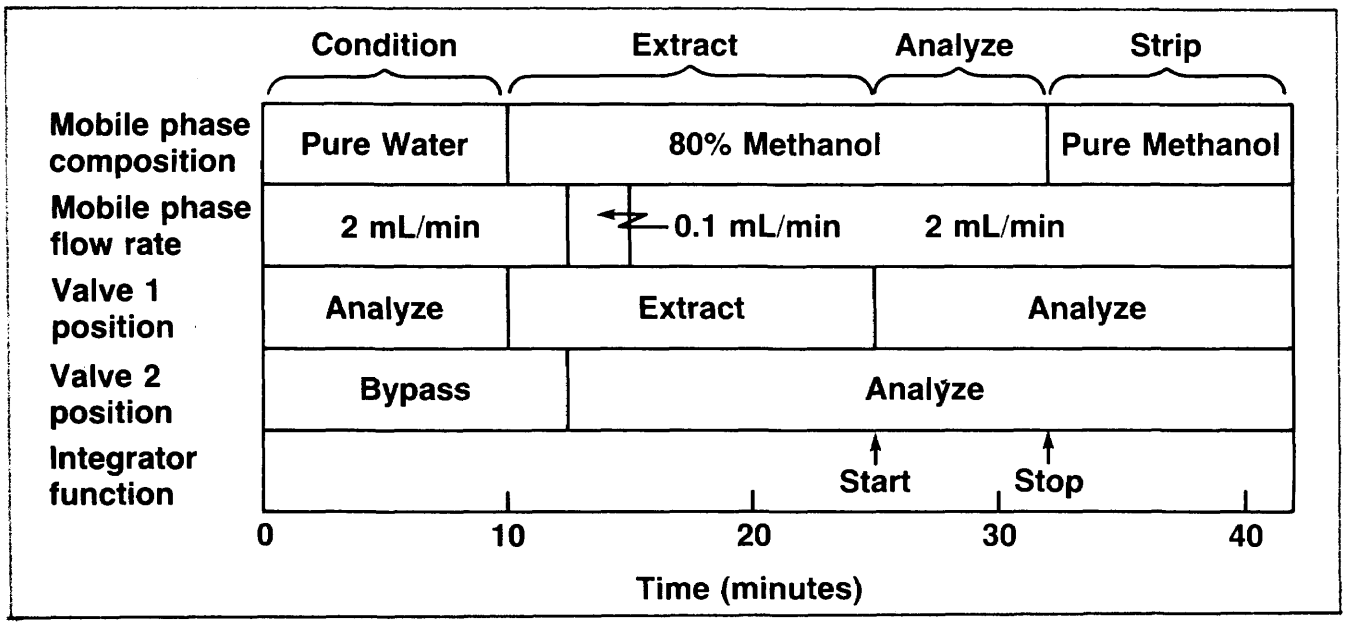

Figure 2–Timing diagram for a typical solubility run. In this example the solute is ethylbenzene and the flow rate through the generator column is 0.3 mL/min. Time along the horizontal axis is measured from the beginning of the Condition step.

to the Analyze position and the mobile phase enters the analytical column. The flow rate of the mobile phase is reduced to 0.1 mL/min to conserve solvents, and later it is returned to the value needed for HPLC analysis (2 mL/min in the example shown in fig. 2). (The microcomputer program calculates the duration of the period of reduced flow rate so as to condition the analytical column with a predetermined volumn of mobile phase. This period is longer for runs with less-soluble solutes requiring longer extraction times.) The Extract step is precisely timed for later calculations.

3. **Analyze.** Valve 1 is changed to the Analyze position and the integrator is started. The methanol-water mobile phase elutes the solute, extracted during the preceding Extract step, from the extractor column and focuses it on the head of the analytical column where chromatographic analysis begins. The eluted solute includes the total amount that was present in the extracted aqueous solution, provided that there was no breakthrough of solute from the extractor column during the preceding Extract step. The integrator plots a chromatogram during the analysis. After the solute peak has been integrated, the integration is stopped and the integrator prints the peak area on the chromatogram chart.

4. **Strip.** Pure methanol is pumped from the HPLC pump through the extractor and analytical columns to strip off any organic impurities that were retained by these columns.

After the strip step, there is a choice of operations which in the case of automated control is preprogramed by the operator. The choices are three: a new run at the same temperature can be started; the bath temperature can be changed and the next run begun after a time delay for re-equilibration of the generator column at the new temperature; or the measurements can be ended.

3. Components and Interfaces

The columns, pumps, valves, and detector are connected by 1/16-in (1.6 mm) OD stainless steel (ss) tubing and standard tube connectors. The appendix lists the sources of certain of the components used in the CCLC system.

3.1 Columns

Figure 3 shows the design of a generator column that is suitable for generating saturated aqueous solutions of an organic liquid. The column is constructed from stainless steel for strength.

The body of the column consists of a 25-cm length of 1/4-in (0.64 cm) o.d. ss tubing connected to a 3.8-cm length of 3/8-in (0.95 cm) o.d. ss tubing. These two sections were joined by inserting one end of the 3/8-inch

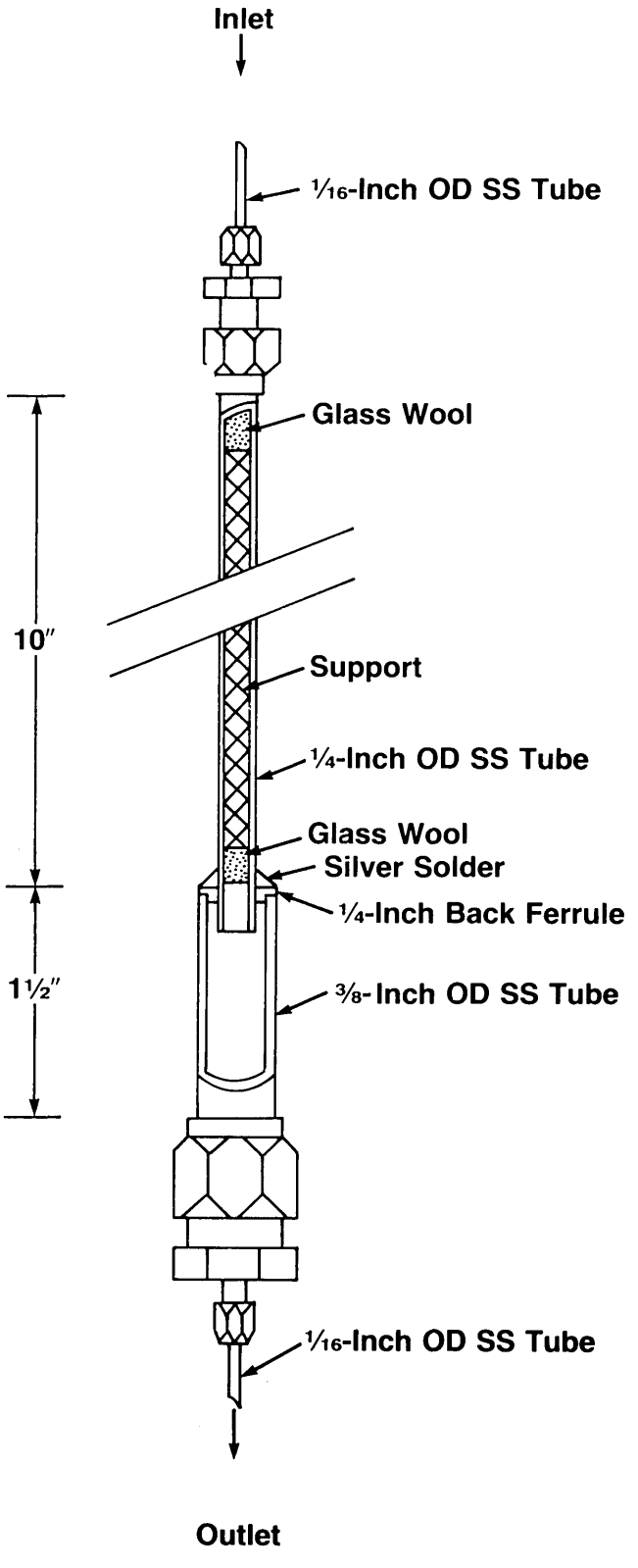

Figure 3–Stainless steel generator column for producing a saturated aqueous solution of a liquid solute. See text for details.

tube over the smaller-diameter end of a ss back ferrule designed for 1/4-in tubing; placing one end of the 1/4-in tube through the back ferrule; and silver soldering the three pieces together. The column has ss reducing end fittings for 1/16-in ss tubing, and is packed with a silanized diatomaceous silica support that is retained in the smaller-diameter section of the body by two plugs of glass wool.

To load the generator column with an organic solute for a series of runs, the column is mounted vertically (as shown in fig. 3) and about 1 mL of solute is pulled downward through the packing using gentle suction. The column is then filled slowly from the bottom with water so as to avoid trapping air. During runs the column remains in this vertical position but the flow of water is downwards. The short section of larger-diameter tubing at the bottom of the column serves as a trap for droplets of the organic liquid pushed off the packing, preventing them from reaching the outlet tube. The organic liquid, being less dense than the aqueous solution, stays at the top of the trap; this behavior has been observed in a glass version of the generator column [3].

The extractor column is a 5.1 cm×0.6 cm ss tube with ss end fittings containing 5-μm frits, filled with a superficially porous reverse phase packing. The analytical column is a commercial 30 cm×0.6 cm ss column containing a 10-μm totally porous reverse phase C_{18} packing.

3.2 Pumps

Water (HPLC grade) is delivered to the generator column with a solvent metering pump capable of pumping at pressures up to 34 MPa (5,000 psi). The flow rate can be selected in increments of 0.1 mL/min.

The HPLC pump mixes two solvents in any desired proportion, pressurizes the mixture, and delivers it at pressures up to 51 MPa with any desired flow rate between 0.06 and 10.23 mL/min. HPLC-grade water and methanol are the solvents in our measurements. They are degassed before use by rapidly bubbling helium through them in their separate containers for 10 minutes, and kept degassed during runs with a continuous reduced flow of helium. The mobile phase composition and flow rate are controlled by a pump controller connected electronically with the HPLC pump. This pump controller is interfaced to the microcomputer by an RS-232 serial port provided on the controller for remote control.

3.3 Valves

Valve 1 is a 10-port high pressure switching valve turned by an air actuator operated with pneumatic pulses from a digital valve interface. (Figure 1 shows only the seven functional ports of Valve 1.) Valve 2 is a 4-port high pressure switching valve turned by an electric actuator. Both valves are built of 300 series stainless steel and Valcon S fluorocarbon, and are designed for a temperature range of -198 °C to 175 °C and for pressures up to 48 MPa. The microcomputer controls the positions of both valves with TTL logic pulses.

3.4 Detector and Integrator

The absorbance signal from the ultraviolet detector (wavelength 254 nm) goes to a recording integrator equipped with a digital input port for remote starting and stopping of integration. The integrator automatically prints peak areas after integration is stopped.

3.5 Temperature Control

Valve 1 and the extractor column are immersed in a 5-liter water bath stirred with a stirrer-circulator. The generator column, mounted over the bath in a vertical position, is enclosed in a glass jacket through which water from the bath is circulated. The bottom of the jacket dips into the bath so that the generator column and the tubing connecting its lower end to Valve 1 are at the same temperature as the bath. The water entering the top of the generator column is brought to the temperature of the bath in a length of stainless steel tubing coiled inside the jacket.

The bath is heated by two independent heating elements and cooled by refrigerated water circulated through a cooling coil. The microcomputer controls the bath temperature with TTL logic pulses that switch solid-state relays to turn the heating elements on and off. One heating element is used to regulate the bath temperature while both are used to raise the temperature to a higher setting.

The microcomputer monitors the bath temperature during runs by reading the frequency of a quartz crystal oscillator thermometer immersed in the bath. The oscillator frequency was calibrated as a function of temperature.

3.6 Microcomputer

A microcomputer with monitor, disk drive, and printer is used for automated control of the system.

A data acquisition card added to the microcomputer provides a timer and two digital 8-bit (parallel) input/output ports. The timer is used to count the time intervals between control signals. Six of the bits from one digital output port are used to control the positions of Valves 1 and 2, the integrator start/stop function, and relays for power to the generator column pump and the two bath heater elements.

A multifunction card added to the microcomputer provides a real-time clock, a parallel port and a serial port. The parallel port is connected to a printer. The serial port is used to control the HPLC pump parameters (mobile phase composition and flow rate) with serial commands to the pump controller.

A custom made interface card enables the microcomputer to read the nine binary coded decimal digits of the frequency counter two at a time.

The microcomputer control program for the CCLC system is written in BASIC. Flowcharts of the program are given in figure 4. After loading the generator column with solute and installing it in the system, the operator starts the program and enters appropriate parameter values into the microcomputer. These parameters include the desired temperatures and number of runs at each temperature, the time delays needed for re-equilibration of the generator column after each temperature change, the mobile phase composition and flow rate for analysis, and the time intervals of the various steps for each run. The runs are then performed under microcomputer control as shown in figure 4(a).

Each interval between control signals for the pumps, valves and integrator is timed by the subroutine shown in figure 4(b). During the interval, the subroutine continuously reads the frequency of the quartz crystal thermometer, computes the bath temperature to an accuracy of 0.002 °C from a linear function of the frequency, and turns a bath heater element on or off to regulate the temperature. The subroutine also updates a monitor display of the bath temperature and the current status of the CCLC system. At the beginning and end of each Extract step, the printer provides permanent hard copy of the clock time (from the multifunction card) and bath temperature. From this information the duration of the Extract step can be calculated to the nearest second.

After all runs for a solute are completed, the microcomputer turns the pumps and bath heaters off. The monitor displays the time at which the experiment ended.

4. Results

The flow rate of the generator column pump was measured by weighing the water delivered during timed intervals, and was found to have a reproducibility at the lowest pump settings of ±0.001 mL/min. The microcomputer regulated the bath temperature, as monitored

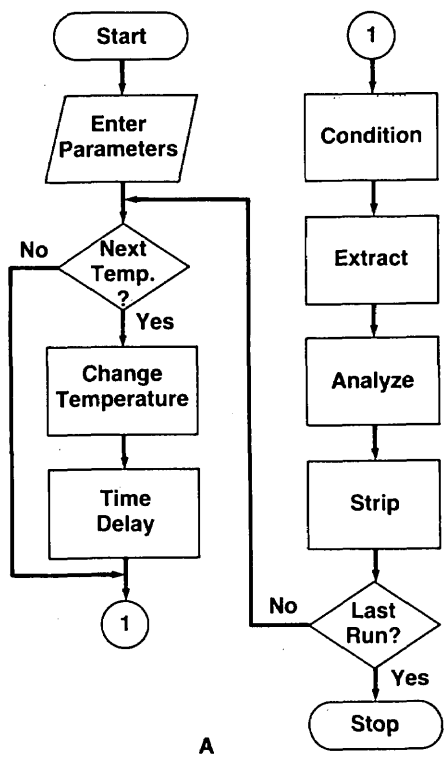

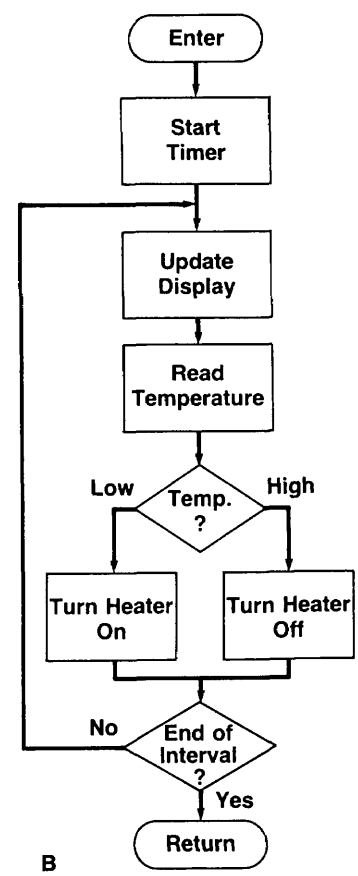

Figure 4–Flowcharts of the control program: A, left, the logic for a series of runs with one solute at one or more temperatures, and B, the subroutine for timing an interval between control signals for the pumps, valves, and integrator.

by the quartz crystal thermometer, to within ±0.025 °C of the set point at all temperatures.

The system described here has been used with the generator column shown in figure 3 for measurements of the aqueous solubilities of five liquid *n*-alkylbenzenes in the range 10–45 °C. The solubility, *s*, was calculated from each run using the relation

$$s = n/V$$

where

n = moles of solute
= measured peak area × detector response factor
V = solution volume
= extract step duration time × generator column flow rate

The detector response factor for each solute was evaluated by injections of a standard methanol solution of the solute into the analytical column from a sample loop, the loop volume having been determined by a spectroscopic method [3].

Figure 5 shows data obtained for ethylbenzene. There is a total of 87 solubility values at 16 temperatures in the range 10–45 °C. The standard deviation of solubilities measured at any one temperature ranges from 0.006 mM to 0.10 mM, with an average standard deviation for all temperatures of 0.05 mM (3% of the mean). The points are scattered, but their large number allows the dependence of solubility on temperature to be determined statistically with reasonable certainty. A solubility minimum is evident at 20–24 °C; Bohen and Claussen [5] observed such a minimum for ethylbenzene at about 18 °C. The solubility and 95% confidence limit at 25 °C were calculated by the method of Clarke and Glew [6] to be (1.74±0.02) mM, in good agreement with the value (1.76±0.02) mM obtained by Tewari et al. [7] at this temperature with the manual CCLC method. Other methods have yielded solubility values for 25 °C ranging from 1.23 mM to 2.00 mM [5, 8–16]. The detailed results of our measurements on *n*-alkylbenzenes will be submitted for publication elsewhere.

5. Conclusions

The automated CCLC system described in this paper for measuring aqueous solubilities has proved to be convenient to use and considerably reduces the time needed to obtain reliable solubility values at many different temperatures.

The generator column described in this paper was built by Albert Ledford of NBS, and the oscillator frequency of the quartz crystal oscillator thermometer that was used in the work was calibrated by David Ditmars, also of NBS.

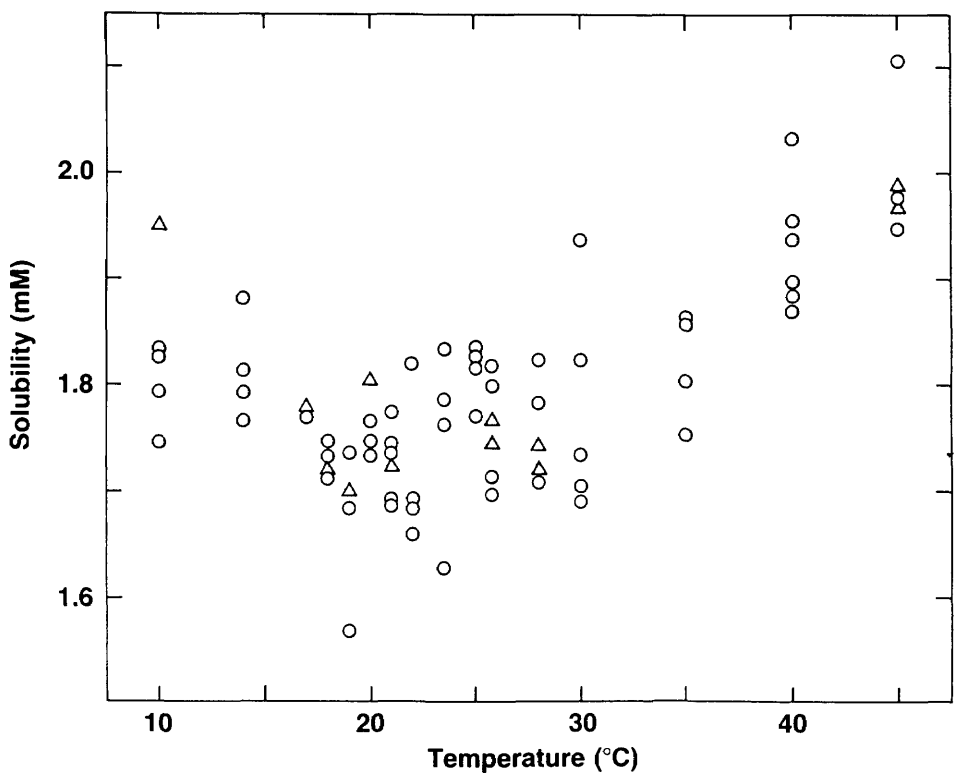

Figure 5–Measurements of the aqueous solubility of ethylbenzene at different temperatures. Each circle shows the result of an individual run. Sometimes two or more runs at the same temperature gave solubility values too close together (0.005 mM or less) to be drawn as individual points; in these instances, the average of the values is shown as a triangle.

6. Appendix: Sources of Components (partial list)

Certain trade names and company products are identified in order to adequately specify the apparatus and experimental procedure. In no case does such identification imply recommendation or endorsement by the National Bureau of Standards, nor does it imply that the products are necessarily the best available for the purpose.

Generator column packing—Chromosorb W, 100–120 mesh, high performance grade, Johns-Manville.

Extractor column packing—Bondapak C_{18}/Corasil, Waters Associates.

Generator column pump—Beckman model 110A.

HPLC pump—DuPont 8800 series analytical binary pump module.

Pump controller—DuPont 8800 series binary solvent controller.

Valve 1—Valco model AC10U valve and air actuator with 6-in standoff.

Valve 2—Valco model EC4U valve and electric actuator.

Digital valve interface—Valco DVI digital interface.

Quartz crystal thermometer—Hewlett-Packard model 2830A.

Integrator—Hewlett-Packard model 3390A recording integrator with 19402A remote start/stop board.

Microcomputer—Apple II+.

Microcomputer cards—ADALAB data acquisition card, Interactive Microwave, Inc.; CPS multifunction card, Mountain Computer, Inc.

7. References

[1] May, W. E.; S. P. Wasik and D. H. Freeman. Determination of the aqueous solubility of polynuclear aromatic hydrocarbons by a coupled column liquid chromatographic technique, Anal. Chem. **50**: 175–179 (1978).

[2] May, W. E.; S. P. Wasik and D. H. Freeman. Determination of the solubility behavior of some polycyclic aromatic hydrocarbons in water, Anal. Chem. **50**: 997–1000 (1978).

[3] DeVoe, H.; M. M. Miller and S. P. Wasik. Generator columns and high pressure liquid chromatography for determining aqueous solubilities and octanol-water partition coefficients of hydrophobic substances, J. Res. Natl. Bur. Stand. **86**: 361–366 (1981).

[4] Wasik, S. P.; M. M. Miller, Y. B. Tewari, W. E. May, W. J. Sonnefeld, H. DeVoe and W. H. Zoller. Determination of the vapor pressure, aqueous solubility, and octanol/water partition coefficient of hydrophobic substances by coupled generator column/liquid chromatographic methods, Residue Reviews **85**: 29–42 (1983).

[5] Bohen, R. L., and W. F. Claussen. The solubility of aromatic hydrocarbons in water, J. Am. Chem. Soc. **73**: 1571–1578 (1951).

[6] Clarke, E. C. W., and D. N. Glew. Evaluation of thermodynamic functions from equilibrium constants, Trans. Faraday Soc. **62**: 539–547 (1966).

[7] Tewari, Y. B.; M. M. Miller, S. P. Wasik, and D. E. Martire. Aqueous solubility and octanol/water partition coefficient of organic compounds at 25.0 °C, J. Chem. Eng. Data **27**: 451–454 (1982).

[8] Andrews, L. J., and R. M. Keefer. Further studies on the argentation of substituted benzenes, J. Am. Chem. Soc. **72**: 5034–5037 (1950).

[9] Klevens, H. B. Solubilization of polycyclic hydrocarbons, J. Phys. Colloid Chem. **54**: 283–298 (1950).

[10] Morrison, T. J., and F. Billet. The salting-out of non-electrolytes. II. The effect of variation in non-electrolyte, J. Chem. Soc. 3819–3822 (1952).

[11] McAuliffe, C. Solubility in water of paraffin, cycloparaffin, olefin, acetylene, cycloolefin, and aromatic hydrocarbons, J. Phys. Chem. **70**: 1267–1275 (1966).

[12] Polak, J., and B. C. Lu. Mutual solubilities of hydrocarbons and water at 0 and 25 °C, Can J. Chem. **51**: 4018–4023 (1973).

[13] Sutton, C., and J. A. Calder. Solubility of alkylbenzenes indistilled water and seawater at 25.0 °C, J. Chem. Eng. Data **20**: 320–327 (1975).

[14] Price, L. C. Aqueous solubility of petroleum as applied to its origin and primary migration, Bull. Am. Soc. Assoc. Pet. Geol. **60**: 213–244 (1976).

[15] Ben-Naim, A. and J. Wilf. Solubilities and hydrophobic interactions in aqueous solutions of monalkylbenzene molecules, J. Phys. Chem. **84**: 583–586 (1980).

[16] Sanemasa, I.; M. Araki, T. Deguchi, and H. Nagai. Solubility measurements of benzene and the alkylbenzenes in water by making use of solute vapor, Bull. Chem. Soc. Japan **55**: 1054–1062 (1982).

conference report

FIBER OPTICS EMPHASIS ON SINGLE MODE

The third biennial Symposium on Optical Fiber Measurements, sponsored by NBS in cooperation with the IEEE Optical Waveguide Communications Committee and the Optical Society of America, drew some 300 attendees to Boulder Oct. 2–3 to hear 25 contributed papers, several invited papers, and to attend two workshops on the general subject of optical fiber measurements. Papers reflected the international interest in fiber optics, with speakers coming from seven countries outside the U.S.

At the first symposium in 1980, the topic of major concern was attenuation in multimode fibers. Two years later at the 1982 meeting, the emphasis turned to bandwidth in multimode fibers with special interest in the prediction of bandwidth for concatenated fibers. At the most recent meeting, the attention was on single-mode fibers with less interest in multimode. This progression of topics follows the industrial trend, which started with multimode fibers and then shifted to single-mode in more recent years.

At the 1984 meeting, the main single-mode fiber concern was with the measurement of chromatic dispersion. In fact, a whole session was devoted to this topic. The remainder of this brief meeting report will summarize the single-mode topics and mention a few specific contributions.

Agreement Lacking

For single-mode fibers there is a need to determine the cutoff wavelength of the second-order mode and the mode field diameter of the fundamental mode. Both of these parameters are under study by standards groups and at present there is no international agreement on how mode field diameter should be measured or specified.

C. A. Millar of British Telecom Research Laboratories reported on a near-field method which gives both the shape of the mode field radial intensity distribution and the refractive index profile. R. Caponi et al. of CSELT, Italy, presented a novel approach to the determination of mode field diameter using an "optical computing" technique whereby a specially prepared mask is inserted in an optical system and mode field diameter is obtained by taking three single data points. Three papers were concerned with cutoff wavelength measurements. The results were interesting because conflicting curvature dependencies were reported. It appears more work needs to be done on how cutoff wavelength depends on fiber-bend curvature. N. K. Cheung and P. Kaiser of Bell Communications Research discussed cutoff wavelength values with respect to the system's operational wavelength. Those investigations measured modal noise, which can occur if operation is too close to the cutoff wavelength. They conclude that effective cutoff wavelength can be slightly greater (1.35 μm) than the system wavelength (1.30 μm).

Chromatic Dispersion

Chromatic dispersion in single-mode fibers was the subject of seven papers. A knowledge of chromatic dispersion allows one to determine the wavelength of zero dispersion and pulse broadening due to source linewidth. The earliest and most common method for determining chromatic dispersion utilizes a high-power Nd:YAG laser to produce Raman scattering in a single-mode fiber, thereby producing a tunable wavelength source of 150-ps-wide pulses.

R. A. Modavis and W. F. Love of the Corning Glass Works reported on a technique using five pulsed laser diodes and curve fitting to yield chromatic dispersion. K. Tatekura et al. of KDD, Japan, described a similar technique but instead measured the phase shift of cw light from sine-wave modulated laser diodes. Chromatic dispersion can also be determined on fiber lengths less than 1 m using an interferometric technique with a tungsten lamp and monochromator. M. J. Saunders and W. B. Gardner of AT&T Bell Laboratories reported using this technique to determine minimum dispersion wavelength and group delay per unit length. L. Oksanen and S. J. Halme of Helsinki University of Technology described numerical methods to extract group delays from interferometric data.

The Technical Digest for the Symposium on Optical Fiber Measurements, 1984, containing three- to four-page summaries of the papers, is available as NBS Special Publication 683 from the Superintendent of Documents, U.S. Government Printing Office, Washington, DC 20402 ($5.00)

Prepared by *Douglas L. Franzen and Gordon W. Day of the Electromagnetic Technology Division, National Bureau of Standards, Boulder, CO 80303.*

conference report

PROMISES OF LARGE-SCALE COMPUTATION

A conference on the Forefronts of Large-Scale Computational Problems (FF84), held at the National Bureau of Standards in Gaithersburg, MD, was organized on the hypothesis that large-scale computation will play an increasingly important role in science and industry, and that the spectrum of applications of large-scale computation will grow rapidly. Sponsorship was obtained through a consortium of industrial, academic, and government organizations, and the conference steering committee was chaired by Dr. David Wehrly of IBM.

Attending the June 25-27 conference were more than 400 engineers, scientists and others interested in current applications, new approaches and future trends in large-scale computation. A distinctive feature of the audience was the mix of researchers from academe and industry, hardware manufacturers, computer laboratory directors, and managers of R&D. Emerging computational methods and requirements which are held in common by a wide range of research activities were also featured prominently in FF84. The breadth of applications of speakers from industrial laboratories provided persuasive evidence that large-scale computation is being realized as a powerful, economic approach to seemingly intractable problems.

The application areas covered in the program, organized by B. L. Buzbee of Los Alamos National Laboratory and H. J. Raveche of the National Bureau of Standards, include medical imaging, materials science, pharmacology, biotechnology, physics, chemical synthesis, structural analysis, economics, fluid mechanics and movies.

Recent advances obtained from large-scale computation in such diverse topics as voltage characteristics in semiconductor devices, bone reconstruction in surgery, action of drug molecules at receptor sites, interaction of DNA with water, global economic modeling, and testing laws of nuclear physics were illustrated. The presentations revealed that exciting breakthroughs are possible in these areas if sufficient computing capability is forthcoming. Providing this new capability will require sizeable advances in state-of-the-art computing technology.

The FF84 Steering Committee, which has representation from industry, academe, and national laboratories, operates on the conviction that interdisciplinary interactions are essential to progress in the field of large-scale computation. The Steering Committee

believes that Forefronts Conferences should be repeated. The purpose of the conferences is to provide a forum for researchers from academe and industry, students, computer vendors, lawmakers and R&D managers to discuss emerging applications, interdisciplinary problems, and future requirements in computing technologies.

This report will begin with a brief review of some of the new and emerging applications of high-speed computations as presented at FF84. It will then discuss specific needs for computing technology that are common to all users of high-speed computation.

'Third Scientific Revolution'

In his keynote address, Dr. Roland W. Schmitt, Senior Vice President of Corporate Research and Development at the General Electric Company and Chairman of the National Science Board, referred to the full emergence of large-scale computation as the "third scientific revolution." Dr. Schmitt also remarked that graphics is essential to gain insight from large-scale computations. He claimed that the combination of high-speed graphics and large-scale computation results in a third way of doing science that will stand alongside the well-established methods of laboratory experimentation and theoretical analysis.

For Dr. Schmitt, effective large-scale computing in an R&D environment not only is a matter of fast computers with large memories but also requires the correct design of the entire computing environment to enable a variety of people to do their work efficiently. The environment includes algorithm development, graphics, individual work stations, micros, minis, mainframes, array processors, and so on. As for improvements, he called for advances in communicating huge data sets to large-scale computers quickly and reliably, and advances in program development tools.

While Dr. Schmitt is generally dubious about government intervention in the commercial development of products, he feels that large-scale computer technology is an exception primarily because the Federal government is one of the principal users of this technology. In addition to Federal assistance for distributing state-of-the-art technology to universities, Dr. Schmitt indicated that the receiving universities should have the responsibility for devising campus-wide networks for their particular computing environment.

Changes for Synthetic Chemistry

Speakers in chemistry included Dr. David Pensak of DuPont and Dr. Enrico Clementi of IBM. Dr. Pensak remarked that, apart from some new reactions and instrumentation, the practice of synthetic chemistry has not changed substantially for more than a century. He added, however, that the introduction of large-scale computational techniques is changing the way synthetic chemistry is being done even though no molecule of any commercial importance has ever been designed on a computer. The combination of high-speed computation and high-speed color graphics provides the chemist with three-dimensional views of molecular geometry and it allows chemists to change geometry readily through, for example, the addition or deletion of functional groups.

Dr. Pensak furnished numerous examples of research areas in the chemical industry where large-scale computation offers substantial promise. These applications include the modeling of: chemical plant processing, requiring the solution of hundreds of simultaneous differential equations; drug molecules on receptor sites, requiring 3-dimensional finite element models; substance-specific membranes to separate alcohol from water or purify synthesis gas obtained from coal, requiring processors 1000 times faster than current technology; cellular kinetics and the metabolism of bacteria, requiring the solution of 15,000 differential equations; chemical reactions on the surface of catalysts; the efficacy of anti-tumor agents; and the toxicity of herbicides and pesticides. He pointed out that advances in such applications require not only advances in processing speed but graphics as well.

Dr. Clementi told the audience that, through research over the last 40 years, quantum chemists have learned how to calculate accurately some properties of molecules with as many as 30 electrons and, with more approximate techniques, the properties of molecules with as many as 400 electrons can be calculated. As an example, he showed results from his computations on the modeling of liquid water. When correlations between many different water molecules were included, the agreement with thermo-

Computer-based imagery is being applied to an increasing number of problems.

dynamic and x-ray experiments approached experimental uncertainties. Such complex calculations, however, approach the limit of current computing capability.

Dr. Clementi provided further examples in the modeling of DNA in water and he reported on the discovery of an unusual arrangement of ions around DNA through these large-scale computations. He explained that the breakthroughs which could shed information on the transmission of genetic information require computing speeds that exceed substantially those now available. To approach these speeds, he is experimenting with a configuration involving as many as 10 FPS-164 array processors attached to three host computers, which are an IBM-4381 and two IBM-4341's. Since each processor is capable of 12 megaflops, he expects peak performance of 120 megaflops with a storage memory of 90 megabytes. Dr. Clementi announced plans for adding to each processor a vector-type feature called 164-MAX. Each MAX-board provides an additional 22 megaflops, and, since he is adding two boards for each of the 10 processors, he projects a maximum speed of 560 megaflops.

Medical Imaging

Speakers in this area were Dr. Gabor T. Herman of the University of Pennsylvania, Dr. Norman J. Pressman of Johns Hopkins Hospital, and Dr. Steven Johnson of the University of Utah. Dr. Herman discussed some fascinating applications of computer tomography, the result of combining high-speed computation with graphics.

For example consider surgery that involves removal or reconstruction of bone, or say the repair of a damaged organ such as the heart. In some cases, the success of the surgery rests on understanding the pre- and post-operative structure of the bone or organ. Surgeons can obtain a three-dimensional model of bones or organs through the use of computer tomography and study these for determining the best way to perform the surgery. Computer-based imagery is being applied to an increasing number of problems, according to Dr. Herman. He cited examples of current research on the three-dimensional visualization of tumors and organs in living patients. With reference to having this imaging technology available to a broad spectrum of patients, Dr. Herman emphasized that the cost of the service is a crucial factor.

Dr. Pressman spoke of the use of special purpose scanning transmission optical microscopes to obtain morphological and biochemical information on cells and tissues. He explained that the computational problems require high processing rates, high bandwidth and the capability of processing large data sets. The computational complexity arises in part from the fact that images need to be collected from all areas on the surface of the slide which is in the microscope's field, and this area can be as large as several square centimeters.

Dr. Johnson presented recent results on ultrasonic imagery which is aimed at obtaining both morphology and material properties. The latter can provide important clues about diseases. Dr Johnson explained that the problem of obtaining this information from ultrasonic imagery involves the solution of complex, nonlinear differential equations. He reported on recent progress involving the use of convolutions and stated that, in order to do three-dimensional imaging, speeds of more than 100 megaflops are required.

Modeling the Non-Linear

Dr. James Gunton of Temple University noted that high-speed computations have been successfully applied to studies of transport properties in semiconductors, devices modeling, and crystal growth. All of these are highly non-linear phenomena, and consequently, modeling them requires large-scale computation. As an example Dr. Gunton discussed the modeling of voltage signals across semiconductor materials. Such studies could be vital in improving the performance of very large scale integrated components used in computers—an example of *computers being used to build better computers.*

For example, consider charge transport under conditions where the magnitude of the electric field could go beyond the region of linear response analysis and hence the validity of Ohm's law can be in doubt. Through the development of powerful Monte Carlo methods, progress has been made in modeling such quantities as the mean energy and drift velocity of electrons in semiconductors which are essential for understanding the speed of solid state devices.

Dr. Gunton also reviewed results on the modeling of electronic transport in silicon and in aluminum-gallium-arsenide devices, and he showed that the agreement with laboratory measurements is promising. Further examples of the impact of large-scale com-

putations in materials science included crystal growth and catalysis. The former entails heat transport in a moving interface, and the latter involve modeling of reacting molecules near metallic surfaces. The complexity of such simulations requires higher computing speeds than those available in current supercomputers or special purpose processors.

Applications in Structural Analysis

Speakers in this area were Dr. John A. Swanson of Swanson Analysis Systems and Carl Henrich of the MacNeal-Schwendler Corporation. These speakers emphasized the tremendous increase in human productivity that accompanies the combination of high-speed computation with high-speed color graphics. Also, their organizations are representative of the third-party software industry wherein companies must offer and maintain their products on a variety of systems while achieving cost-effective performance. It was made clear that portability does not necessarily mean loss in performance. Both organizations are already implementing their products on parallel processors and, currently, do not foresee any insurmountable obstacles. Results were presented on the use of finite element modeling for such varied topics as turbine blades and architectural structures.

The desirability of doing these calculations on dedicated computers with attached array processors versus supercomputers was reviewed. Dr. Swanson speculated that, with multi-ported memory, multiprocessor systems of the future could obtain a 40-fold improvement with many processors, with almost linear improvement for up to eight processors. He forecast that a desk-top-size computer with CRAY-1S capabilities and high-resolution graphics will be commercially available in about four years.

Computer-Generated Movies

Mr. Gary Demos of Digital Productions showed clips from the science fantasy movie, "The Last Starfighter." Digital Productions has developed Digital Science Simulation (SM), which is computer-generated moving imagery that simulates 3-dimensional objects and events realistically. This company has developed technology in computer-generated graphics whereby they can achieve resolution in the range of 4000 by 6000 lines per image. As a consequence, it is difficult in most cases to distinguish between the computer-generated images and actual color photographs. Mr. Demos indicated that computations are done on their CRAY-XMP.

The cost effectiveness of this technology now equals that of alternative techniques for movie production. The quality and cost effectiveness of graphics shown by Mr. Demos are simply not available to scientists and engineers who typically use large-scale computation, but clearly that technology would be of tremendous benefit to them. With respect to the arts, one suspects that Mr. Demos and friends still have some tricks up their sleeves that await the availability of equipment significantly faster than any available today. Future developments include the technology for the forthcoming major motion picture "2010."

Role in Economics Research

Speakers from this area were Dr. Lawrence R. Klein and Dr. Albert Ando, both of the University of Pennsylvania; Dr. Fred Norman of University of Texas; and Dr. Daniel F. X. O'Reilly of Data Resources Incorporated. State-of-the-art economic modeling is used primarily to investigate consequences of changes in economic policy or external events, to test economic theory, and to train students. Economists would like to enhance the capability to specify objectives and be able to explore policy alternatives for achieving them.

Dr. Klein, who is the 1980 Nobel laureate in economics, explained that the role of computers has been instrumental in the way economics and economic research has developed in the last few decades and that this role can only become more important in the future. He discussed a recent experience with international teleconferencing between participants in Europe and the United States. In the course of the conference, a world economic model of more than 10,000 equations was executed in response to a particular aspect of the discussion and the results were "brought up on the screen" and discussed. Unfortunately, approximately one half-hour was required to execute the model. Conferencing would be greatly improved if this time could be cut to about 5 minutes.

. . .one suspects that Mr. Demos and friends still have some tricks up their sleeves. . .

Current research on macroeconomic modeling being done by Drs. Klein, Ando and Norman was reviewed. This work involves computations containing international data bases, time periods as long as 25 years, and as many as 13,000 equations. While inherent uncertainties in macroeconomic models lead to unavoidable limitations in their accuracy, advances in large-scale computing capabilities are necessary to improve existing models and the turnaround time for obtaining a balanced view of the global economy.

Dr. Ando and Dr. Norman amplified Dr. Klein's presentation and noted that a typical econometric model of a country or a group of countries can be characterized as a stochastic nonlinear system of several hundred or thousands of equations. Such models often involve some non-concavity in the system; and therefore, the computational problems involved in merely analyzing the dynamic properties of the system are formidable. The process of search for approximate optimal control strategies for policy authorities, especially when more than one active authority is involved, introduces game theoretic aspects. This is simply beyond the computing resources now available to economists, both in terms of funding and in power of the equipment.

Dr. O'Reilly mentioned that many of the economic models being used are somewhat coupled and that, while each model may entail 10,000 or fewer equations, the correlated aggregate would involve more than 100,000 equations. Such work could, for example, lead to improvements in the forecasting of monthly unemployment by taking into account weekly unemployment insurance claims. Since there are no adequate computational tools, the problem of correlations can only be handled by having modelers meet to estimate the effects of changing parameters. Dr. O'Reilly anticipates requirements in speed and memory in ranges of tens of megaflops and terabytes respectively.

Applications in Physics

Dr. Kenneth G. Wilson of Cornell University, the recipient of the 1982 Nobel Prize in physics, stated that physicists typically have two responsibilities: one is in their specialty area, such as solid state or elementary particle physics, and the other is in maintaining the basic laws of nature. Dr. Wilson's activities in the former area deal with quantum chromodynamics which is capable of predicting such fundamental quantities as the masses of the proton and neutron. The problem of verifying this theory is a computational challenge inasmuch as it entails four dimensions. The approach is to put the problem on a grid or lattice. The state-of-the-art is a 16^4 lattice and Dr. Wilson suggested that at least a 32^4 lattice is necessary. Since there are inherent fluctuations due to the quantum nature of the problem, statistics must be done on these fluctuations and this involves at least 1000 passes through the lattice, but 10^6 passes are likely to be required. The motivation for this work is that quantum chromodynamics shows promise of providing a new theory and an improved understanding of nuclear physics.

Beyond high energy physics, Dr. Wilson is working on the use of large-scale computation to verify basic laws of nature as they apply to many different subjects. In collaboration with Dr. Robert Swenson of Carnegie-Mellon University, he is studying the inherent mismatch encountered in characteristic features of a broad-class of natural phenomena. Consider, for example, the problem of incorporating atmospheric turbulence in global weather forecasts.

Meteorologists find that the basic hydrodynamic equations for global forecasting, which are solved on the most powerful computers available, require a grid with point spacings of about 50 miles. On the other hand, similar computations for describing a turbulent atmosphere require grid spacings of less than a millionth of a mile. How is this wide mismatch in fundamental length scales resolved? The answer given by Dr. Wilson is to develop the basic laws which are correct at each stage of the process of building increasingly larger grids, and to find the connection between the variables on different grid sizes. This follows the renormalization group approach pioneered by Dr. Wilson. The postulate is that the method leads to an equation which involves all the important grid point spacings, and that this equation captures the essence of the problem.

Dr. Wilson pointed out that many of the conference participants have similar computational problems, irrespective of whether they are chemists, engineers, physicists or image processors. This, Dr. Wilson believes, suggests some objectives for the next generation of hardware. One of these is expandability in basic architecture by factors of 10^3 and ideally by factors of 10^6. Dr. Wilson sees parallelism as a means of providing the desired expandability through a configuration of thousands or perhaps millions of processing elements, each having speeds of

at least 20 megaflops. Other guidelines include expandability in data communication, as also mentioned by Dr. Schmitt in his keynote address on large-scale computation in the industrial environment.

Dr. Wilson gave his view of the disadvantages of Fortran, and described a new effort at Cornell called the Gibbs program. The goal of this effort is to provide a modular exposition of programs in a language for researchers to communicate with computers.

Computational Fluid Dynamics

Dr. John E. Bussoletti of the Boeing Company spoke on large-scale calculations used in the design and testing of airplanes, and Dr. Bengt Fornberg of Exxon gave a review of large-scale computers as an introduction to his work on fluid dynamics.

Dr. Bussoletti referred to the powerful computational methods developed for aircraft design and simulation. He cautioned, however, that simulations do not replace wind tunnel and flight tests but instead complement them. Several examples were presented where computations have led to considerable insight and financial savings. Computations played a key role in modifying the design of the 757 cockpit so that it could accommodate the instrument panel of the Boeing 767. In determining the feasibility of 747's to transport a fifth engine from one point to another, simulations revealed that the mounting kit for the extra engine had to be modified in order to avoid a large shock.

While today's supercomputers are capable of processing models for cruise conditions in transonic flow, they are inadequate for many important applications, such as the study of horizontal stabilizers and details of wing structures. Dr. Bussoletti called for bigger and faster machines not only for these types of calculations, but also for the development of improved models. He urged a close relationship between algorithm research and computer architecture.

Dr. Fornberg reported on massive computations for the flow of fluid around a cylinder which involve two space-variables, two velocity-variables, and complex boundary conditions. He said that the power of state-of-the-art technology has led to the discovery of new structure in the flow problem, and that this is stimulating research involving laboratory studies and theoretical analysis.

Dr. Fornberg explained that desired computational requirements in fluid dynamics vary. For the more complex problems, such as chemical reactions in flowing fluids, he projects computational and memory requirements in the range of gigaflops and gigabytes. He speculated that the history of this dynamic technology indicates that sustained rates in the gigaflop range will be available in the 1990's, for example, as some say ETA's GF-10 will achieve.

Public Policy Implications

The speakers in the area of public policy included two members of the U.S. House of Representatives: Rep. George E. Brown Jr. (D. Ca.) and Rep. Rod Chandler (R. Wa.), both of whom are members of the committee on Science and Technology. Dr. James Kane, the Deputy Director of the Office of Energy Research at DOE, and Jo Billy Wyatt, the Chancellor of Vanderbilt University, also spoke.

Rep. Chandler mentioned the importance of educating Congress on what he described as one of America's best kept secrets—large-scale computation and its impact on America's future. He discussed the initiatives of the Republican Task Force on High Technology, of which he is a member, and Task Force recommendations that are designed to promote technology, provide incentives for a vigorous R&D effort in America, and direct resources to universities for equipment modernization. It was explained that the House Science and Technology Committee held two hearings on large-scale computation last year and that these were instrumental in allocating increased support to NSF, NASA, and NBS. Rep. Chandler explained how the R&D joint venture bill, recently passed by the House, should provide some incentives for consortia such as Bobby Ray Inman's Microelectronics Computer and Technology Corporation, MCC.

Dr. Kane recalled how a dynamic partnership between America's computing industry and its national laboratories has been a key factor in building American leadership in computing technology. The responsibilities of DOE in areas of applied and basic research and in new issues, such as climate modeling and the nuclear winter problem, provide opportunities for DOE to continue its strong role in the area of scientific and engineering computations. Dr. Kane said that he has been made aware of the importance of American researchers having greater access to large-scale computing technology and he reviewed various initiatives in the DOE National Laboratories which are designed to provide more access.

Congress is just beginning to understand the connection between large-scale computation and innovation and productivity.

Chancellor Wyatt commented that the current activities in government and universities in the area of computer usage is reminiscent of initiatives taken by the NSF in the 1960's to establish university computational centers. He emphasized the continued importance of basic research in America and stressed the importance of America's ability to transfer technology from the research laboratory to commercialization. Chancellor Wyatt expressed the opinion that the linkages between the Federal government, private sector, and universities are as good as they ever have been for promoting high technology initiatives such as large-scale computations.

Rep. Brown explained that Congress understands the vital importance of computing technology to the continued development of science and engineering, but that it is just beginning to understand the connection between large-scale computations and innovation and productivity. He cited the growing recognition in Congress that, given the existing market, commercial computer manufacturers in the United States have neither the resources nor the motivation to singlehandedly undertake the advancement of high-speed computing technology. Rep. Brown acknowledged that a coordinated effort to maintain America' leadership in computing technology is vital not only for America's scientific strength, but also for its economic competitiveness in world markets. He pointed out that much needs to be done between industry, universities, and the Federal government, and he urged the audience to take a more active role and to view themselves as a transmission belt to opinion makers who have impact on Congress.

Common Technology Needs

Dr. James C. Browne of the University of Texas informed the audience that the next generation of hardware will be more difficult to use, if users expect to exploit the full power of the new technology. He urged more research on algorithms, software, and higher-level languages, and he emphasized the importance of training the current generation of students in these pressing topics.

Dr. Sidney Fernbach of Control Data Corporation corroborated Dr. Browne's remarks. He explained the further need for more research on software that allows one to do symbolic computation. He speculated that the difficulties encountered in the commercialization of large-scale computing technology may go beyond price and extend to the friendliness and versatility of software. Dr. Fernbach agreed that the users of present generation hardware must learn a great deal in order to tap its potential. Another problem is that peripheral equipment is often not designed to match the needs of the host computer.

As evidenced throughout the conference, the cost of computing must include the cost of people not doing science because of either having to wait on slow computers or having to spend time outwitting and coaxing slow computers. The issue is not only economic; it also raises questions about the optimal use of creative resources. This point is widely recognized among traditional users of large-scale computation and has been addressed by combining high-speed interactive graphics with high-speed general purpose computing.

As is evident from the preceding discussion, scientists in these emerging applications have arrived at the same solution. Implicit in this solution is the need for high-speed data communications and large data management facilities. Virtually every application of high-speed computation addressed at the conference showed the promise of major breakthroughs through the availability of more powerful computers, but advances in that area must be accompanied by advances in these other two areas in order to maintain a balanced system.

Equally important are mutual needs in software; for example, efficiency in software, including operating systems, is a clear concern. Improved software for networking and database management is needed. Last, but not least, greater emphasis must be placed on ease of use and quality of documentation.

Prepared by *B. L. Buzbee, Computing and Communications Division, Los Alamos National Laboratory, Los Alamos, NM, 87544, and H. J. Raveche, Thermophysics Division, National Bureau of Standards, Gaithersburg, MD 20899.*